EVALUATION OF THE MESOSCALE ETA MODEL OVER THE WESTERN UNITED STATES

by

Robert Timothy Swanson, Jr.

A thesis submitted to the faculty of
The University of Utah
in partial fulfillment of the requirements for the degree of

Master of Science

Department of Meteorology

The University of Utah

June 1995

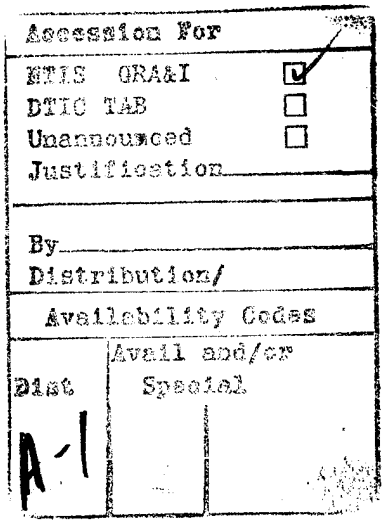

REPORT DOCUMENTATION PAGE

Form Approved
OMB No. 0704-0188

1. AGENCY USE ONLY *(Leave blank)*	2. REPORT DATE	3. REPORT TYPE AND DATES COVERED
	10 Sep 95	

4. TITLE AND SUBTITLE
Evaluation of the Mesoscale Eta Model Over the Western United States

5. FUNDING NUMBERS

6. AUTHOR(S)
Robert Timothy Swanson, Jr.

7. PERFORMING ORGANIZATION NAME(S) AND ADDRESS(ES)
AFIT Students Attending:
Utah University

8. PERFORMING ORGANIZATION REPORT NUMBER
95-092

9. SPONSORING/MONITORING AGENCY NAME(S) AND ADDRESS(ES)
DEPARTMENT OF THE AIR FORCE
AFIT/CI
2950 P STREET, BLDG 125
WRIGHT-PATTERSON AFB OH 45433-7765

10. SPONSORING/MONITORING AGENCY REPORT NUMBER

11. SUPPLEMENTARY NOTES

12a. DISTRIBUTION/AVAILABILITY STATEMENT
Approved for Public Release IAW AFR 190-1
Distribution Unlimited
BRIAN D. GAUTHIER, MSgt, USAF
Chief of Administration

12b. DISTRIBUTION CODE

13. ABSTRACT *(Maximum 200 words)*

14. SUBJECT TERMS	15. NUMBER OF PAGES 113
	16. PRICE CODE

17. SECURITY CLASSIFICATION OF REPORT	18. SECURITY CLASSIFICATION OF THIS PAGE	19. SECURITY CLASSIFICATION OF ABSTRACT	20. LIMITATION OF ABSTRACT

THE UNIVERSITY OF UTAH GRADUATE SCHOOL

SUPERVISORY COMMITTEE APPROVAL

of a thesis submitted by

Robert Timothy Swanson Jr.

This thesis has been read by each member of the following supervisory committee and by majority vote has been found to be satisfactory.

May 24, 1995 — Chair, John D. Horel

May 24, 1995 — Jan Paegle

May 24, 1995 — Lawrence B. Dunn

THE UNIVERSITY OF UTAH GRADUATE SCHOOL

FINAL READING APPROVAL

To the Graduate Council of the University of Utah:

I have read the thesis of Robert Timothy Swanson Jr. in its final form and have found that (1) its format, citations and bibliographic style are consistent and acceptable; (2) its illustrative materials including figures, tables and charts are in place; and (3) the final manuscript is satisfactory to the supervisory committee and is ready for submission to The Graduate School.

May 30, 1995
Date

John D. Horel
Chair, Supervisory Committee

Approved for the Major Department

J.E. Geisler
Chair/Dean

Approved for the Graduate Council

Ann W. Hart
Dean of The Graduate School

ABSTRACT

The skill of the Mesoscale Eta Model is evaluated over a 6-month period from October 1, 1994 to March 31, 1995 over the western United States. This model will continue to undergo changes until and after its projected operational release in July 1995. Many diagnostics and error statistics are created to evaluate its performance as forecasts are received and archived at the University of Utah. These statistics are available on the Internet allowing researchers and operational forecasters access to them in near real-time.

The Mesoscale Eta Model forecast initialized at 1200 UTC, 9 November 1994 is used as a case study to introduce many of the diagnostics developed to evaluate the model. A systematic evaluation of the average and root-mean-squared error over months and seasons reveals little significant bias in upper tropospheric fields such as 300 mb wind or 500 mb geopotential height. Moderate average errors are evident in lower tropospheric temperature. For example, during the period from October 1, 1994 to December 31, 1994 a -1°C to -2°C cold bias was evident between 850 mb and 700 mb over much of the western United States. Root-mean-squared errors for dew point temperature and relative humidity in the lower and middle troposphere are large.

Accumulated precipitation over months and seasons indicates the model's spinup of precipitation during the first 12 hours of the forecast cycle. Comparison of the stable and convective precipitation totals reveals infrequent triggering of the model's convective parameterization away from the coastal regions of the West. A convective precipitation maxima is noted west (offshore) of the coastline.

TABLE OF CONTENTS

ACKNOWLEDGMENTS

I would like to thank my advisor, Dr. John Horel. He was indispensable in keeping this research focused and on track. Without his experience, expertise and guidance this thesis would not have been completed. I would also like to thank my committee members, Dr. Jan Paegle and Dr. Lawrence Dunn for their support and input. Additionally, the computer intensive portions were made possible thanks to the inspired code and system troubleshooting by our computer systems administrator, Lloyd Staley.

Not surprisingly, the hours spent away from home, and the stress related tantrums took their toll on the family, so I would especially like to thank my wife, Linda, and my boys, Ryan and J.R., for their infinite understanding, patience and support.

This research project was made possible with the support and cooperation of the staff of the National Meteorological Center. I would like to thank particularly: Ronald McPherson for permitting access to the model output at the National Meteorological Center and for allowing the distribution of the results over the Internet to the educational, research, and operational communities; Thomas Black for his role in the model development and facilitating this cooperative research; Fedor Mesinger for his feedback concerning this research and thesis; and Keith Baldwin for making available the GEMPAK sounding files.

The National Science Foundation funded a portion of this research under NSF Grant ATM9318491. Additionally, I am attending the University of Utah under an Air Force Institute of Technology (AFIT) scholarship.

Finally, I would like to recognize the students, staff and faculty in the Meteorology Department for their help, encouragement and friendship. In particular, I would like to thank Brett McDonald for his GEMPAK and computer assistance, and Bryan White for his help with the development of the Department of Meteorology's World Wide Web server.

CHAPTER 1

INTRODUCTION

Scientists in the Development Division of the National Meteorological Center (NMC) developed the Eta model to predict the synoptic-scale and mesoscale evolution of weather features over the continental United States (Mesinger et al. 1990). The term 'eta' refers to the model's unique vertical coordinate. The first operational version of the Eta model was released officially to the forecasting community during the summer of 1993 (Black et al. 1993). This version of the model continues to evolve as updates to it are implemented. It will be referred to here as the Early Eta model as it is the first model run in each 12-hour operational forecast cycle of the NMC. Since the Early Eta model currently uses horizontal grid spacing on the order of 80 km, it resolves and predicts primarily synoptic-scale weather features.

A version of the Eta model able to resolve and predict meso-α scale weather phenomena has been under development at the NMC for several years and will be officially released to the forecasting community in the summer of 1995. This version uses horizontal grid spacing on the order of 30 km and is referred to as the Mesoscale Eta Model (abbreviated hereafter as MEM). During 1996, the NMC intends to test a version of the Eta model with horizontal resolution on the order of 10 km, which will be capable of resolving meso-β scale phenomena.

The purpose of this study is to evaluate the skill of the MEM to simulate synoptic-scale and mesoscale weather phenomena over the western United States. Model forecasts from October 1994 through March 1995 are used here. Thus, this study evaluates the model's performance in its preoperational form and during a period in which the model has

undergone significant changes. This research is part of an ongoing National Science Foundation funded project to evaluate the MEM before and after its official release. It is being conducted in cooperation with the NMC, the Scientific Services Division of the Western Region of the National Weather Service (NWS), and selected Weather Service Forecast Offices in the Western Region.

According to Pielke (1984), mesoscale atmospheric systems can be divided into two distinct groups: those primarily forced by surface inhomogeneities (terrain induced) and those that are forced by instabilities traveling in larger scale disturbances (synoptically induced). Mountain-valley circulations, orographic precipitation, and local convergence zones are examples of terrain-induced phenomena that are often difficult to forecast over the western United States whereas banded precipitation features are a common example of synoptically-induced mesoscale instabilities in the West. An understanding of the ability of the MEM to accurately forecast both types of phenomena will be useful to operational forecasters.

The terrain-following sigma coordinate, which was introduced by Philips (1957), has been used in many research and operational models, such as the Nested Grid Model (NGM) and the Medium-Range Forecast (MRF) model. This vertical coordinate has considerable utility; however, large errors may develop in regions of steeply sloped terrain (Mesinger et al. 1988). First, the pressure gradient term in the horizontal momentum equation is a weak residual of two strongly opposing terms on steeply sloped sigma surfaces. Further, the horizontal diffusion terms in the momentum, thermodynamic, and moisture equations lead to incorrect transports of momentum, heat and moisture in regions of complex terrain.

Although several methods have been explored to alleviate these problems (e.g., Kuo et al. 1988), Mesinger et al. (1988) demonstrated that a modified sigma coordinate, the eta coordinate, improves the numerical treatment of the pressure gradient force and diffusion in regions of complex terrain. This coordinate, which is used in all versions of

the Eta model, treats topography in a stair-step fashion so that individual eta surfaces are quasi-horizontal. A more detailed explanation of the eta coordinate follows in the next chapter.

The skill of the Early Eta model has been evaluated in many studies, with particular attention placed on the model's ability to predict precipitation over the central and eastern portions of the United States. Mesinger et al. (1988) analyzed a storm system over the eastern United States and Mesinger et al. (1990) contrasted the Early Eta model's skill to that of the NGM for a 20-day period in 1989. Other studies by Black and Mesinger (1989) and Zhao et al. (1991) demonstrated improved precipitation predictions compared to those of the NGM.

An evaluation of the Early Eta model was performed by the Forecast Systems Laboratory by Cairns et al. (1993). Their research concentrated on parameters of interest to the aviation community and focused on four locations: the northeast United States, Florida, Colorado, and the Central Plains. They determined that biases in the moisture fields were present that contributed to biases in temperature and height fields.

A study of the Eta model's ability to predict summer convective precipitation over Arizona has been performed (Dunn 1993; Dunn and Horel 1994a,b). The NGM and Early Eta model failed to predict the occurrence of several episodes of widespread precipitation over Arizona. The version of the MEM available during 1993 also did not predict the occurrence of precipitation in the one case available. Even though the Eta model's prediction of precipitation was poor, other model parameters may provide clues to the occurrence of major precipitation episodes during the Arizona Monsoon.

The impact of improved horizontal resolution in the Eta model has been assessed in several studies. Black and Mesinger (1991) showed that the NGM and the Early Eta model were incapable of delineating two distinct precipitation bands. However, an Eta model forecast with horizontal resolution on the order of 30 km was more successful. Mesinger et

al. (1994) found that the 40 km version of the MEM was more accurate in the light and medium intensity precipitation compared to that predicted by the Early Eta model.

In a detailed examination of the 1994 version of the MEM's performance over the central United States, Black (1994) showed that the model's increased resolution did, indeed, capture smaller scale circulations associated with a frontal band passing through the area. However, it was still unable to adequately capture the very heavy rainfall in the warm sector ahead of the front. Black (1994) also examined the model's ability to simulate orographic effects by examining a system moving onshore near Vancouver Island in the Pacific Northwest. He determined that the enhanced resolution of the MEM generated local maxima in precipitation that were not evident in the Early Eta model. He notes that some of these improvements may be due to the model's higher-resolution representation of the area's land-forms. Additionally, Black and Baldwin (1995) demonstrated the increased horizontal and vertical resolution led to a vastly improved (over the Early Eta) forecast of a cold air damming precipitation event east of the Appalachians. The increased number of levels permitted better modeling of the cold dry air beneath the warmer moist overrunning air, and the increased horizontal resolution led to a more accurate depiction of the Appalachian orography and of the strong thermal gradient.

The goals of this research can be summarized as follows:

- To develop the capability to archive the MEM forecasts over the western United States on a continual basis.
- To routinely determine the magnitude of the errors in the MEM, relative to soundings, MEM analyses, and the Rapid Update Cycle (RUC) analyses as a function of forecast duration, time of year, variable type, and vertical level.
- To summarize the skill of the MEM in terms of average errors and root-mean-squared errors averaged over sample sizes of months and seasons.
- To focus on the skill of the MEM as a function of level with respect to the variables: geopotential height, wind, temperature and moisture.

- To make all of this information available as soon as possible to interested researchers and the operational community over the Internet.

Evaluation of operational model performance is an ongoing effort at the NMC. For example, for several years, the NMC Seasonal Performance Summary was published routinely as a means to document the skill of the operational models. However, given the complexity and coverage of the operational models at the NMC, it is difficult to monitor and evaluate all aspects of the model's forecasts. This research focuses only on the MEM forecasts over the western United States where the documentation of the model's performance is less complete than that for other regions. In many respects, this effort is a pilot study that serves as the basis for further in depth analysis of the model's skill over the western United States.

The last of the above listed objectives reflects a novel aspect of this study. Normally, model verification statistics are disseminated in journal articles or technical reports. However, the World Wide Web provides a mechanism to make available much more effectively information of interest to both the research and operational communities. Only a fraction of the results developed in this study are presented in this thesis. Directions to other 'on-line' pages of information, which are analogous to interactive appendices, will be given.

Characteristics of the MEM are described in the next chapter. This summarizes the numerical schemes and parameterizations used in the model, as well as recent and planned modifications. The data used to verify the model forecasts are summarized in Chapter 3. A detailed case study is presented in Chapter 4 using the statistics generated to evaluate the model's skill. The model statistics over the period October 1994 through March 1995 are examined in Chapter 5. Finally, conclusions drawn from this research and suggested areas for further research are presented in the final chapter.

CHAPTER 2

MODEL DESCRIPTION

Eta Vertical Coordinate

The eta coordinate (Mesinger et al. 1988) is defined by the relation:

$$\eta = \left(\frac{p - p_T}{p_{sfc} - p_T} \right) \left[\frac{p_{ref}(z_{sfc}) - p_T}{p_{ref}(0) - P_T} \right] \tag{2.1}$$

where p_T is the pressure at the top of the domain (currently 50 mb), p_{sfc} and z_{sfc} are the pressure and elevation of the model's lower boundary, and p_{ref} is a reference pressure state that is a function of distance above sea level. Notice that the term on the right hand side of Equation 2.1 collapses to the sigma coordinate (Philips 1957) when $z_{sfc} = 0$:

$$\sigma = \left(\frac{p - p_T}{p_{sfc} - p_T} \right). \tag{2.2}$$

The eta coordinate treats the topography in a stair-step fashion so that individual eta surfaces are quasi-horizontal. Further, it preserves the simplified lower boundary condition found in terrain following vertical coordinates. A schematic comparison of the sigma and eta coordinates is shown in Figure 2.1. Notice that the sigma coordinate system is a terrain following coordinate system and that two adjacent points on the same sigma surface can vary greatly in height. As mentioned in Chapter 1, this can introduce large errors when the pressure gradient force term is computed over steeply sloping terrain.

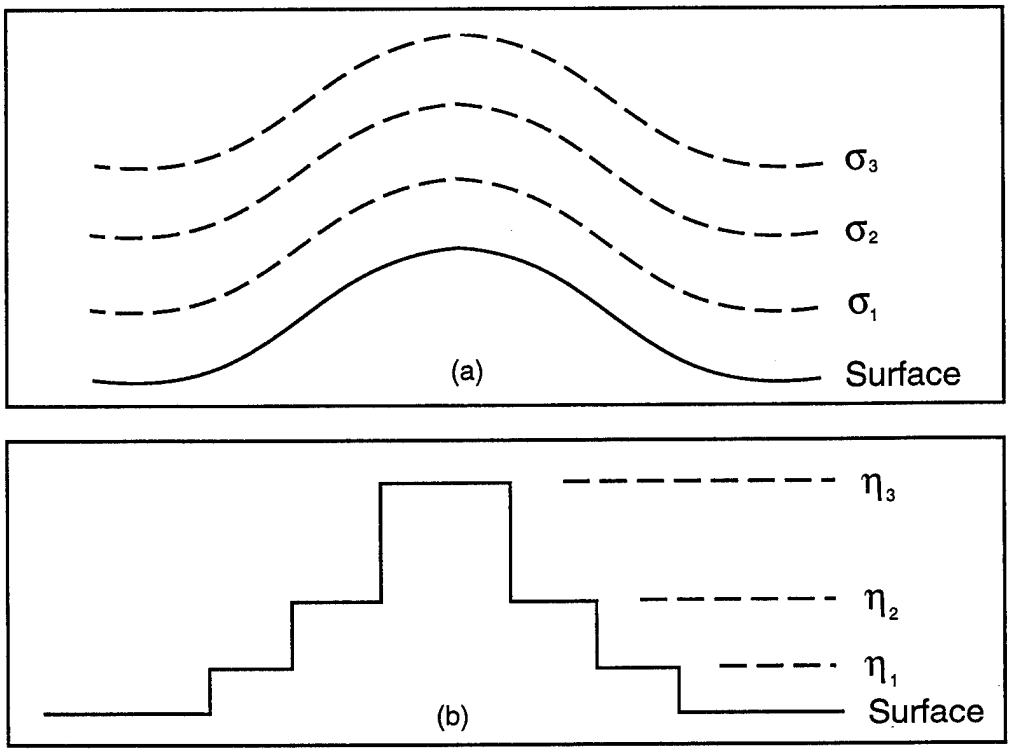

Figure 2.1. Schematic of the two vertical coordinates: (a) sigma and (b) eta.

It is readily seen in Figure 2.1 that the spacing between eta surfaces is dependent on the altitude of the surface (z_{sfc}). This feature may cause problems over regions of elevated terrain where the large spacing between model levels leads to coarse resolution of the boundary layer. Figure 2.2 shows vertical profiles of wind at Quillayute (UIL), WA and Salt Lake City (SLC), UT. At a location near sea level (e.g., UIL), there are 17 eta surfaces from the surface to 2 km whereas only 9 eta surfaces are found in the lowest 2 km at SLC.

Mesoscale Eta Model

The Mesoscale Eta Model (MEM) was described recently by Black (1994). As will be discussed further below, the model has undergone additional revisions since last year. It is currently a 50 layer hydrostatic model with greatest vertical resolution near sea level and near the mean height of the tropopause. The MEM uses a semistaggered Arakawa E-grid (Black 1994). This grid staggers the mass variables and the wind variables and is designed

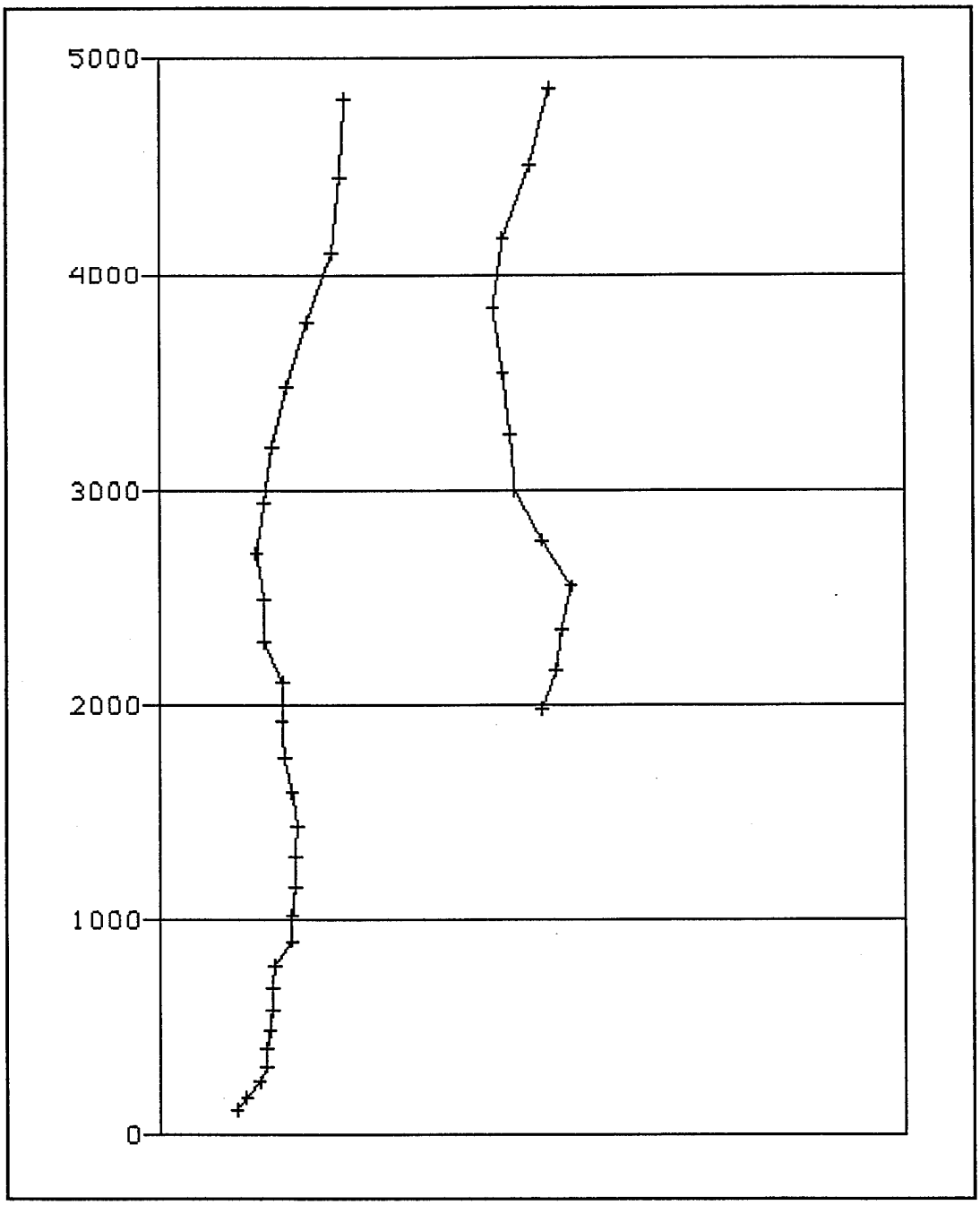

Figure 2.2 Relative vertical spacing between eta surfaces (crosses) at a station near sea level, Quillayute (UIL), WA (left), and a station in the intermountain region, Salt Lake City (SLC), UT (right).

to minimize errors that occur with other horizontal grid domains associated with geostrophic adjustment and topographic forcing. It uses a split-explicit integration scheme that minimizes the calculations required per forecast time step. The fundamental time step used is that required for inertial gravity waves (about 72 seconds). The time step required for advective processes is twice that.

The initial conditions are derived from the Eta Data Assimilation System (EDAS), described by Rogers et al. (1995), which is analogous to the Regional Data Assimilation System (RDAS) that initializes the NGM. The continuous assimilation approach proceeds at 3-hour intervals and model forecasts last 33 hours (36 hours prior to April, 1995). The lateral boundary conditions are derived from the Aviation run of the global spectral MRF model using a one-way interactive scheme.

Two types of precipitation are handled by the model. Grid scale precipitation is forecast if the relative humidity in a grid box exceeds 95%. Part or all of this precipitation may evaporate as it falls through layers where the relative humidity is less than 95%. As described by Janjic´ (1994), a modified Betts-Miller cumulus parameterization (Betts 1986; Betts and Miller 1986) handles the convective precipitation. In this scheme, nonprecipitating shallow convection carries moisture upward and helps maintain low-level inversions. Deep convection transports heat and moisture upwards and produces rainfall. In both types of precipitation, model variables are relaxed to reference profiles. Rainfall amounts are deduced from the net negative change in the specific humidity in deep convective clouds.

The vertical turbulent exchange uses a modified Mellor-Yamada Level 2.5 scheme (Gerrity et al. 1994; Black 1994). In this approach, turbulent kinetic energy (TKE) is a fully prognostic variable. The predicted TKE is then used to compute the exchange coefficients for the transfer of heat, moisture, and momentum between adjacent model layers. The Mellor-Yamada Level 2 scheme governs the exchange between the earth's surface and the lowest model layer where the TKE is assumed to be constant in height.

Surface fluxes are computed using Monin-Obukov functions (Black 1994). Currently, this model has only one prognostic ground layer. Temperature and moisture are updated over the ground surface; over the open water, however, these quantities are held constant. The surface soil temperature is computed using a force-restore relation.

The model's radiation package is virtually identical to that of the MRF model as developed at the Geophysical Fluid Dynamics Laboratory. The model's carbon dioxide and ozone distributions are taken from climatology and held constant. The initial surface albedo is also taken from climatology, but is allowed to evolve during the forecast. Both stratiform and cumuliform clouds are diagnosed following the approach developed by Slingo (1987) and determined from the model's relative humidity and collective rainfall rate.

Code Updates and Changes

A log of model and postprocessor changes has been maintained since January, 1992 (Black 1994). Many of the changes involved fixing problems discovered during the development and testing of the MEM. A summary of the changes that may affect the interpretation of the results presented here, as well as the evaluation of the model, are listed in Table 2.1. Additionally, several significant changes to the model are expected to be implemented by Summer 1995. These include:

- a 20 m surface above ground level at each grid point.
- improvements to surface fluxes over the ocean.
- major changes to the treatment of soil moisture and soil heat exchanges.
- a new turbulence package.

Table 2.1. Chronological listing of significant Mesoscale Eta code changes since those described by Black (1994).

Date	Changes
09/27/94	Fixed the topography file to correct for some elevated water points along the coasts.
09/27/94	The underground and edge wind components were fixed to be identically zero in the assimilation for the static analysis run.
10/12/94	The hourly profiler output was modified to specify the base flow-ground water runoff as missing throughout the forecast.
10/12/94	Fixed an error in computing Richardson's number (improper averaging of the winds surrounding each mass point).
10/17/94	10 m winds are now included in the hourly profiler output.
10/21/94	A bug was removed which loaded the lowest levels in the profiler output of temperature tendencies due to shortwave radiation and grid scale rain with zeroes.
10/26/94	Modifications to the decision tree for precipitation types were made.
10/26/94	Code for computing the time averaged cloud fraction was added.
11/09/94	An evolving albedo was added to the model.
12/05/94	The 50-layer carbon dioxide transmission functions were erroneous (increasing with height) and were corrected.
12/20/94	A bug was removed which erroneously equivalenced the 2 m and surface temps together.
02/02/95	The first operational Mesoscale Eta code was established at this point.
03/08/95	A fix was made to the saturation vapor pressure over ice. The critical value of q needed for precipitation was modified.
03/21/95	The new SST analysis was incorporated. The resolution is 50 km over the oceans and a relaxed 14 km over the Great Lakes.
03/28/95	The mesoscale run commenced running with operational priority with the forecast code current as of 2 February.

CHAPTER 3

DATA AND METHOD

Data Resources

All available MEM forecasts have been archived routinely beginning in August 1994. The forecasts were accessed at the NMC and transported over the Internet to the University of Utah. The 6-month period October 1994 through March 1995 is emphasized here. During that period, 288 forecasts were received, processed, and archived out of a total possible of 364. The missing forecasts were mainly due to data retrieval difficulties. Thus, a large sample of model forecasts have been examined. The model output is post processed at the NMC from the model's Arakawa E-grid to the GRIB grid 106, which has horizontal resolution on the order of 40 km (Treadon 1993). In addition, the model output is interpolated from the model's eta levels to 50 mb surfaces from 1000 mb to 100 mb. Selected model output is available at the surface and other levels of interest, e.g., tropopause and freezing level. In addition to the model's analysis fields, output during this study was available at 6-hour intervals through 36 hours. Standard meteorological variables are archived in GEMPAK format (des Jardins et al. 1991) at levels above the surface: temperature, geopotential height, vector wind, relative humidity, and vertical velocity.

The interpolation procedures performed at the NMC may introduce discrepancies between what the model actually forecast compared to that available after interpolation. However, these steps are necessary for post analysis. The staggered Arakawa E grid and eta vertical coordinate are not supported presently by GEMPAK software (des Jardins et al. 1991). Further, operational use of the model output is planned to occur on postprocessing grids, such as the AWIPS GRIB grid 212.

The postprocessed output from each MEM forecast is on the order of 30 Mbytes. Thus, the total amount of model output stored to date at the University of Utah is roughly 10 Gbytes. For convenience and to speed processing of the information, a separate archive of model forecasts was created in which the horizontal domain is restricted to the western United States (Figure 3.1). This reduces each model forecast to roughly 5.5 Mbytes.

Figure 3.1 shows the MEM's terrain in the western United States. The heights are plotted on the GRIB grid 106, used in processing most of the data. Figure 3.2 displays the rawinsonde station locations used in this research.

Soundings from the MEM in GEMPAK format that were created by Keith Baldwin of the NMC were obtained on a routine basis (personal communication, 1994). The model field grid point deemed most representative of a given location is used as the 'sounding' location. The primary advantages of this archive are: model soundings are available at hourly intervals; the model output has not been interpolated to pressure surfaces; and other diagnostic fields are available in the files. However, fewer of these model sounding files are available than the complete MEM forecast files. Thus, soundings at rawinsonde sites in the western United States are generated from the MEM forecast files using a simple bilinear interpolation from the output on the GRIB 106 grid to the rawinsonde locations.

In order to verify that this additional interpolation step does not introduce large errors, Figure 3.3 compares a typical model temperature sounding at Salt Lake City extracted from the MEM forecast file to that obtained from the MEM sounding file generated at the NMC. The differences between the two lines are barely distinguishable. Here, the solid line is the actual MEM sounding generated at the NMC whereas the dashed line show the temperature sounding generated by interpolating MEM data to sounding locations. The small differences in this case are representative of most of those that have been examined. As a general rule, large differences are evident only at the lowest 50 mb level near mountain ranges where the horizontal interpolation may combine information from the free atmosphere and below ground.

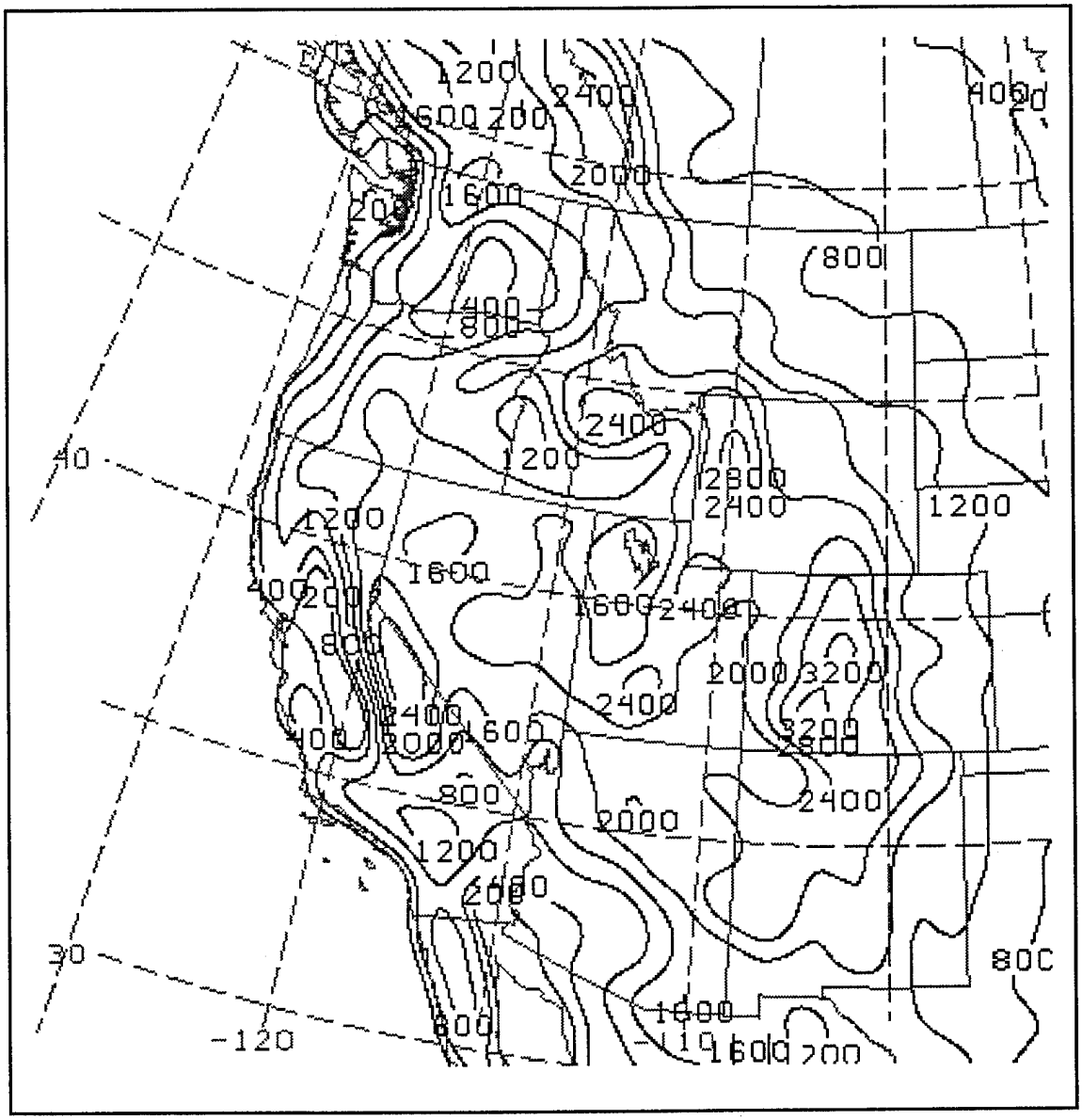

Figure 3.1. MEM terrain over the western United States. Elevations here are contoured at 200 m, and 400 m to 3200 m in 400 m intervals.

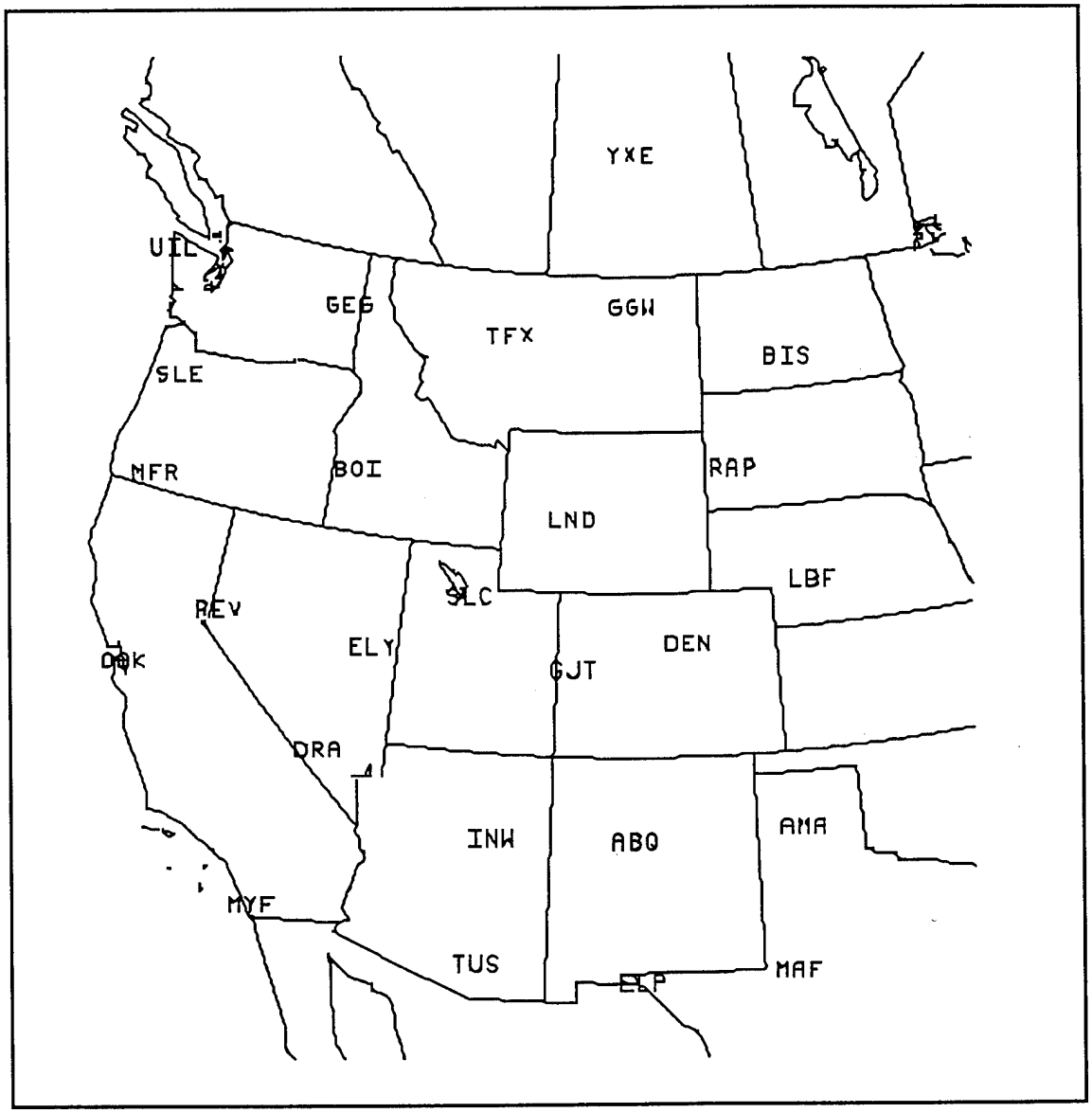

Figure 3.2. Rawinsonde locations over the western United States and Canada used in this research.

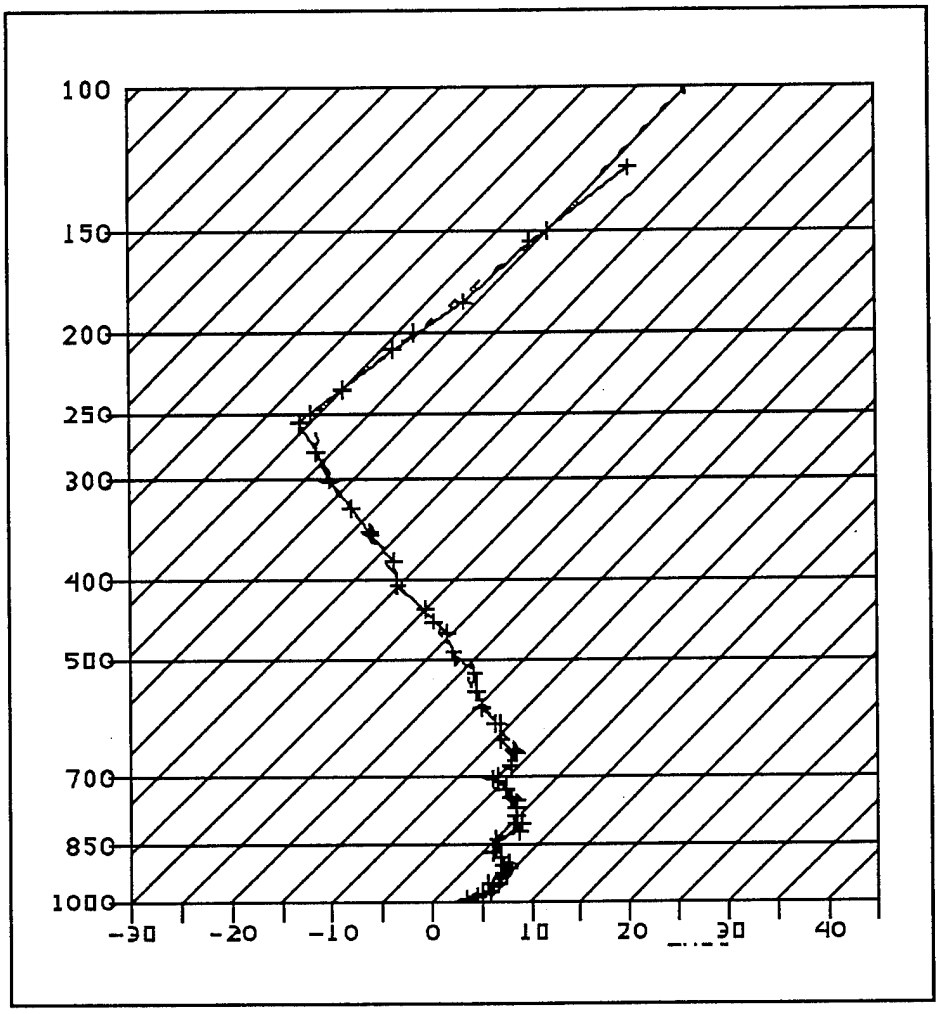

Figure 3.3. Comparison of Salt Lake City temperature soundings for 0000 UTC, January 2 1995. The solid line is the MEM sounding from NMC and the dashed line is the MEM sounding generated by interpolating gridded data to sounding locations.

The MEM forecast skill is evaluated in comparison to the model's analysis at later times, rawinsonde observations, and the RUC analyses of the NMC. Since MEM analyses are available for this project only at 12-hour intervals, it was possible to verify the 12-hour, 24-hour, and 36-hour forecasts only. Rawinsonde observations at all sites in the western United States have been received, processed, and archived routinely as part of the Unidata initiative to distribute weather information to universities over the Internet. Soundings are generally available at 12-hour intervals; thus, only the analysis, 12-hour, 24-hour, and 36-hour forecasts can be verified. The observed soundings are interpolated to 50 mb intervals in the vertical for comparison to the model soundings.

To verify MEM forecasts at 6-hour intervals, the RUC analyses from the NMC were obtained, archived, and postprocessed to the same GRIB 106 grid on which the MEM forecasts are stored. The RUC model was developed at the Forecast Systems Laboratory and provides an analysis that incorporates all available information over the continental United States (Bleck and Benjamin 1993).

Model Skill

Forecast skill is examined here in terms of the errors between the MEM forecasts and: (1) MEM analyses; (2) RUC analyses; and (3) rawinsonde observations. The errors are determined as a function of variable, level, forecast duration, and time of year. To reduce the volume of the error statistics, one approach is to summarize the characteristics of the model errors in terms of the average error (or bias) and the root-mean-squared (RMS) error, a measure of their typical magnitude. The average error, B, is the average difference between the forecast and observed summed over a specified number of model forecasts, such as a month or season:

$$B = \frac{\sum_{i=1}^{n} (f_i - o_i)}{n} \tag{3.1}$$

where n is the total number of forecasts, f_i is the i^{th} forecast, and o_i is the i^{th} analysis. A positive average error indicates that the forecast typically exceeds the observed value. The bias information is useful only if the sample size is sufficiently large to reflect a typical mix of weather regimes. The RMS error is determined as follows:

$$RMS = \left(\frac{\sum_{i=1}^{n} (f_i - o_i)^2}{n} \right)^{\frac{1}{2}}. \qquad (3.2)$$

The RMS error reflects the typical size of the errors, irregardless of their sign. A few poor forecasts in the sample may lead to large RMS errors.

Comparing the MEM forecasts to real-time upper-air sounding data requires careful treatment of the observed soundings, i.e., sporadic and varied reporting must be taken into account. Also, unrealistic errors must be identified and discarded. Thus, the following thresholds are used to eliminate unrealistic values: ± 15° C for temperature and dew point temperature, ± 50 m s^{-1} errors for wind speed, and ± 200 m for geopotential height. Errors of this magnitude were rarely present in the data.

Interactive Access to Graphical Information

As mentioned in Chapter 1, a novel aspect of this study is the interactive access to the research results via the Internet. To achieve this goal, new technology has been exploited by placing all of the error statistics, as well as several case studies of model forecasts, on a World Wide Web server in the University of Utah Department of Meteorology. In addition, graphics from the most recent MEM forecast are available. At the request of the Director of the NMC, access to this information is restricted to government and educational institutions until the MEM becomes operational later this year.

Graphics and on-line documentation are available via the Department of Meteorology's Web server. This information is accessed by setting the Uniform Resource Locator (URL) to: **http://www.met.utah.edu**, the 'home page' of the Department of Meteorology's Web server. Throughout this work, bold face type will indicate the appropriate URL to access other pages of information. The term 'page' refers to a collection of information accessible from a Web server with a single command.

In the following subsections, the different types of graphic resources available on-line are described. The development of these resources reflects the combined efforts of J. Horel, R. Swanson, B. White, and B. McDonald. Conversion of the color graphics available on-line to the monochrome figures of this thesis has affected the quality of some of the figures with extensive shading; viewing the color originals available on-line may help to differentiate between different gray shades presented here.

MEM Forecasts

Graphics from the latest MEM forecast are made available as soon as they are processed. Two sets of diagnostic fields are presented as four-panel graphics as a function of forecast time. The information contained in the first set of diagnostics consists of:

- upper-left panel - 300 mb wind, isotachs, and divergence
- upper-right panel - 500 mb height and absolute vorticity
- lower-left panel - 700 mb wind, temperature, and relative humidity
- lower-right panel - mean sea level pressure (Mesinger and Treadon 1995), accumulated precipitation, and upper-tropospheric potential vorticity.

Examples of these diagnostic fields are presented in the next chapter and further documentation is available on-line by selecting the **INFO** button. The second set of diagnostic fields is comprised of the following:

- upper-left panel - 200 mb wind, isotachs, and divergence
- upper-right panel - 10 m wind, precipitable water, and 2 m equivalent potential temperature

- lower-left panel - 700 mb equivalent potential temperature and relative humidity
- lower-right panel - Convective Available Potential Energy (CAPE) and accumulated precipitation.

A three day archive is maintained on-line. These diagnostics and archives can be accessed on-line via URL: **http://www.met.utah.edu/html/meso/model_mesoeta.html**. These diagnostic fields can also be recreated from the archived data.

MEM Case Studies

For selected periods, collections of graphic fields have been assembled for comprehensive evaluations of the MEM forecasts. To date, several case studies are on line including:

- November 9-11, 1994 - first major winter storm of the season
- January 7-13, 1995 - severe California flooding
- March 7-12, 1995 - second episode of severe California flooding

These are available via: **http://www.met.utah.edu/html/case/case_master.html**.

MEM Analysis Height Fields and Potential Vorticity

As a means to quickly review the synoptic situation of any of the available MEM forecasts, MPEG files have been created of the 200-300 mb (upper tropospheric) potential vorticity anomalies along with their corresponding 500 mb height fields. These MPEG files can be accessed via URL: **http://www.met.utah.edu/html/meso/meso_mpg.html**. They are intended to provide an overview of the weather patterns, and should be used in conjunction with the other error statistics (particularly the time series) to see which synoptic situations the MEM handles well. For reference, potential vorticity values greater than two Potential Vorticity Units (PVUs) (1 PVU = 10^{-6} m^2 s^{-1} K kg^{-1}) indicate an intrusion of stable stratospheric air into the lower atmosphere. Figure 3.4 shows an example of this graphic. This is the upper-tropospheric potential vorticity and 500 mb height for 1200 UTC, November 9 1994, the synoptic situation presented in the case study in Chapter 4.

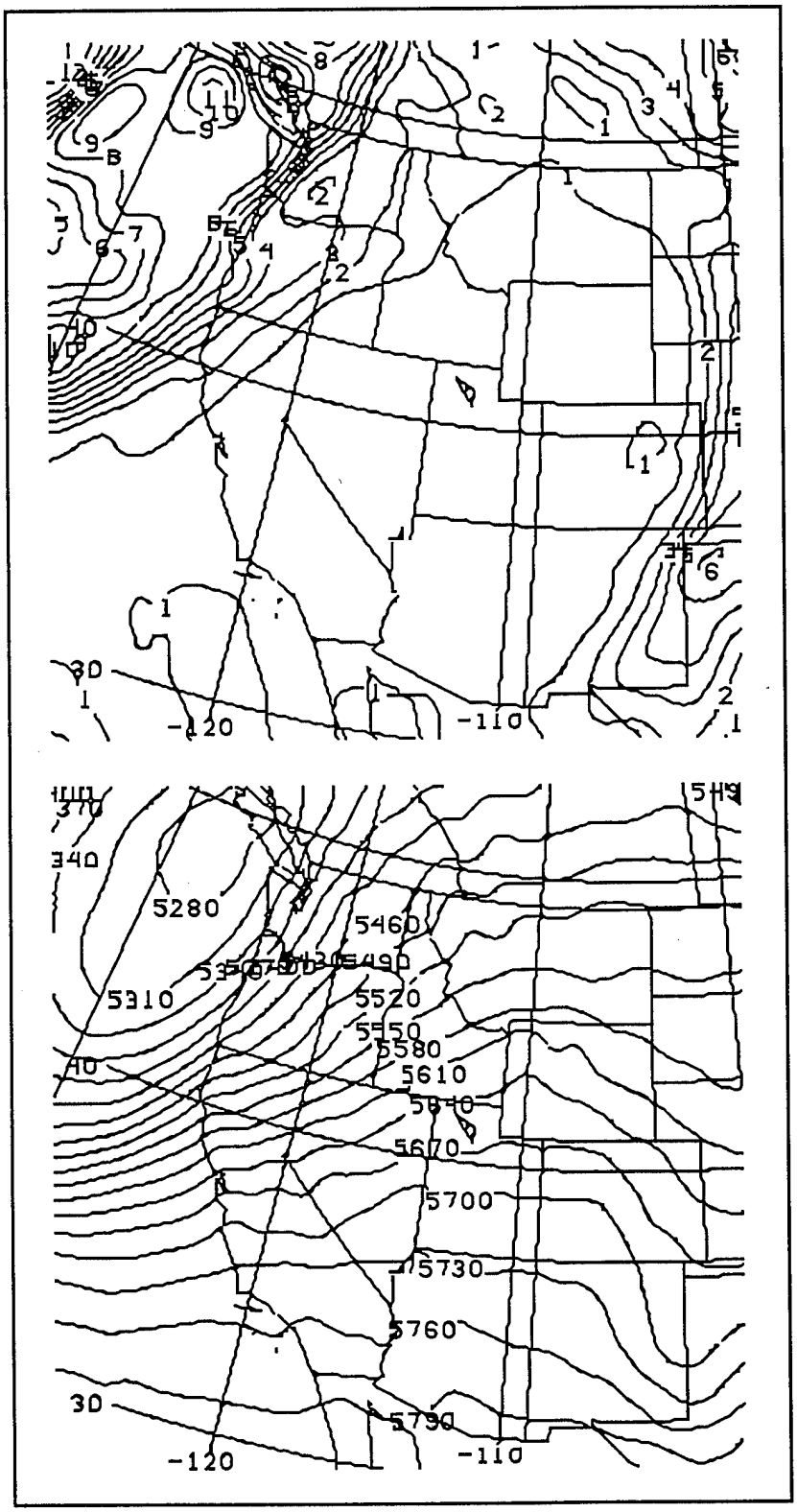

Figure 3.4. Upper tropospheric potential vorticity (upper panel) contoured at an interval of 1 PVU (10^{-6} m^2 s^{-1} K kg^{-1}) and 500 mb geopotential height (lower panel) contoured at 30 m intervals for 1200 UTC, November 9 1994.

Error Time Series

Model errors with respect to rawinsonde observations are available as monthly time series. These differences are computed for the 26 western United States rawinsonde locations used in this study for the following parameters: temperature, dew point temperature, zonal and meridional wind, relative humidity and geopotential height. They can be plotted for any level (every 50 mb from 1000 mb to 100 mb). Here the output is restricted to four standard levels (300 mb, 500 mb, 700 mb, and 850 mb) and five parameters (temperature, dew point temperature, wind speed, geopotential height and relative humidity). Examples of these plots are presented in Chapters 4 and 5. The time series plots can be viewed by month, station and parameter on-line by accessing URL: **http://www.met.utah.edu/html/meso/meso_time_series.html**.

Average and RMS Error with Respect to Observed Soundings

Time-averaged RMS and average errors are plotted at the rawinsonde locations. A complete description of this graphic appears in Chapter 5. These can be accessed via Internet using the following URLs:

http://www.met.utah.edu/html/meso/meso_verification_bias.html

http://www.met.utah.edu/html/meso/meso_verification_rms.html.

Further documentation is available on-line by selecting the **INFO** button. Monthly, as well as seasonal, statistics are presented.

Average Error and RMS Errors with Respect to MEM Analyses

The MEM's own analyses are used to verify its previous forecasts. While the error measures are determined for all of the model prognostic variables at all vertical levels available in the archive, graphics are presented on-line for only a small sample of the fields. They are available on-line using the following URLs:

http://www.met.utah.edu/html/meso/meso_bias.html

http://www.met.utah.edu/html/meso/meso_rms.html.

Average Error and RMS Error with Respect to RUC Analyses

Monthly and seasonal RMS error and average error statistics are generated for the MEM with respect to the RUC analyses. As in the case of the MEM verification against the MEM analysis, verification is conducted for all available prognostic variables and levels in the archive. The RUC is used here since its analysis procedure is quite different from that employed by the static analysis and EDAS used by the MEM. Further, it allows verification of the MEM forecasts at 6-hour forecast intervals. This information is available via Internet by accessing the following URLs:

http://www.met.utah.edu/html/meso/meso_ruc_bias.html

http://www.met.utah.edu/html/meso/meso_ruc_rms.html.

Accumulated Precipitation Totals

To evaluate the MEM's handling of precipitation, both convective and total, cumulative precipitation totals are available for monthly and seasonal time periods. Assuming that all forecasts are available, the monthly or seasonal precipitation totals should be independent of forecast duration. However, there are gaps in the archive developed here. Examples of these accumulated precipitation fields appear in Chapter 5. They can be accessed via URL: **http://www.met.utah.edu/html/meso/meso_rain.html**.

CHAPTER 4

NOVEMBER 1994 CASE STUDY

The period November 9-12, 1994 was selected for further analysis. A major winter storm, one of the first of the winter season, approached the west coast of the United States on November 9. All of the operational NMC models moved a vigorous trough into the intermountain region by November 11. Widespread precipitation over the intermountain region was forecast with large snow totals expected in the mountains as the storm moved through. However, the storm weakened and headed further south than forecast and conditions remained dry and mild over much of the state of Utah. The overall skill of the MEM forecast is comparable in this case to that of the other operational models. The largest model errors were found in the 700 mb temperature field and relative humidity in the lower troposphere over Utah.

A variety of information is available for the three day period from November 9 to November 11, 1994 by accessing the following pages:

http://www.met.utah.edu/html/case/case_nov09_94.html

http://www.met.utah.edu/html/case/case_nov10_94.html

http://www.met.utah.edu/html/case/case_nov11_94.html.

For brevity, only the MEM model forecast initialized at 1200 UTC November 9, 1994 is discussed here. The MEM forecast can be compared on-line to those of the Early Eta model, the NGM, and the Aviation run of the MRF model. All of these model forecasts can be compared on-line to later model analyses, RUC analyses, and satellite photos.

Surface Observations and Visible Satellite Imagery

Satellite imagery for the entire period is available on-line. A sequence of three visible satellite images are presented in Figure 4.1. Shortly after the initial time of the MEM forecast (Figure 4.1a.), a baroclinic zone extends from northern California through Oregon and Washington. Moderate rain is occurring at Redding, California and light snow is falling at Klamath Falls, Oregon. Later that afternoon (Figure 4.1b), the front has sagged southward and eastward. A well-defined cyclonic circulation is evident off the coast of Oregon. The surface observations over western Nevada indicate strong southerly winds and sharply falling pressures that are associated with the development of a trough in the lee of the Sierra Mountains. Over the next 24 hours (Figure 4.1c), the baroclinic zone shifts slowly to the southeast with light rain reported at Tonopah, Nevada while the upper-level circulation located earlier off the coast of Oregon has plummeted directly southward to a position off central California. While pressures fell 6-9 mb at stations in Utah, no precipitation is found at the stations available.

Surface conditions over the 3-day period are shown for Salt Lake City (Figure 4.2a) and Reno (Figure 4.2b). The passage of a vigorous cold front is evident at Reno during the afternoon of the 9th. Winds of 40 knots and gusts to over 55 knots were observed as lee-side cyclogenesis developed that afternoon. Overnight, rain showers turned to snow and it snowed again the next evening. The widespread effects of the lee-side cyclogenesis are evident from the meteogram at Salt Lake City during the afternoon of the 9th: falling pressures, strong southerly winds, and low relative humidity. However, no significant front passed through Salt Lake City during the next 24 hours. Instead, the weather conditions reflect predominantly the combined effects of the local diurnal mountain/valley and land/lake breezes.

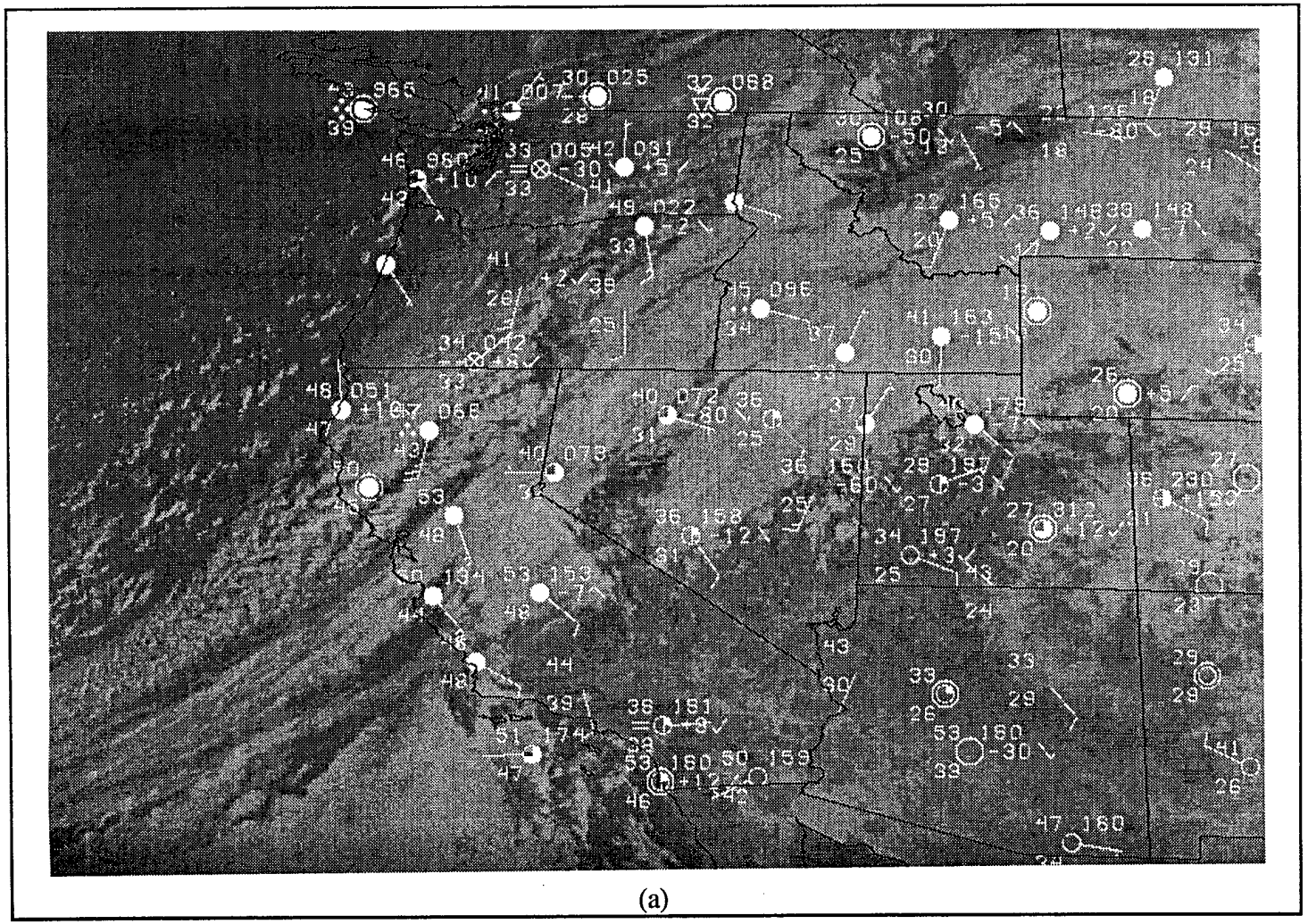

(a)

Figure 4.1. Visible satellite picture with surface observations valid at (a) 1500 UTC, November 9 1994 (b) 2200 UTC, November 9 1994 (c) 2200 UTC, November 10 1994.

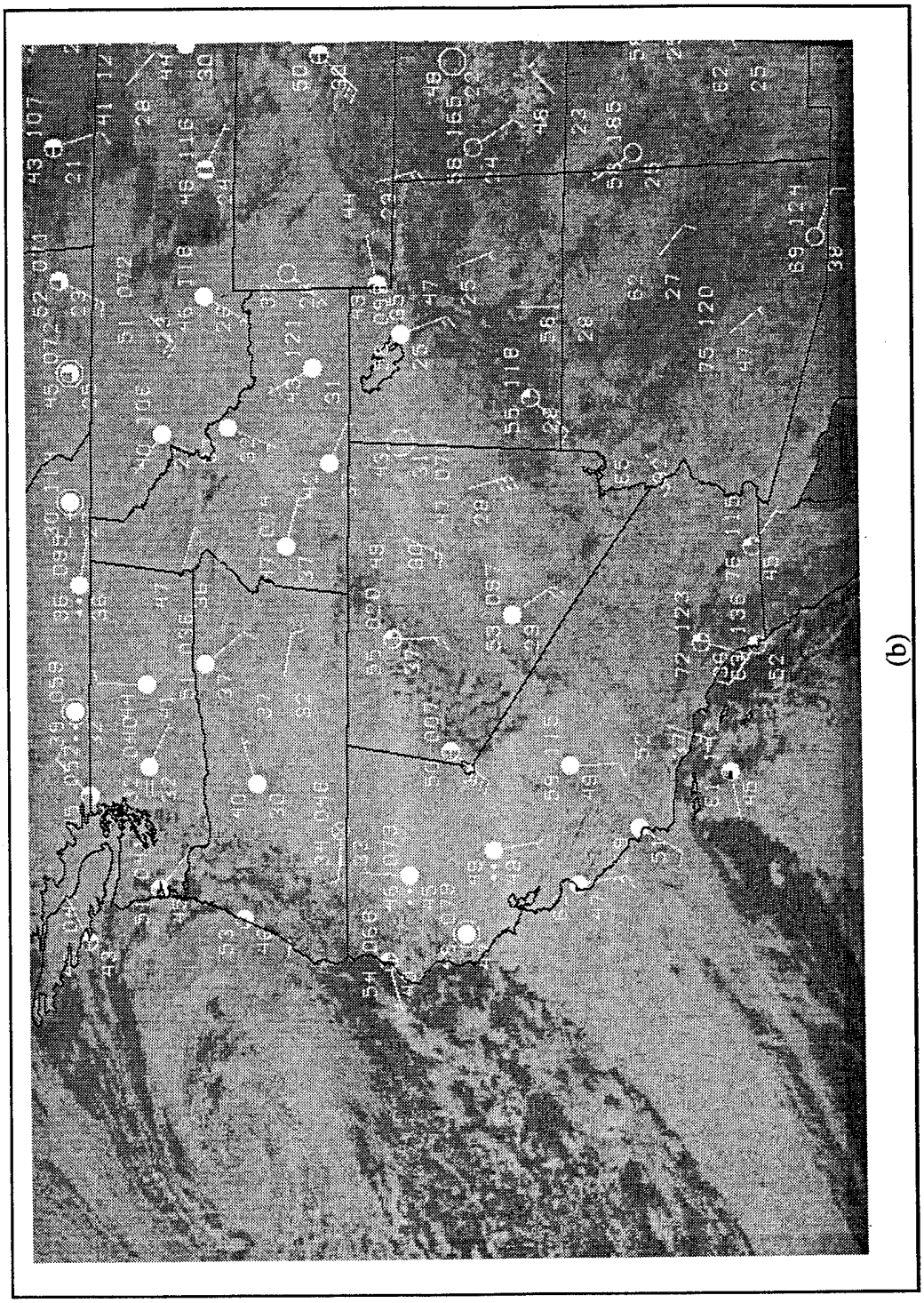

(b)

Figure 4.1. (Continued)

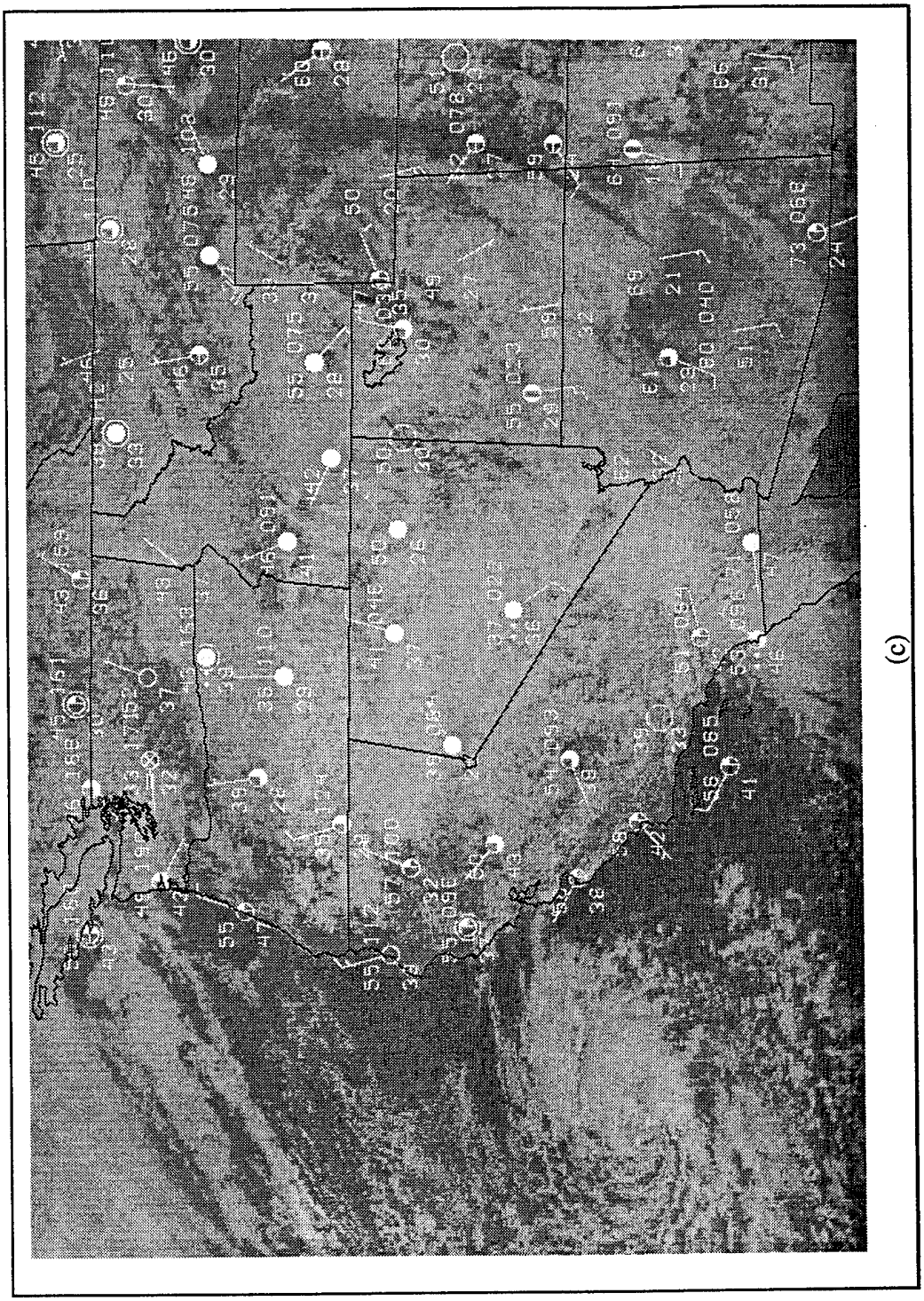

(c)

Figure 4.1. (Continued)

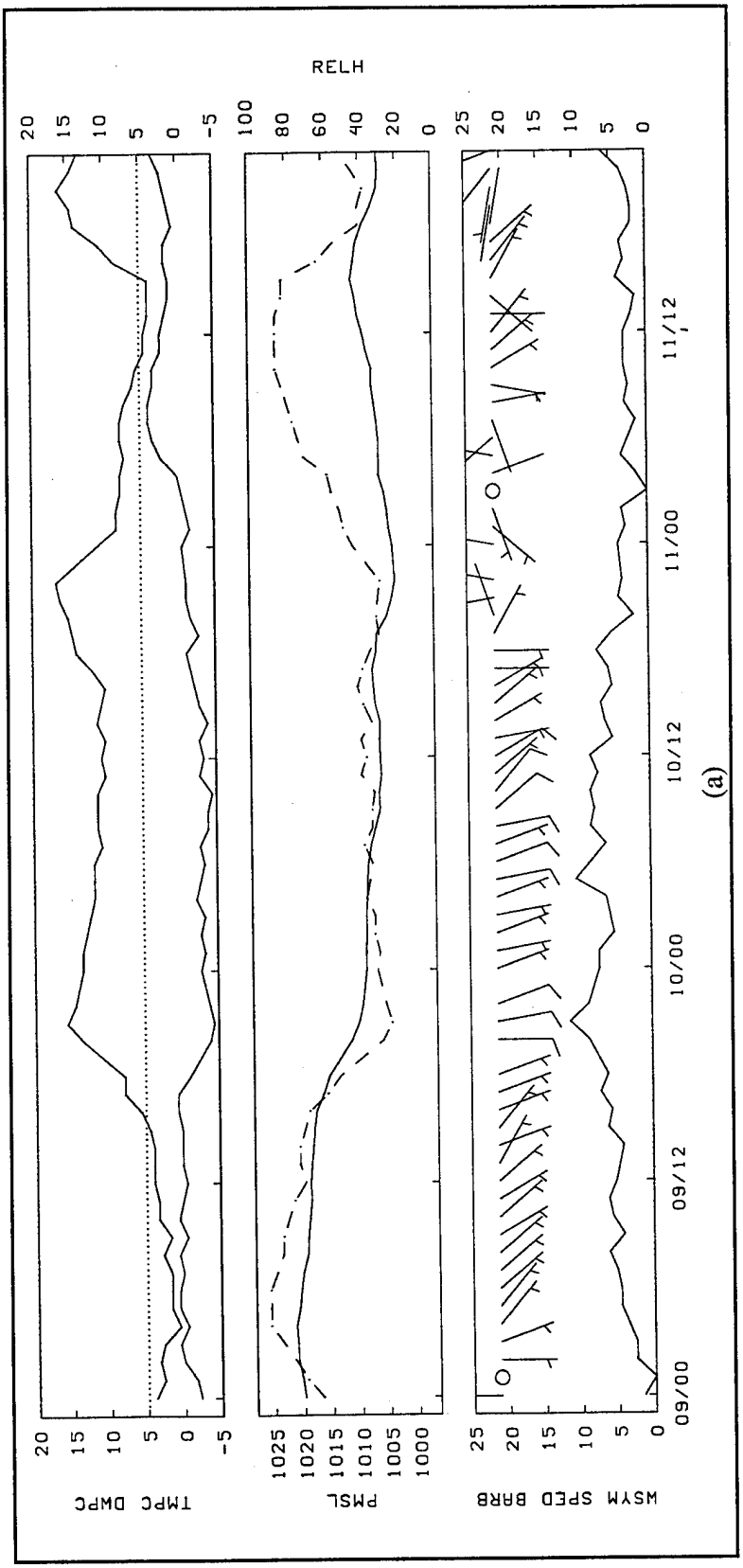

Figure 4.2. Surface conditions for (a) Salt Lake City, Utah (b) Reno, Nevada from 0000 UTC, November 9, through 2200 UTC, November 11. Temperatures are shown in the upper panel (dew point temperature is the lower solid line) in °C. Pressure (solid line) in mb and relative humidity (dash-dot line) in % are shown in the middle panel. Wind speed (barbs and solid line) in m s^{-1} is displayed in the lower panel and surface conditions are plotted along the bottom of Figure 4.2b.

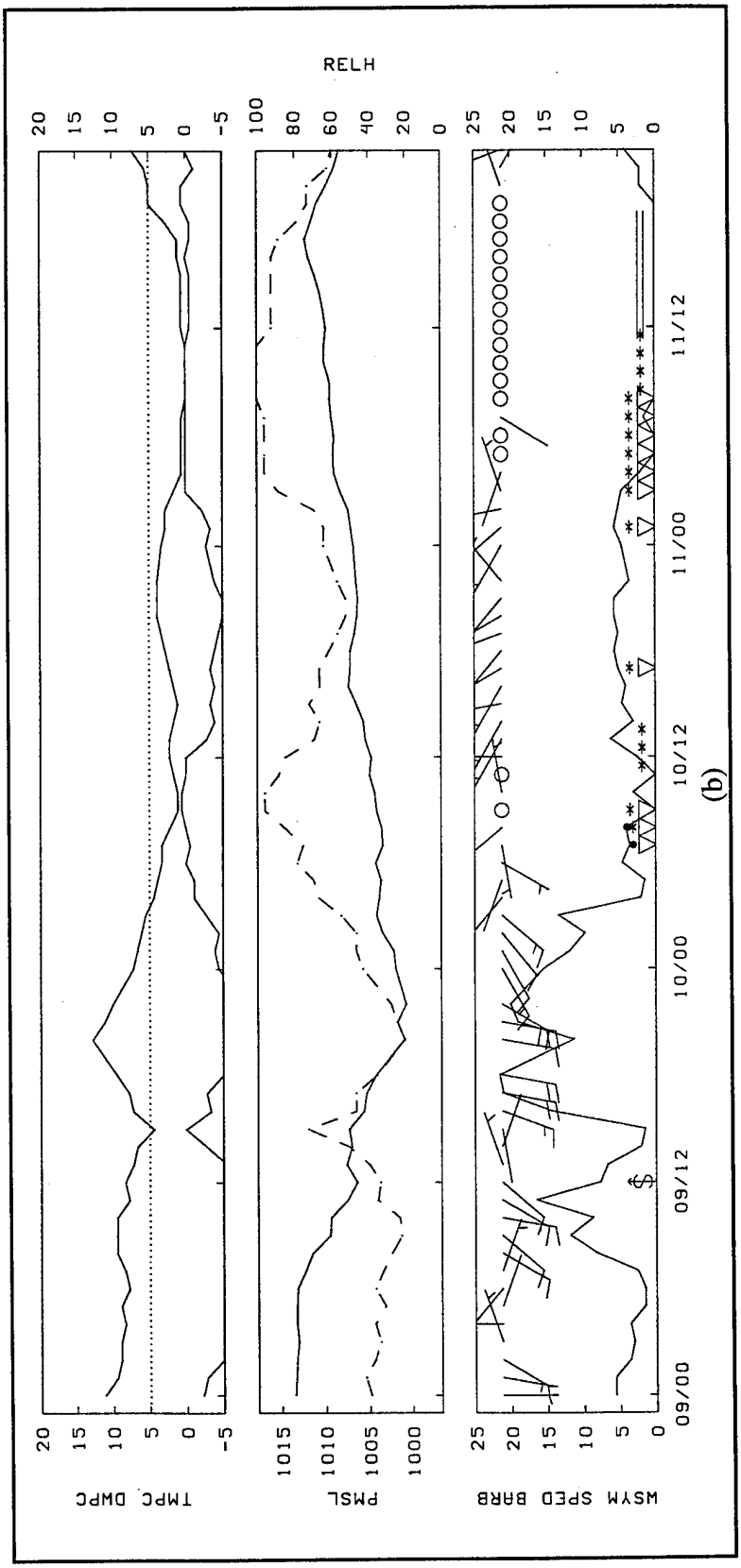

Figure 4.2. (Continued)

Potential Vorticity and Sea-Level Pressure

The upper-tropospheric potential vorticity and sea-level pressures are presented in Figure 4.3 for the analysis (Figure 4.3a), the 36-hour forecast (Figure 4.3b) and the verifying analysis (Figure 4.3c). At the initial time of the MEM model forecast, high values of potential vorticity are found off the west coast (Figure 4.3a). The development of a lee trough downwind of the Sierra Mountains is evident in the sea level pressure field. The evolution of potential vorticity and sea level pressure over the next 36 hours can be examined on-line. Here, the final distribution of these two fields are presented in Figure 4.3b. In addition, the 12-hour accumulation of precipitation forecast by the model is shaded. The lee-side trough has been forecast to move to western Utah while high values of upper tropospheric potential vorticity are centered over western Nevada. The surface low associated with the offshore circulation is forecast to move southward to a position off the coast of San Francisco. Widespread precipitation is forecast in the wake of the trough over the intermountain region.

Verification of this 36-hour forecast of sea level pressure and potential vorticity can be obtained by contrasting Figures 4.3b and 4.3c. The surface low in the intermountain region at the verification time is observed to lie over eastern Nevada. Thus, the model moved the surface trough too rapidly to the east. The surface low off the west coast is located further south than that forecast. The region of high potential vorticity observed at the verification time extends further south and exhibits more fine-scale structure than that forecast by the MEM. The greater amount of structure in the analysis field than that forecast is common in diagnostic fields such as potential vorticity and divergence. It apparently results from a combination of two factors: (1) the static analysis used at that time tends to introduce imbalances between the dynamical fields and (2) the model tends to damp fine-scale structures with time.

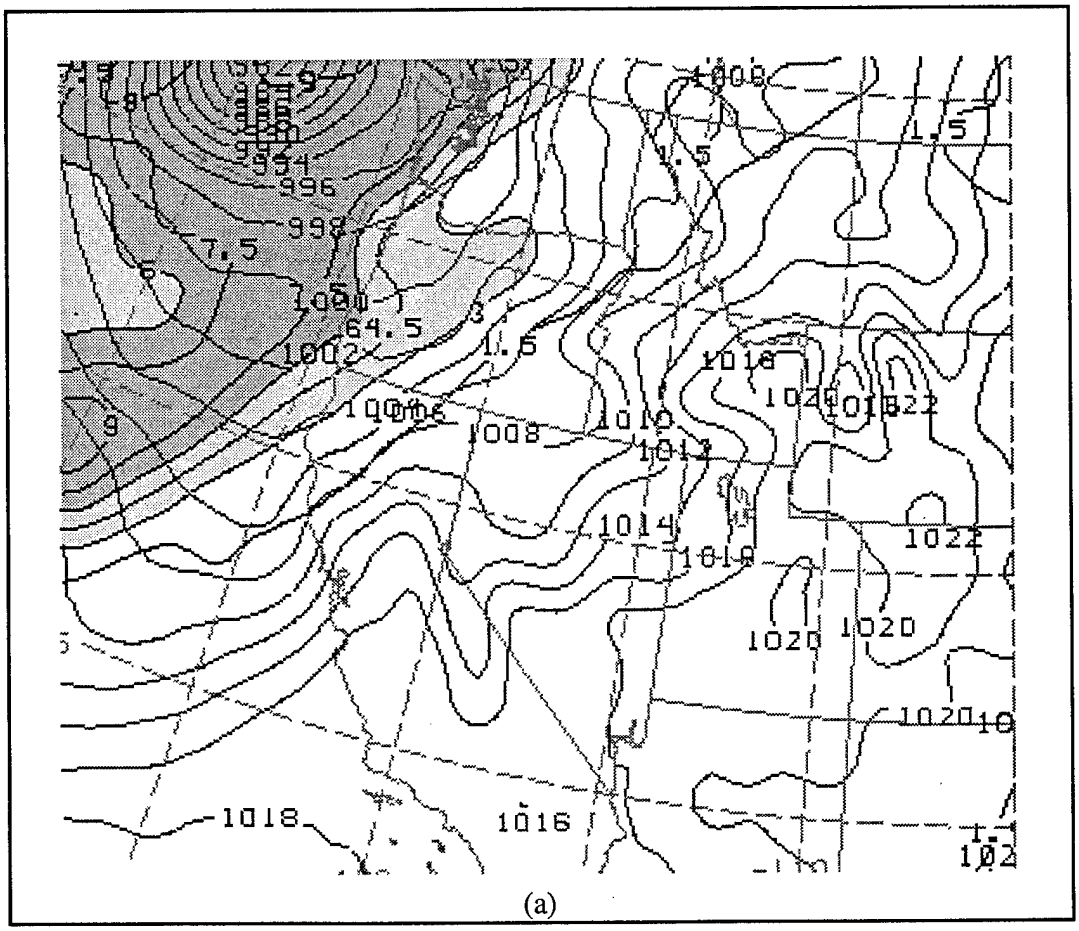

Figure 4.3. Sea level pressure and potential vorticity for (a) the analysis valid 1200 UTC, November 9 1994; (b) the 36-hour forecast valid 0000 UTC, November 11 1994; and (c) the analysis valid 0000 UTC, November 11 1994. Sea level pressure (light lines) is contoured at 2 mb intervals while potential vorticity (dark lines) is contoured at 1.5 PVU intervals (10^{-6} m^2 s^{-1} K kg^{-1}). Light (dark) shading in (a) and (c) reflects potential vorticity between 3 and 6 PVU (6-9 PVU). The 12-hour accumulated precipitation is shaded in (b); increasingly darker shading reflected precipitation amounts from 0.01 to 0.5 inches.

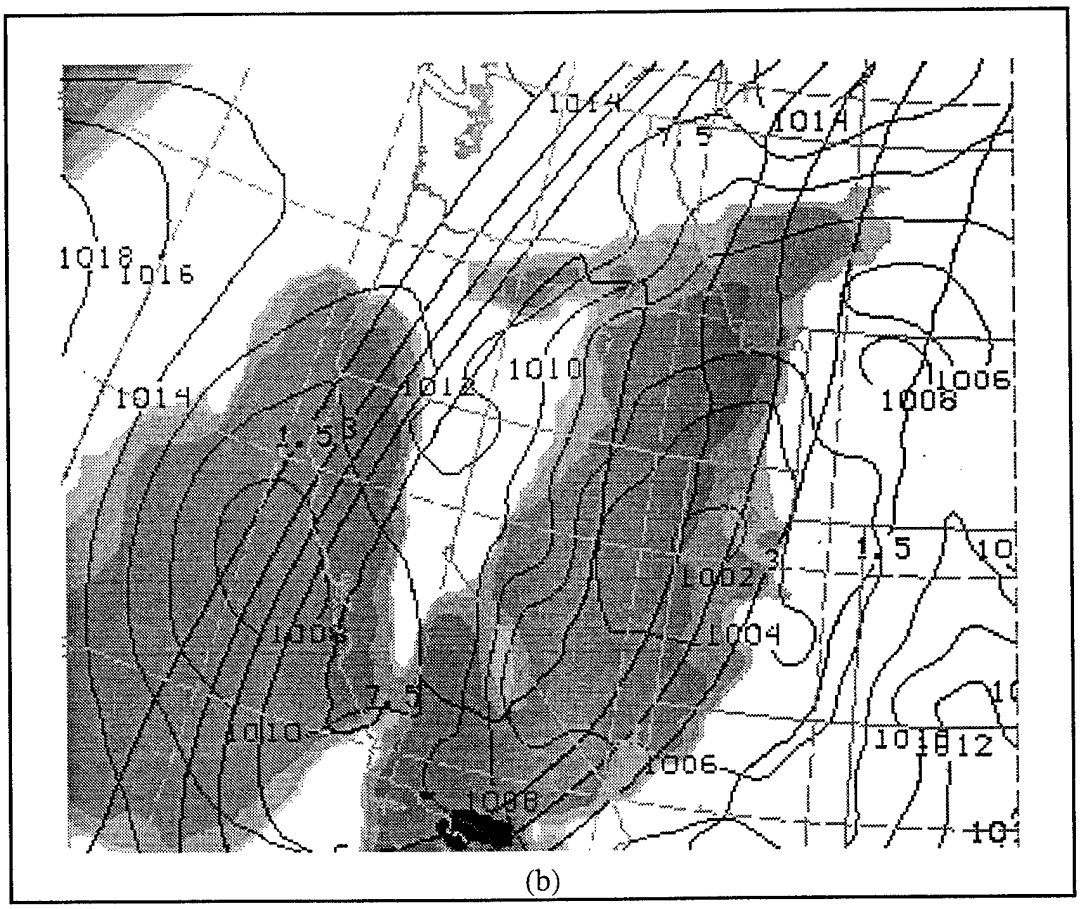

Figure 4.3. (Continued)

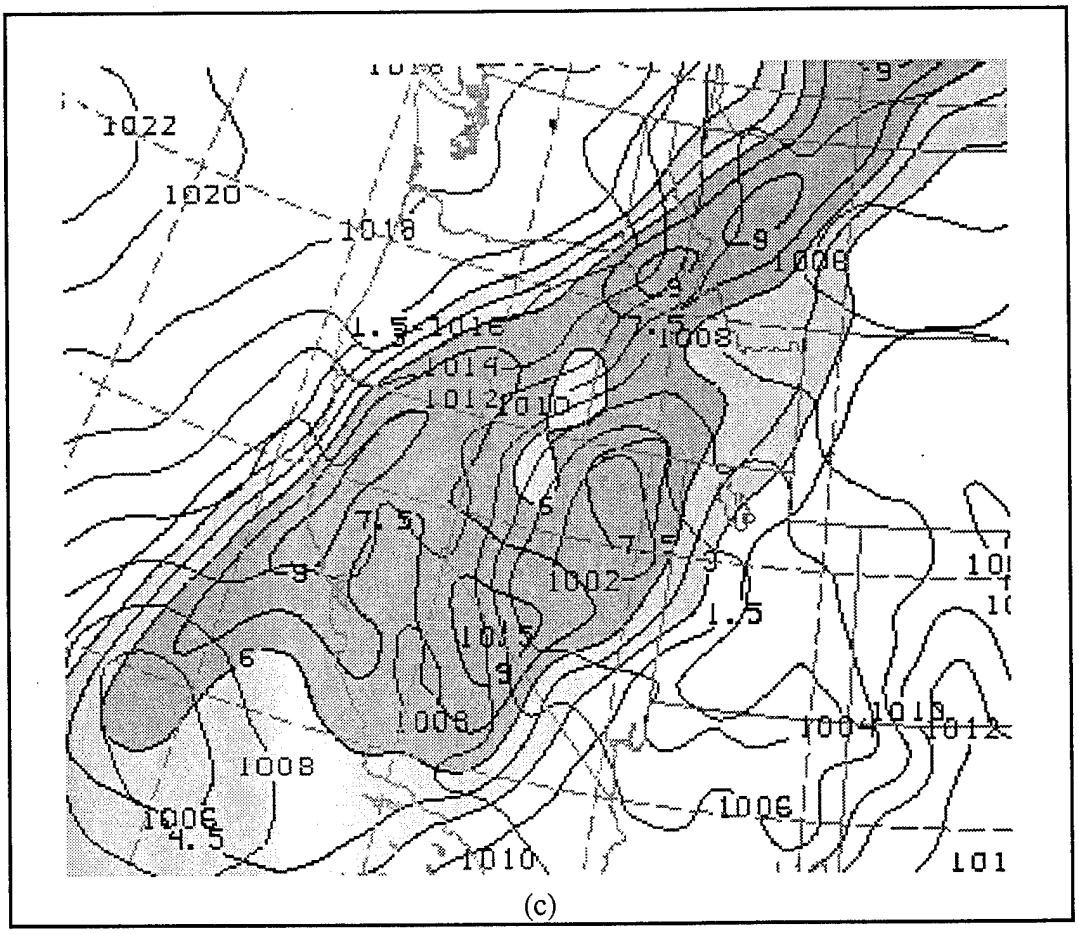

Figure 4.3. (Continued)

500 mb Geopotential Height and Absolute Vorticity

Geopotential height and absolute vorticity are displayed in Figure 4.4 for the initial analysis (Figure 4.4a), the 36-hour forecast (Figure 4.4b), and the verifying analysis (Figure 4.4c). Overall, the forecast is quite good with vorticity centers located on the western and southeastern flank of the synoptic-scale trough. However, as was evident in the distribution of upper-tropospheric potential vorticity, the model moved the trough along the coast too far to the east and not far enough south. Subjective evaluation of the Early Eta Model has led many forecasters in the western United States to suggest that the Eta model digs troughs too much; in this case, the model did not dig the system enough.

300 mb Wind and Divergence Fields

Vector wind and divergence at the 300 mb level are shown at the initial time (Figure 4.5a), the 36-hour forecast (Figure 4.5b), and the verifying analysis (Figure 4.5c). The jet near the west coast at the initial time is positively tilted. As mentioned with respect to the potential vorticity field, the divergence field has considerable fine-scale structure that appears to be overdone. This jet is forecast to move inland through the forecast period while another jet develops on the western flank of the upper tropospheric trough. By the 36 hour forecast, the jet and associated divergence lie over Utah. The progression of the jet on the eastern side of the trough was forecast quite well. However, larger errors are evident on the western flank of the trough where the western jet was underforecast by a significant amount, on the order of 20 m s^{-1}.

700 mb Temperature and Relative Humidity

Figure 4.6 shows the 700 mb temperature, wind, and relative humidity at the initial time (Figure 4.6a), the 36-hour forecast (Figure 4.6b), and the verifying analysis (Figure 4.6c). The initial baroclinic zone (Figure 4.6a) is evident over northern California with high relative humidity in a broad band. Significant warm air advection is forecast over Utah and

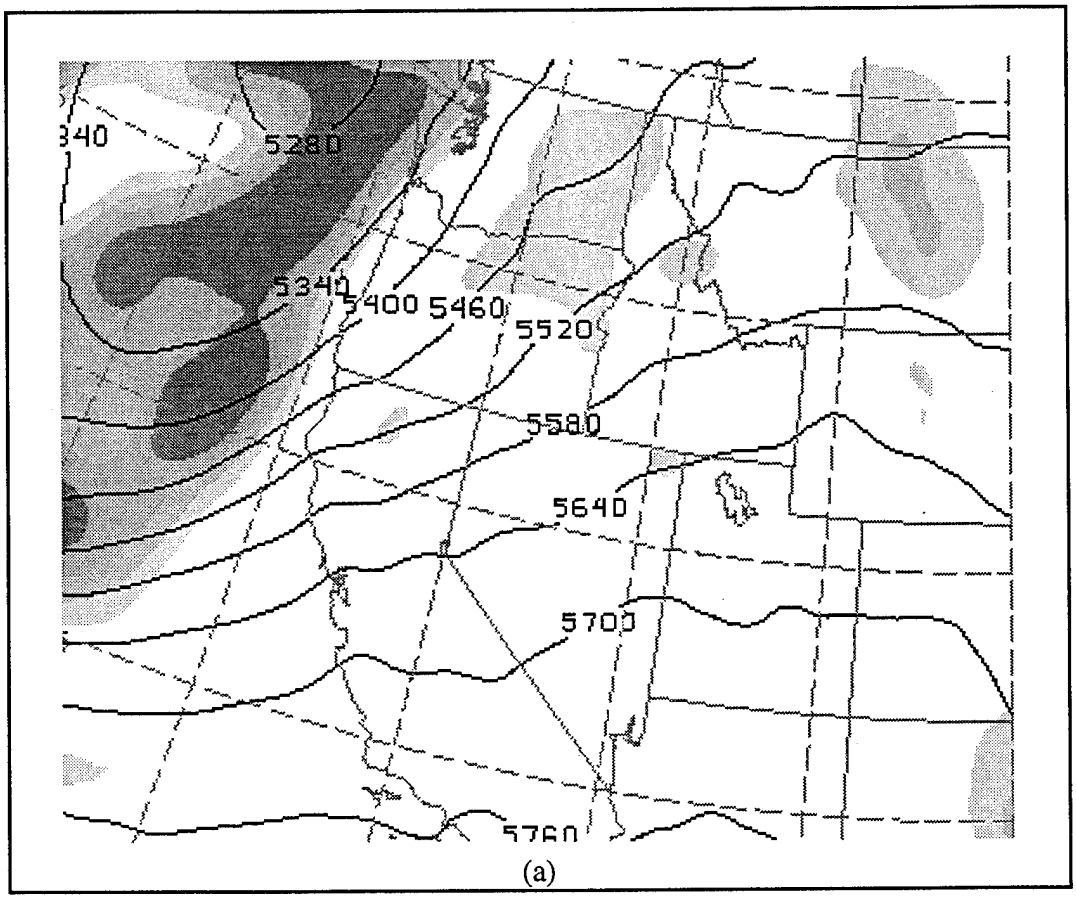

Figure 4.4. 500 mb geopotential height and absolute vorticity (a) analysis valid 1200 UTC, November 9 1994; (b) 36-hour forecast valid 0000 UTC, November 11 1994; and (c) analysis valid 0000 UTC, November 11 1994. Height contours are in meters. Increasingly darker shading reflects increasing values of absolute vorticity from 12 x 10^{-5} s^{-1} to 24 x 10^{-5} s^{-1} at intervals of 4 x 10^{-5} s^{-1}.

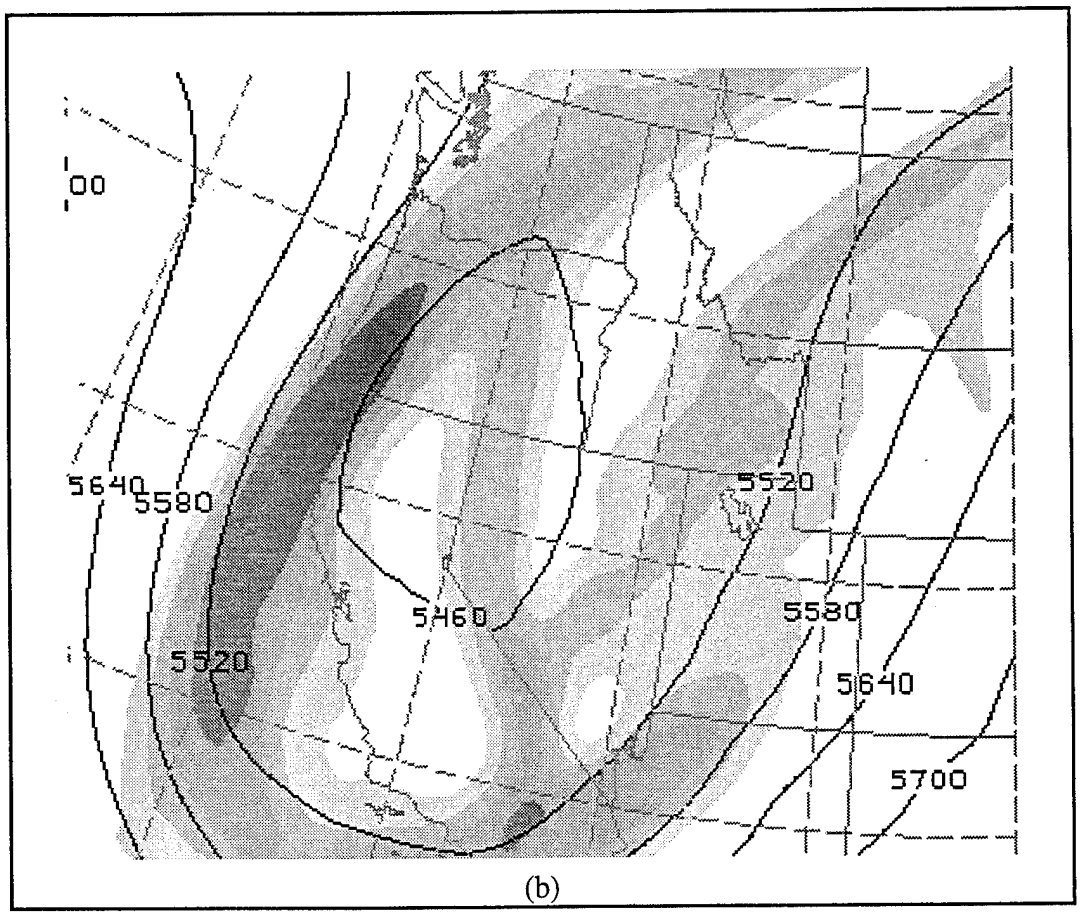

(b)

Figure 4.4. (Continued)

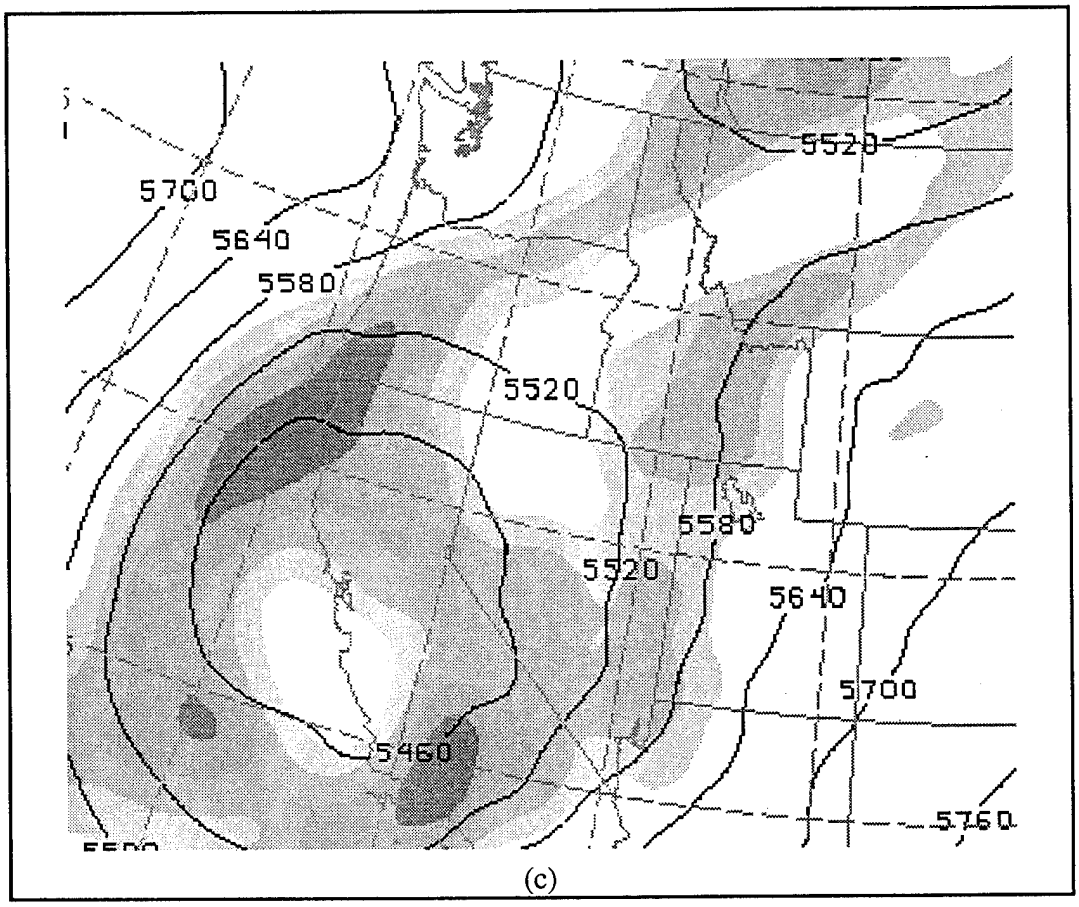

Figure 4.4. (Continued)

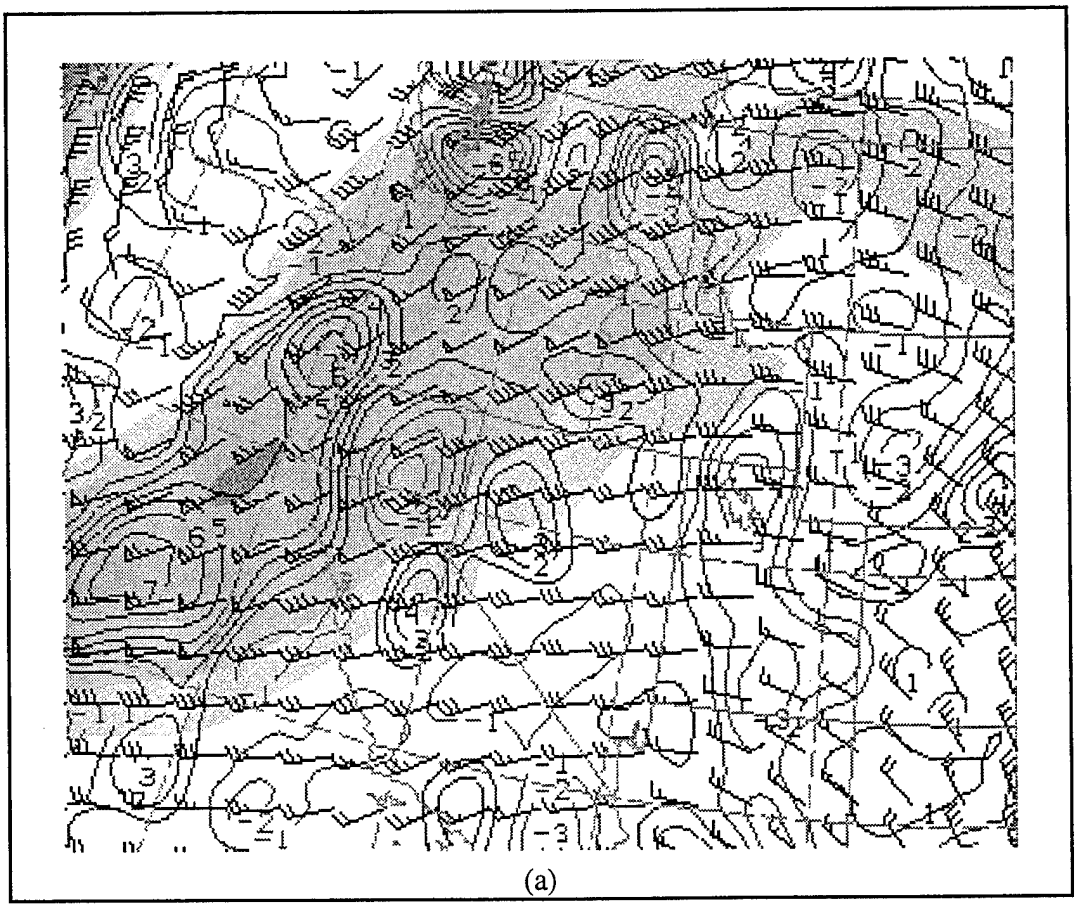

(a)

Figure 4.5. 300 mb wind and divergence (a) analysis valid 1200 UTC, November 9 1994; (b) 36-hour forecast valid 0000 UTC, November 11 1994; and (c) analysis valid 0000 UTC, November 11 1994. The contours show divergence in units of 10^{-5} s^{-1} (negative values denote convergence). The wind barbs show winds in units of m s^{-1}. Increasingly darker shading reflect wind speeds ranging from 35 m s^{-1} to 65 m s^{-1} in steps of 10 m s^{-1}.

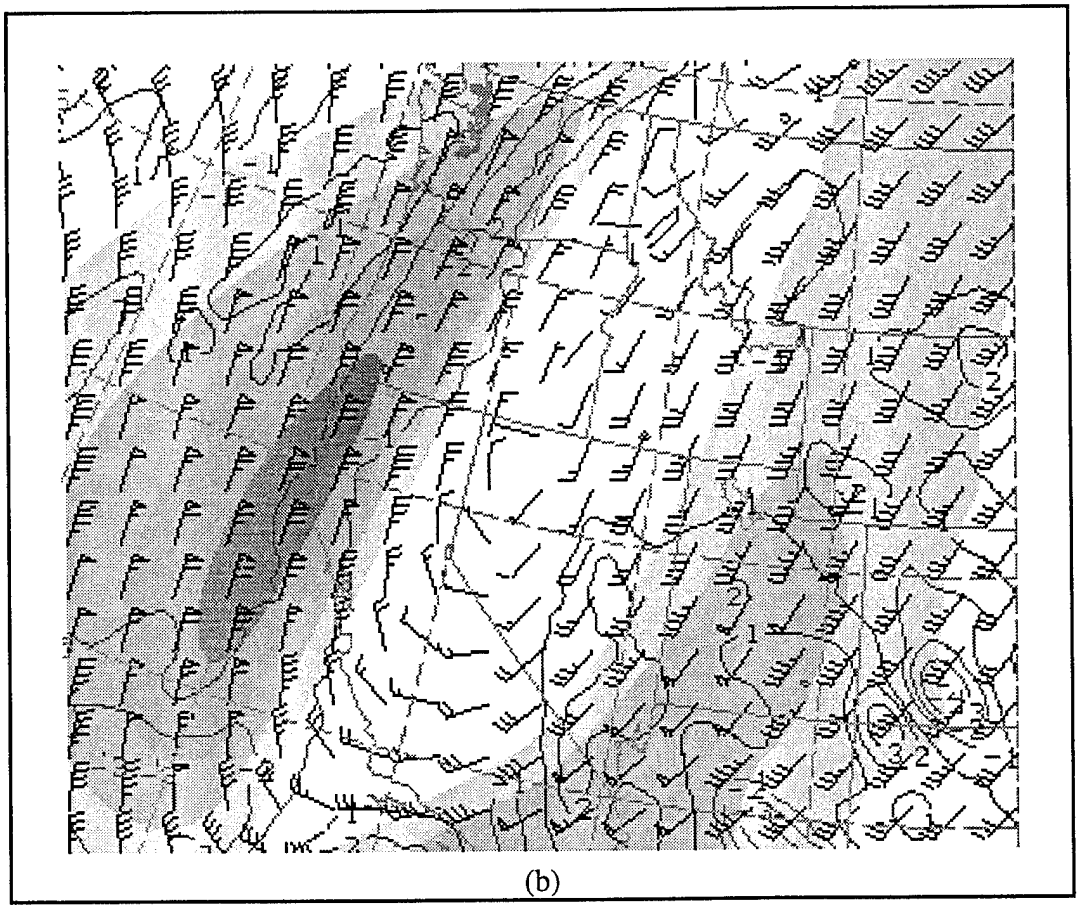

(b)

Figure 4.5. (Continued)

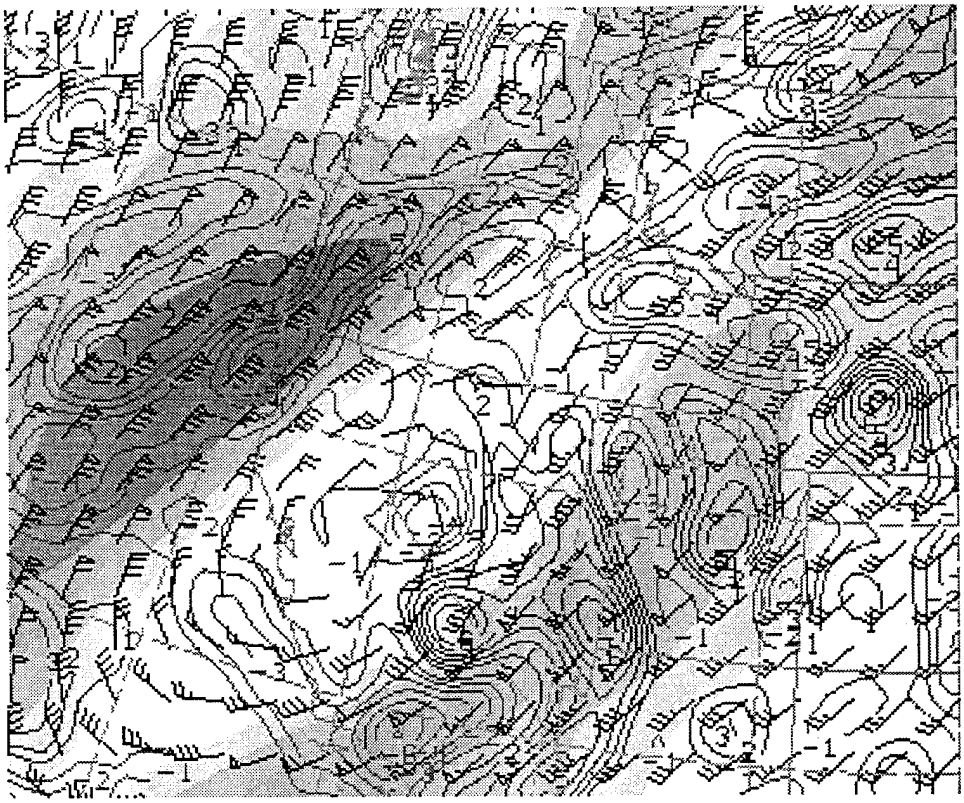

(c)

Figure 4.5. (Continued)

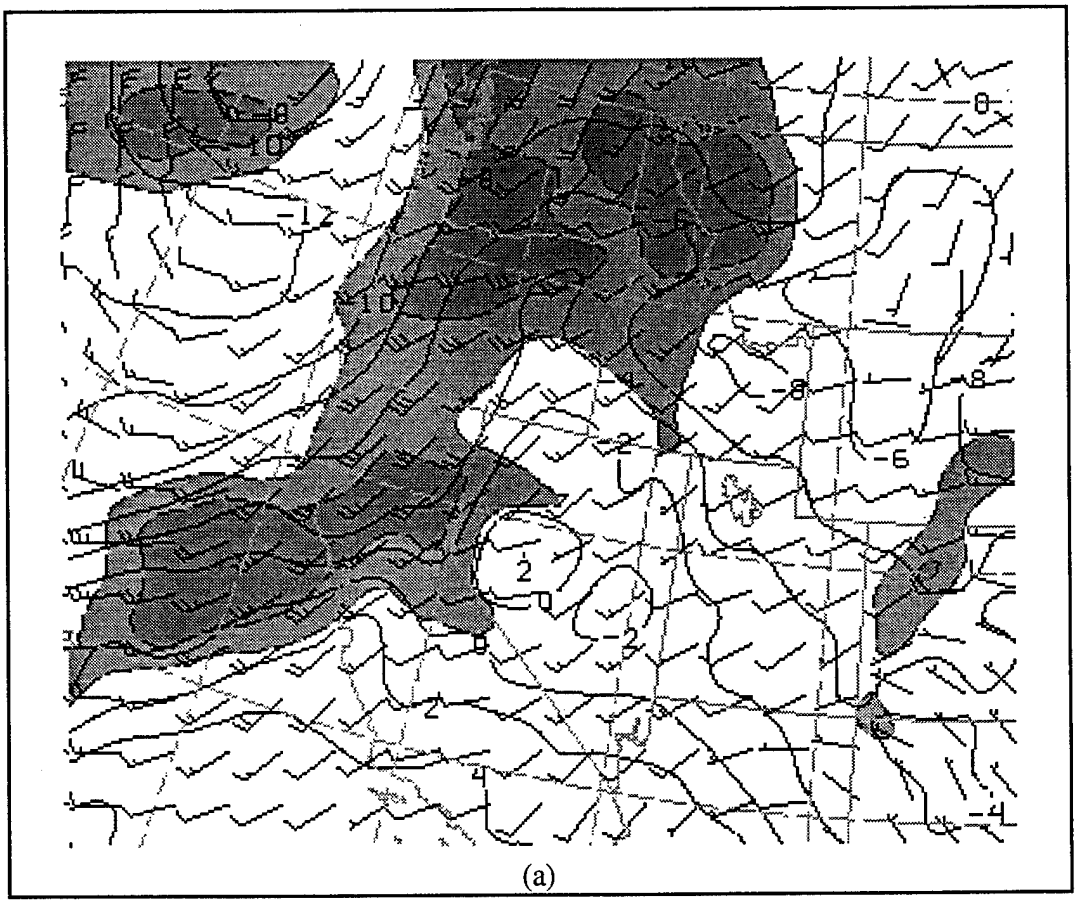

Figure 4.6. 700 mb temperature, wind, and relative humidity (a) analysis valid 1200 UTC, November 9 1994; (b) 36-hour forecast valid 0000 UTC, November 11 1994; and (c) analysis valid 0000 UTC, November 11 1994. Wind barbs are plotted in m s^{-1}. Isotherms are in °C plotted at 2°C intervals. Relative humidity is shaded: light (dark) shading denotes relative humidity between 70% and 90% (greater than 90%).

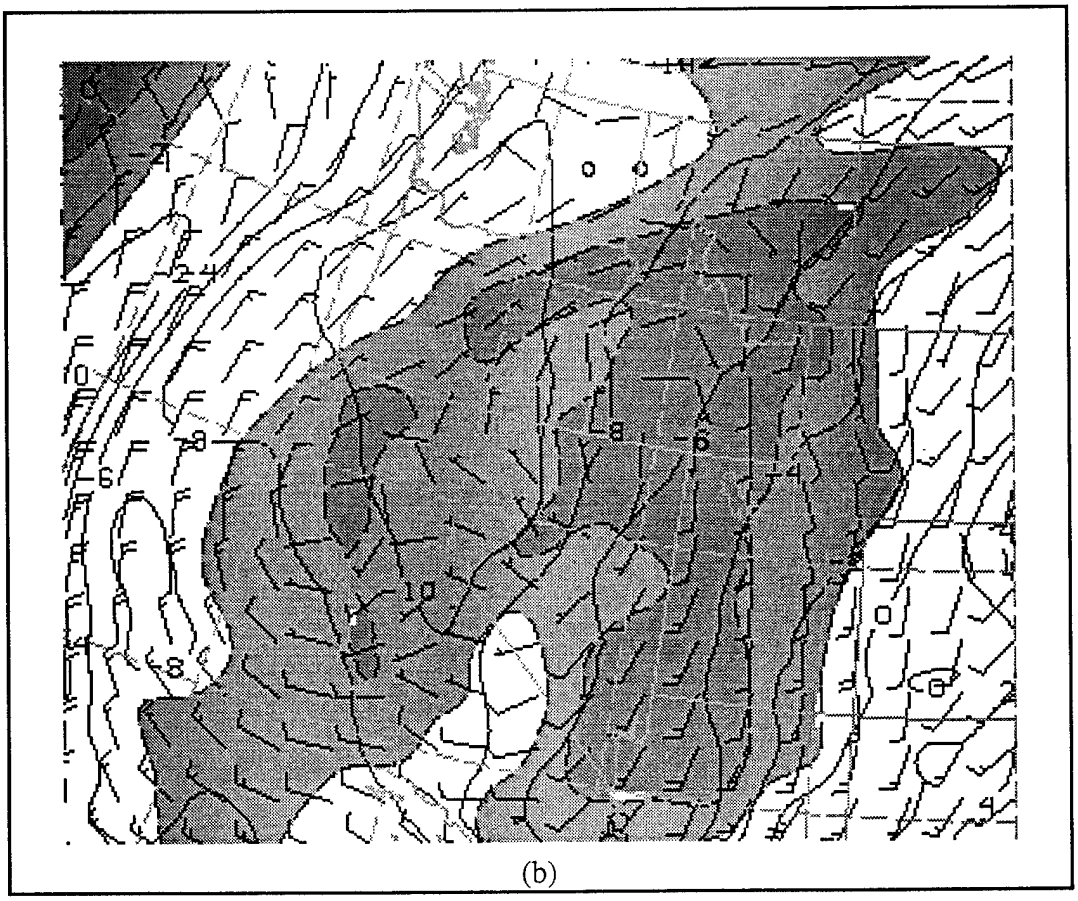

(b)

Figure 4.6. (Continued)

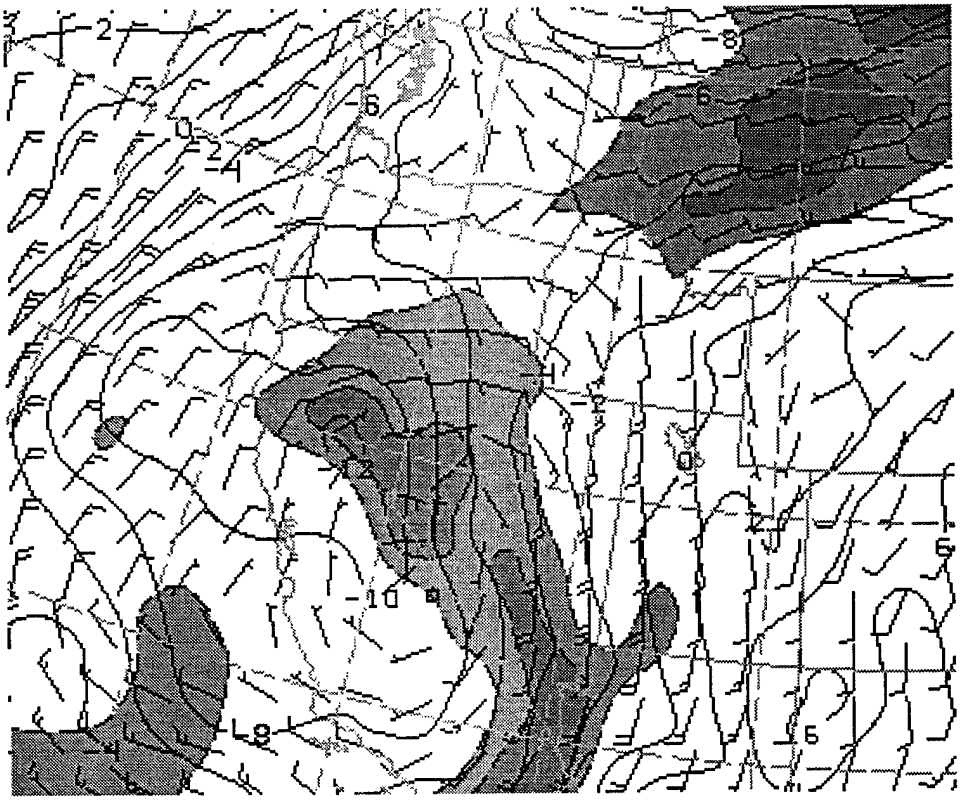

(c)

Figure 4.6. (Continued)

the model forecasts that the 700 mb temperature should rise from -4°C to 0°C at Salt Lake City by 0000 UTC 10 November. The actual temperature at that time at Salt Lake was 2°C; thus, the warm air advection associated with the developing trough over the intermountain region was underforecast. However, over the next 24 hours, the MEM predicted that 700 mb temperatures should drop sharply reaching -5°C at Salt Lake after 36 hours (Figure 4.6b). The observed temperature at that time was 1°C and analyzed by the MEM analysis to a value close to that (Figure 4.6c). Clouds inferred from the 700 mb relative humidity at 36 hours to cover much of the West. However, as already seen in the satellite photo valid near this time (Figure 4.1c) and the analysis in Figure 4.6c, the area of cloudiness is restricted in the lower troposphere to a well-defined band stretching from northern California to Arizona.

The temperature error for Salt Lake City is shown in Figure 4.7a, and the dew point temperature errors in Figure 4.7b. Notice the 1200 UTC, November 9 1994, 24- and 36-hour forecasts are greater than 5°C colder than actually observed. Contrast this with the 36-hour forecast shown in Figure 4.6b valid at 0000 UTC, November 11 1994. This agrees with the MEM's own analysis valid at 0000 UTC, November 11 1994 as shown in Figure 4.6c. Additionally, notice that the 36-hour forecast (Figure 4.6b) shows that the relative humidity exceeds 90% over SLC, whereas the analysis for the same time (Figure 4.6c) is much less.

Summary

Several aspects of the MEM forecast in this case study are good. The rotation of short waves within the developing and southward moving synoptic-scale trough is handled quite well. As a final summary of the principal results of this chapter, Figure 4.8 presents cross-sections along 40°N of potential vorticity, wind speed, and relative humidity. The 36-hour forecast (Figure 4.8a) shows a clear tropopause fold on the western flank of the trough with a strong jet on its flank. The detailed structure of the tropopause fold is an

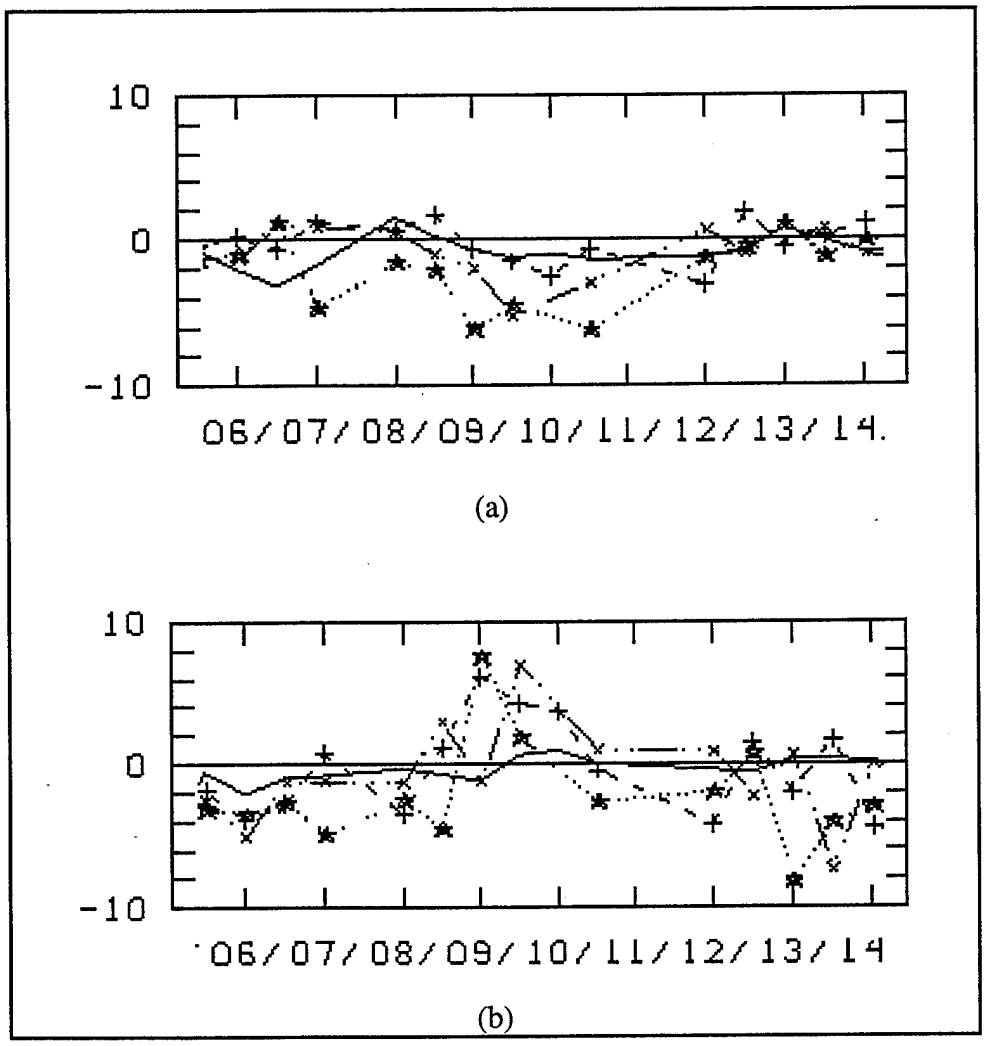

Figure 4.7. Time series of (a) 700 mb temperature error (forecast minus observed) and (b) 700 mb dew point temperature error at Salt Lake City. The solid line, dashed line, dash-dot line and dotted line represent the 00-, 12-, 24- and 36-hour forecasts, respectively. The scale on the left is in units of °C.

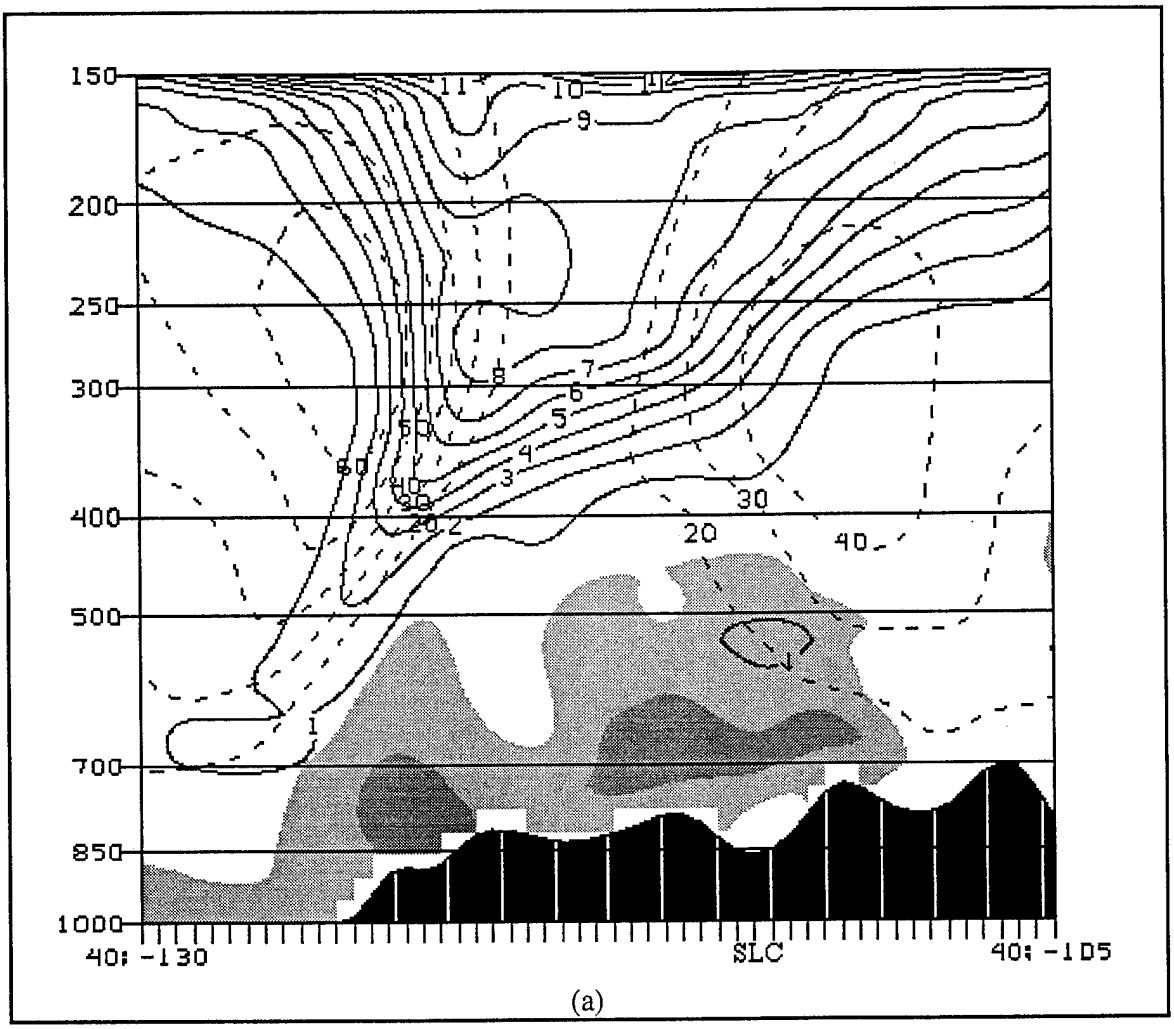

Figure 4.8. Vertical cross section along 40°N of potential vorticity, wind speed and relative humidity for (a) the 36-hour forecast and (b) the analysis valid at 0000 UTC, November 11 1994. The dashed contours denote wind speed in m s^{-1} that are plotted in 20 m s^{-1} intervals. Solid contours denote potential vorticity at intervals of 1 PVU (10^{-6} m^2 s^{-1} K kg^{-1}).

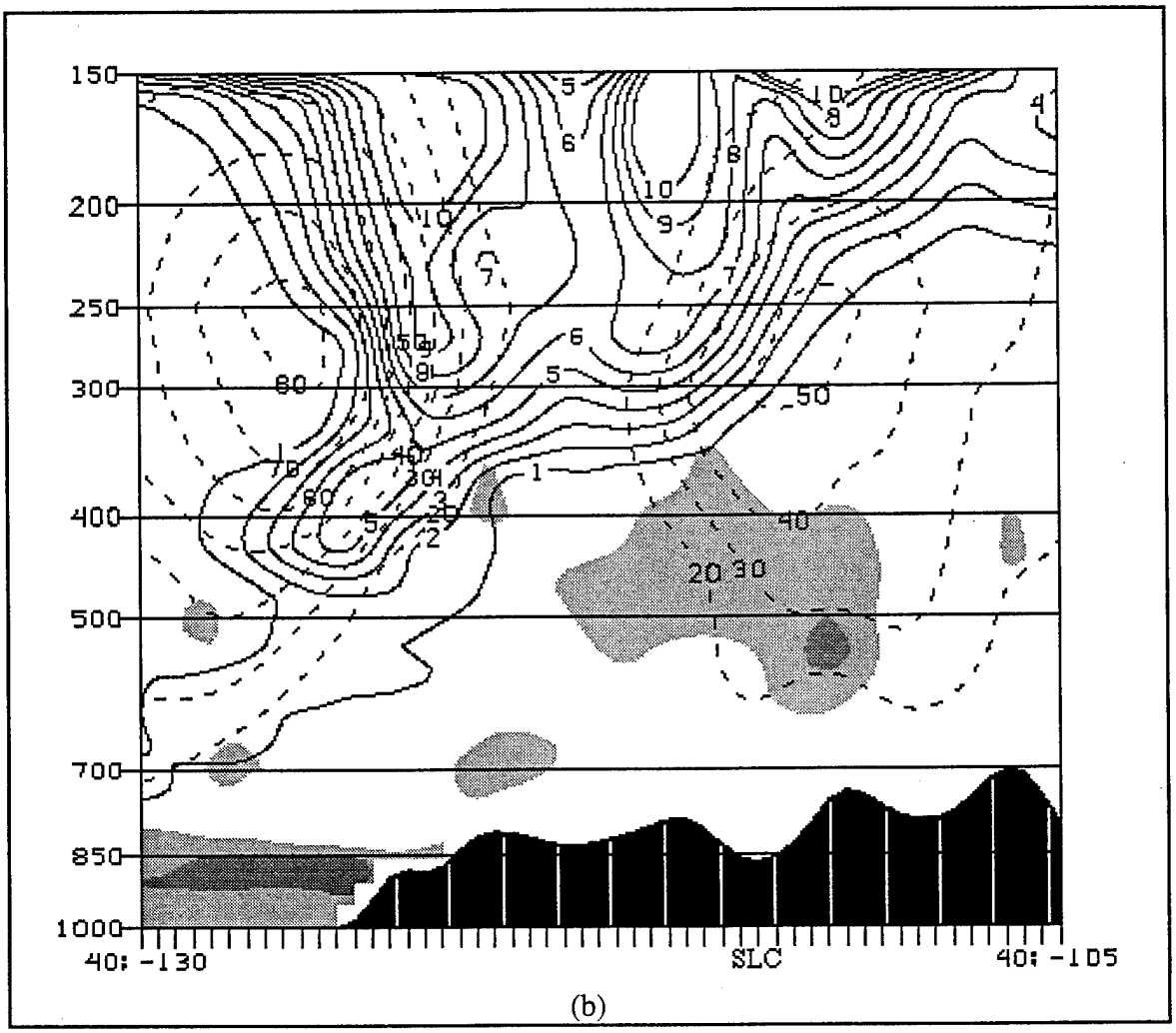

Figure 4.8. (Continued)

example of the utility of the MEM to forecast meso-α scale weather features. This fold is not evident in the output from the other operational models (not shown). A weaker jet in the upper troposphere with less tropopause folding is evident on the eastern flank. High relative humidity in the lower troposphere (and precipitation) is associated with each of the induced baroclinic zones.

In the corresponding verifying analysis (Figure 4.8b), the pool of high potential vorticity has more structure than that found in the forecast. The tropopause fold on the western flank is accentuated with higher values at 400 mb and a stronger associated jet. A stronger jet in the upper troposphere is analyzed by the MEM on the eastern flank than that forecast. However, the induced baroclinic zone in the lower troposphere is weaker with less vertical motion and lower relative humidity. Operationally, these errors would have a significant negative impact on forecast decisions at the time that the forecasts became available since the model guidance of lower tropospheric temperature and moisture fields is relied on heavily.

CHAPTER 5

CUMULATIVE STATISTICS

A major goal of this study is to provide a baseline of the MEM's performance over a large sample of model forecasts. The focus here is on the model's skill at predicting dynamical and thermodynamical variables in the free atmosphere. In addition, the distribution of precipitation accumulated over months or seasons will be examined as a function of forecast duration.

This baseline also serves as a means to evaluate later the impact of the model enhancements to be implemented during May 1995. As mentioned before in Chapter 2, most of these planned enhancements affect the model's treatment of surface and boundary layer processes. Thus, the evaluation of the model's skill in the free atmosphere should remain relevant even after the MEM becomes operational.

Typical Average and RMS Errors

The statistics of the MEM's forecast skill can be evaluated in many ways. One approach is to consider the information available on-line through the page **http://www.met.utah.edu/html/meso/meso_error.html**. As a means to summarize a major portion of this information, Tables 5.1 and 5.2 present 'typical' average errors and RMS errors respectively for selected variables as a function of forecast duration and season. Typical refers here to values that reflect the average and RMS errors independent of location over the western United States. They are based on an evaluation of the MEM forecast skill with respect to its own later analyses, RUC analyses, and rawinsonde observations.

Table 5.1. Typical average errors for selected variables as a function of forecast duration and season. Fall 94 refers to the period October-December 1994 while Wtr 95 refers to the period January-March 1995.

	Fall 94			Wtr 95		
Variable/ Forecast Duration	12 hour	24 hour	36 hour	12 hour	24 hour	36 hour
300 mb wind speed (m s^{-1})	0	-1	-2	0	-1	-1
500 mb height (m)	0	0	0	0	4	8
700 mb temperature (^{o}C)	-.5	-1.0	-1.5	0	-.5	-1.0
700 mb dew point temp.(^{o}C)	0	-0.1	-0.1	-0.2	-0.4	-0.3
700 mb relative humidity (%)	0	-1	-2	0	0	1

Table 5.2. Typical RMS error for selected variables as a function of forecast duration and season. Fall 94 refers to the period October-December 1994 while Wtr 95 refers to the period January-March 1995.

	Fall 94			Wtr 95		
Variable/ Forecast Duration	12 hour	24 hour	36 hour	12 hour	24 hour	36 hour
300 mb wind speed (m s^{-1})	5	8	10	5	7	9
500 mb height (m)	14	22	30	14	22	30
700 mb temperature (^{o}C)	1.0	1.5	2.5	1.0	1.5	2.0
700 mb dew point temp.(^{o}C)	5.8	5.7	6.2	4.8	5.2	5.7
700 mb relative humidity (%)	17	19	22	18	19	21

According to the values presented in Table 5.1, the average errors of 300 mb wind speed and 500 mb height are quite small during both seasons. Thus, the model exhibits little bias in these fields for forecast lengths up to 36 hours. An increasing cold bias at 700 mb as a function of forecast duration is evident in Table 5.1, however. This cold bias in the lower troposphere will be examined in greater detail in the next section. The dew point temperature and relative humidity biases are minimal when considered over the western United States.

Typical RMS errors over the western United States after 36 hours are on the order of 10 m s^{-1} for 300 mb wind speed, 30 m for 500 mb geopotential height, and 2 ^{o}C for 700 mb temperature. These values are consistent with other operational models' performance, such as the NGM, for the entire continental United States as reported in the NMC Seasonal Performance Summary for earlier years. It is interesting to note that while the 700 mb dew point temperature and relative humidity average errors are small (Table 5.1), the corresponding RMS errors (Table 5.2) are quite large indicating frequent poor forecasts of moisture. The values for the 12-, 24- and 36-hour forecasts are similar and are independent of forecast duration. However, as will be shown later, the typical RMS error between the model's analyses and observed soundings is much smaller. Thus, these large errors are not necessarily a reflection of the methodology used here to evaluate them.

The spatial distribution of the average and RMS errors can be viewed on-line for each variable as a function of month and season. This distribution of 300 mb wind speed and 500 mb geopotential height error fluctuate somewhat as a function of the changes from month-to-month in the mean position of the jet stream or ridge/trough axes. The spatial distribution of the average and RMS errors in the 700 mb temperature field of the MEM forecast verified against its own later analyses for the Fall 1994 and Winter 1995 seasons are shown in Figure 5.1. The verification with respect to the RUC analyses is quite similar to that shown here. The largest cold bias is evident in the Fall over the high terrain of the Rocky Mountains (Figure 5.1a) and the largest RMS errors are also evident during the Fall

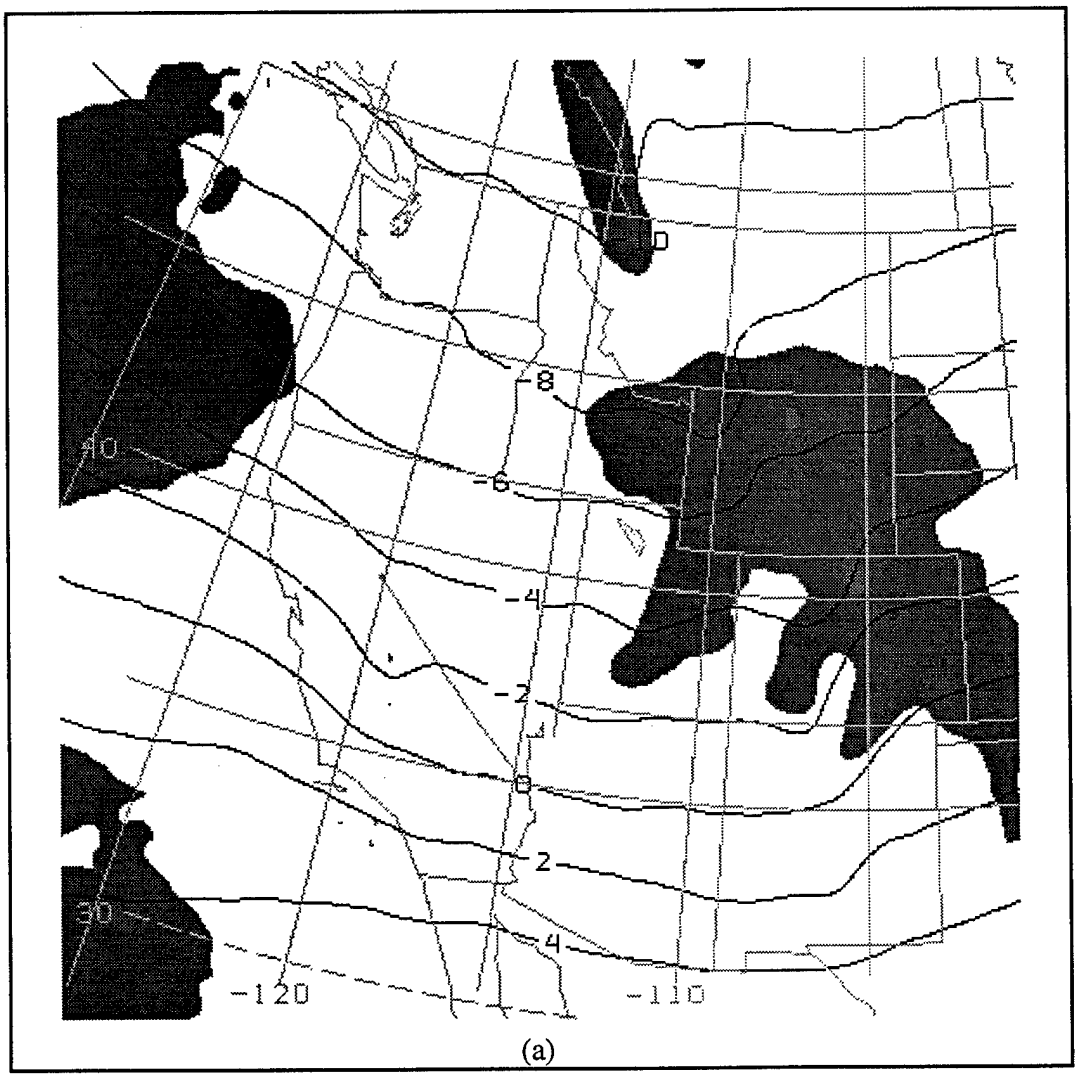

Figure 5.1. 700 mb temperature (a) average error during Fall 1994; (b) average error during Winter 1995; (c) RMS error during Fall 1994; (d) RMS error during Winter 1995 for 36-hour forecasts superimposed on the mean 700 mb temperature field, contoured at 2°C intervals. For (a) and (b), the light (dark) shading denotes average errors less than -1°C (-2°C). For (c) and (d), the shading denotes RMS errors of 1°C, 2°C and 3°C (light to dark).

Figure 5.1. (Continued)

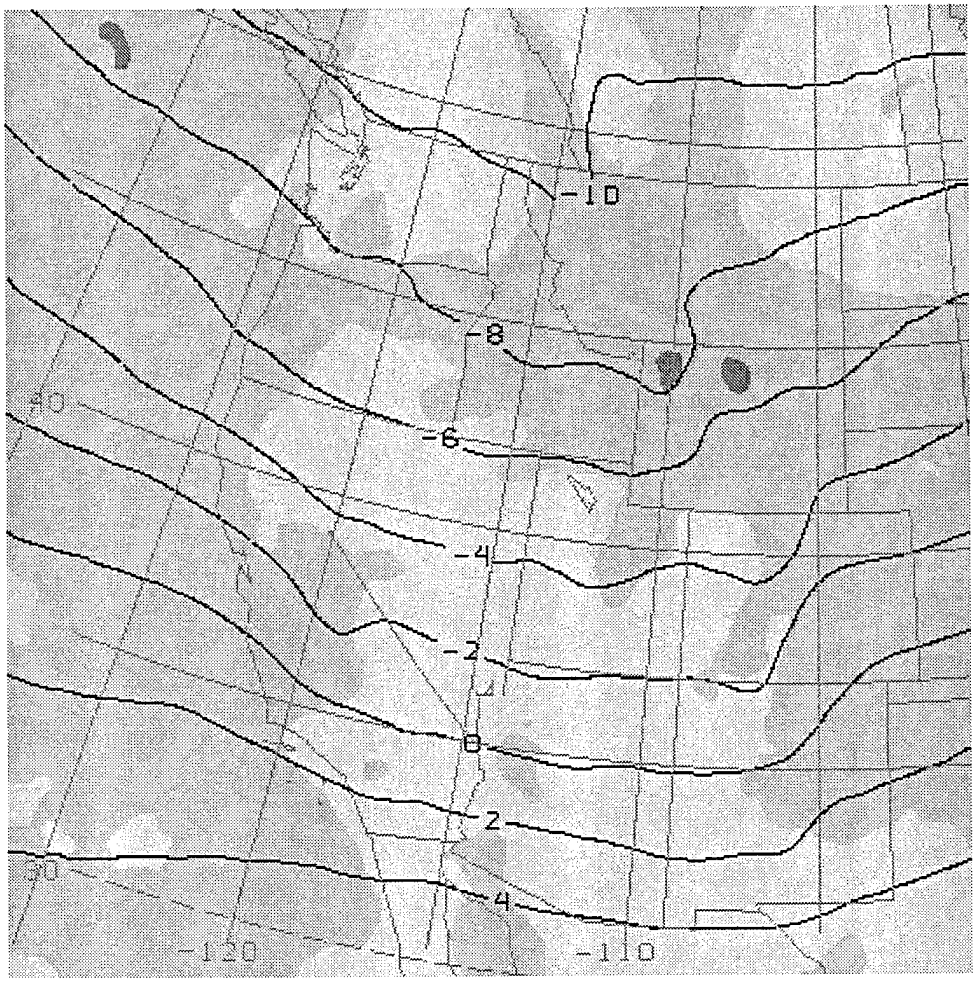

(c)

Figure 5.1. (Continued)

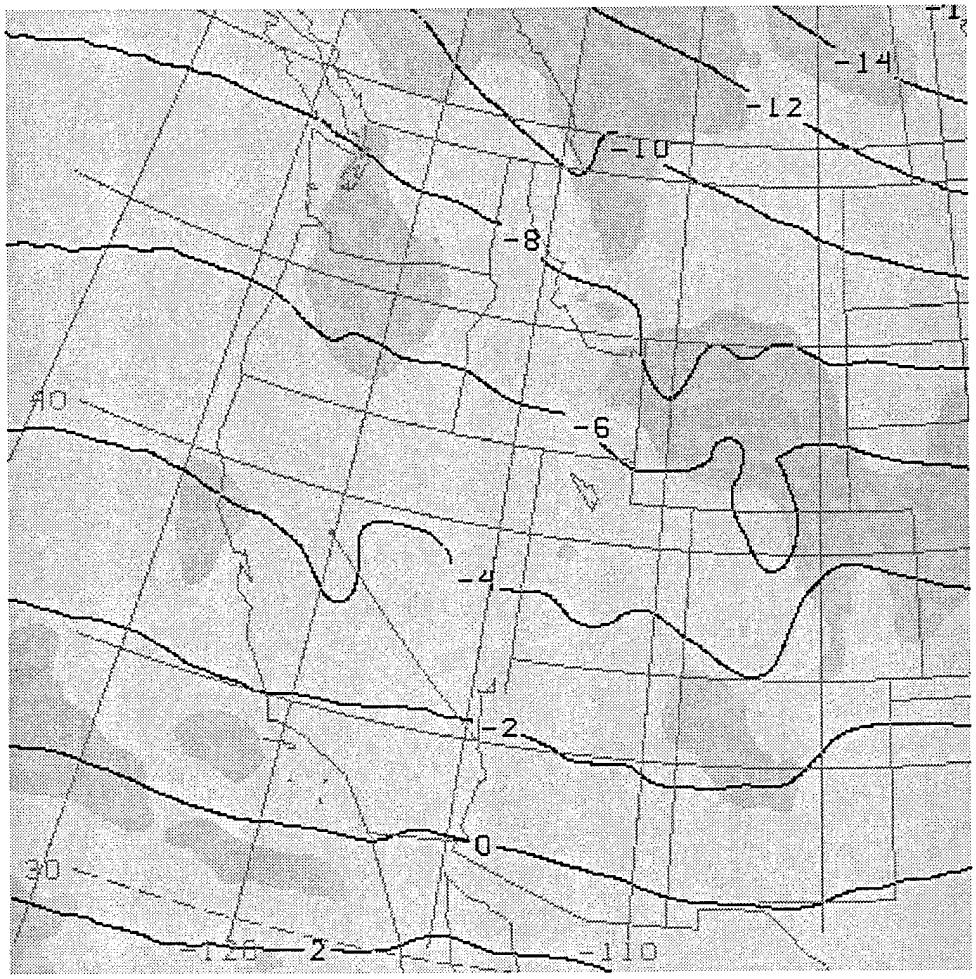

(d)

Figure 5.1. (Continued)

in that same region (Figure 5.1c). The errors have been superimposed on the mean 700 mb forecast temperature field in order to evaluate the relationship between the model's errors and the mean state of the atmosphere. In this instance, there does not appear to be any strong relationship between the model's cold bias and the mean north-south temperature gradient. However, during August and September 1994 (not shown), the cold bias at 700 mb was larger and tied directly to the position of the mean baroclinic zone. Also, it appears the model's mean local response to the terrain of the Sierra and Rocky Mountains is colder mean temperatures over the high terrain and warmer mean temperatures downstream.

Forecast Verification with Respect to Rawinsonde Observations

Routine comparison of MEM forecasts to rawinsonde observations is accomplished each forecast cycle. At the end of each month and season, the average and RMS errors are computed for selected variables at 50 mb levels in the vertical according to the procedures outlined in Chapter 3. The errors for Fall 1994 and Winter 1995 are presented here for the 36-hour forecast only. Seasonal statistics at other forecast lead times are available via URL: **http://www.met.utah.edu/html/meso/meso_verification_seasonal.html**. Monthly average and RMS errors can be examined on-line via the following URLs:

http://www.met.utah.edu/html/meso/meso_verification_bias.html

http://www.met.utah.edu/html/meso/meso_verification_rms.html.

The average error of the 36-hour MEM forecasts at the 300 mb level during Fall 1994 is presented in Figure 5.2a for the variables: temperature, dew point temperature, wind speed, vector wind, geopotential height, and relative humidity. The plotting convention is described in the figure caption. All of the average errors tend to be small, e.g., height errors are typically 10 m or less. Large negative 'errors' are apparent at many stations in dew point temperature (middle left) and relative humidity (middle right). However, this results more from erroneous specification of moisture at this level in the rawinsonde observations rather than any identifiable problem with the model.

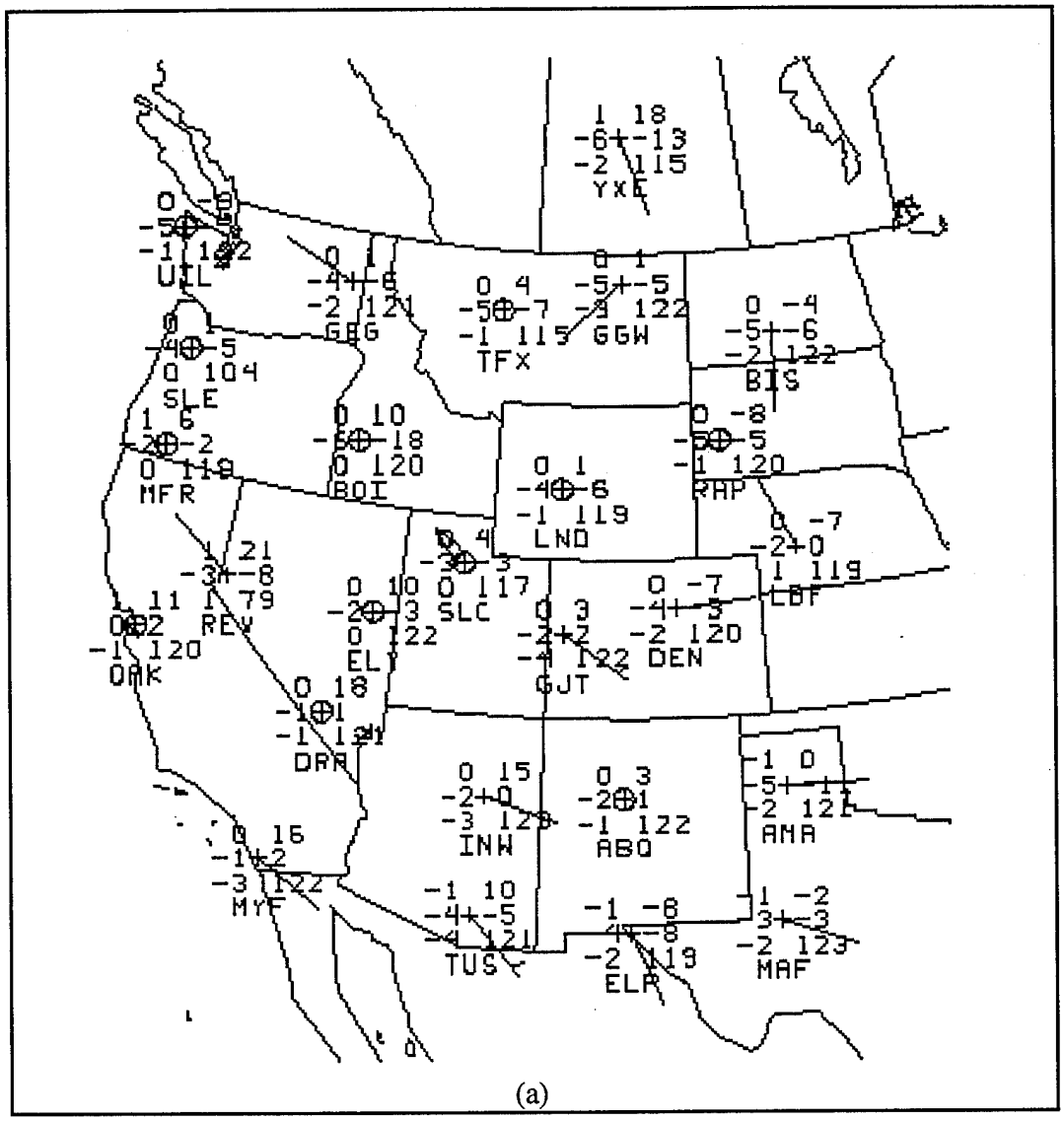

Figure 5.2. Average error of 36-hour MEM forecasts during Fall 1994 for selected variables at: (a) 300 mb; (b) 500 mb; (c) 700 mb; and (d) 850 mb. The errors are computed with respect to rawinsonde observations at the stations identified by the plus sign and three-letter ID numbers. The average errors are plotted for each variable according to the following: temperature (^{o}C, upper left); dew point temperature (^{o}C, middle left); wind speed (m s^{-1}, lower left); geopotential height (m, upper right); relative humidity (%, middle right); number of verified forecasts (lower right); and vector wind (wind barb where a half barb reflects 5 m s^{-1} and a circle around the station indicates a wind speed error less than 2.5 m s^{-1}). Stations whose surface elevations lie above 850 mb verify only geopotential height on the 850 mb surface.

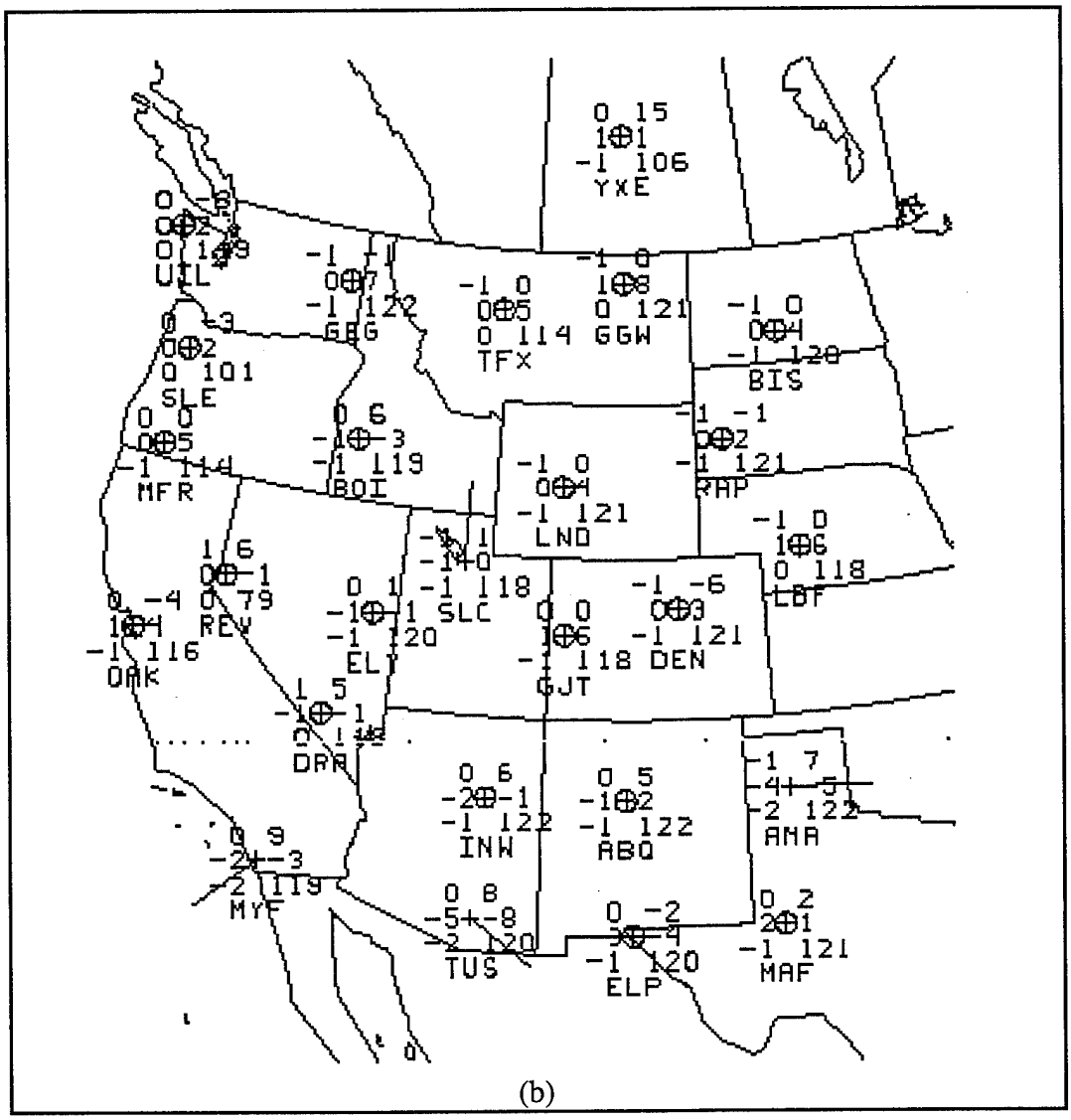

(b)

Figure 5.2. (Continued)

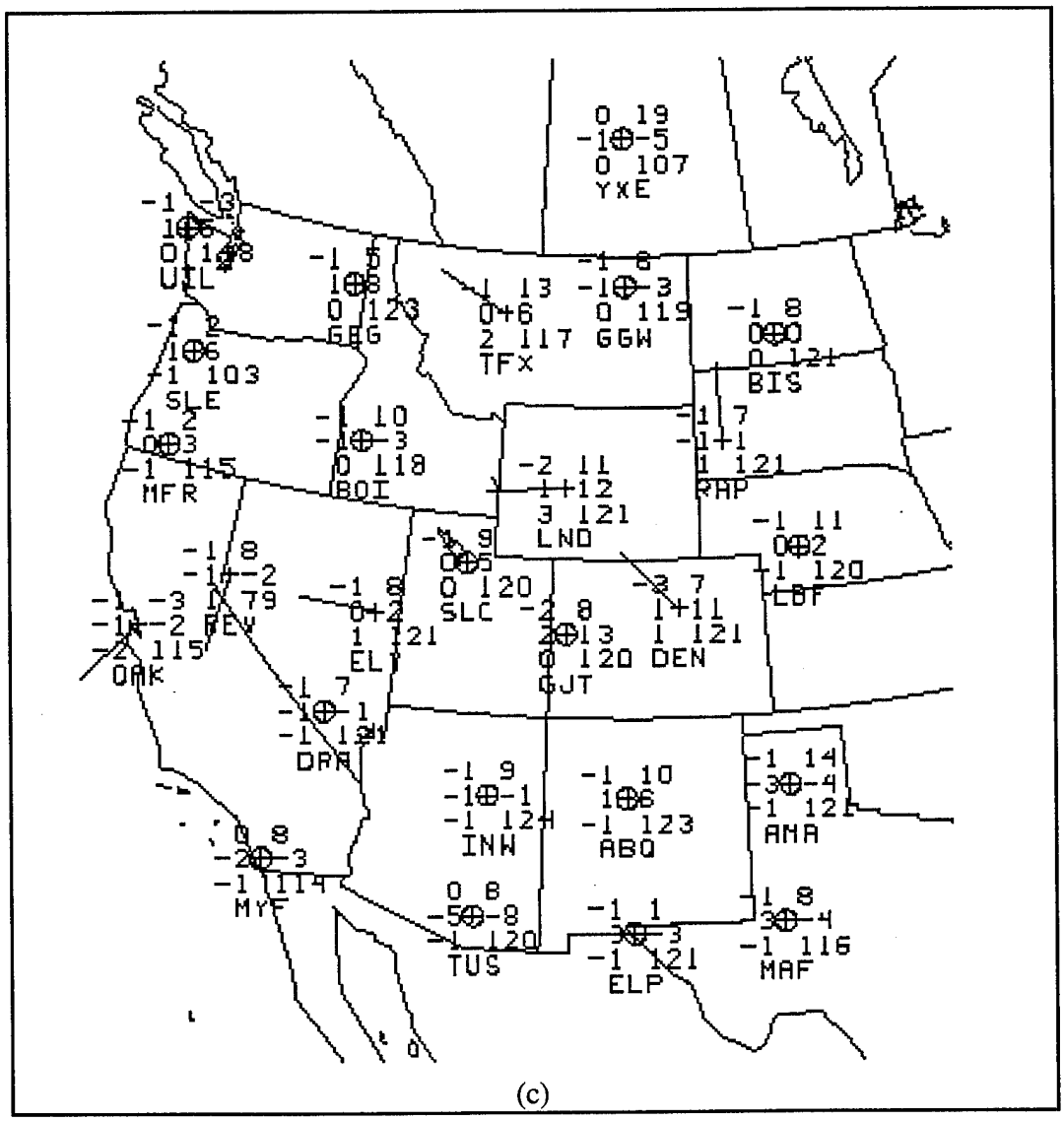

(c)

Figure 5.2. (Continued)

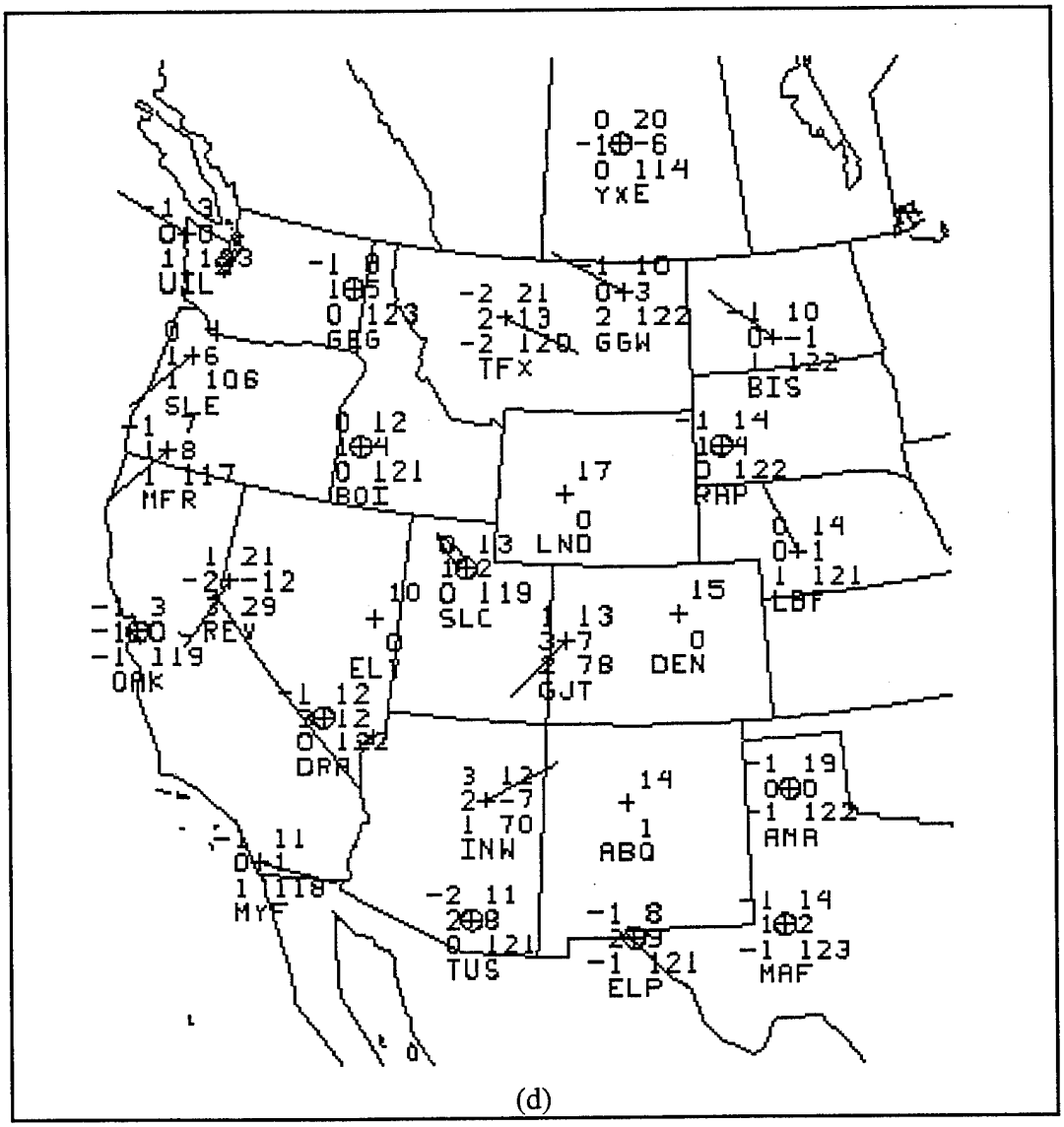

(d)

Figure 5.2. (Continued)

The average error for the same set of variables at the 500 mb level for Fall 1994 is shown in Figure 5.2b. The magnitudes of the average errors are again small; the model exhibits a slight cold, dry bias with respect to the rawinsonde observations at many stations in the West. At 700 mb (Figure 5.2c), a significant cold bias (i.e., over 2°C) is evident at Lander, Wyoming (LND) and Denver, Colorado (DEN) that is consistent with the spatial distribution of the temperature bias exhibited in Figure 5.1a. Finally, at 850 mb (Figure 5.2d), positive height biases on the order of 10-20 m are evident at many stations.

The average errors during Winter 1995 are presented in Figure 5.3 for the four levels. As in the case of the 300 mb level for the Fall 1994, the errors at 300 mb (Figure 5.3a) are small with the exception of dew point temperature and relative humidity. The 500 mb average errors are shown in Figure 5.3b. As in the Fall case the magnitudes of the errors are small. However, the geopotential height values are over the southern and eastern portion of the evaluation domain are slightly higher with the magnitude of some errors as high as 18 m. The 700 mb temperatures (Figure 5.3c) display what has become a characteristic cold bias at LND and DEN. Additionally, geopotential height errors are about twice that of the Fall 1994 season on the southern and eastern edges of this domain. At 850 mb (Figure 5.3d), the geopotential height biases are again on par with those exhibited during the Fall season.

The RMS errors for 36-hour MEM forecasts during Fall 1994 are summarized on the four standard pressure surfaces in Figure 5.4. At 300 mb (Figure 5.4a), geopotential height errors on the order of 45-50 m, vector wind errors on the order of 10 m s^{-1}, and temperature errors on the order of 2°C are common. The large dew point temperature and relative humidity errors, again, reflect the poor procedures for specifying moisture in observed soundings rather than any problem in the model. However, at 500 mb (Figure 5.4b), the observed dew point temperature and relative humidity values are more reliable and typical RMS errors are on the order of 7°C and 20% respectively.

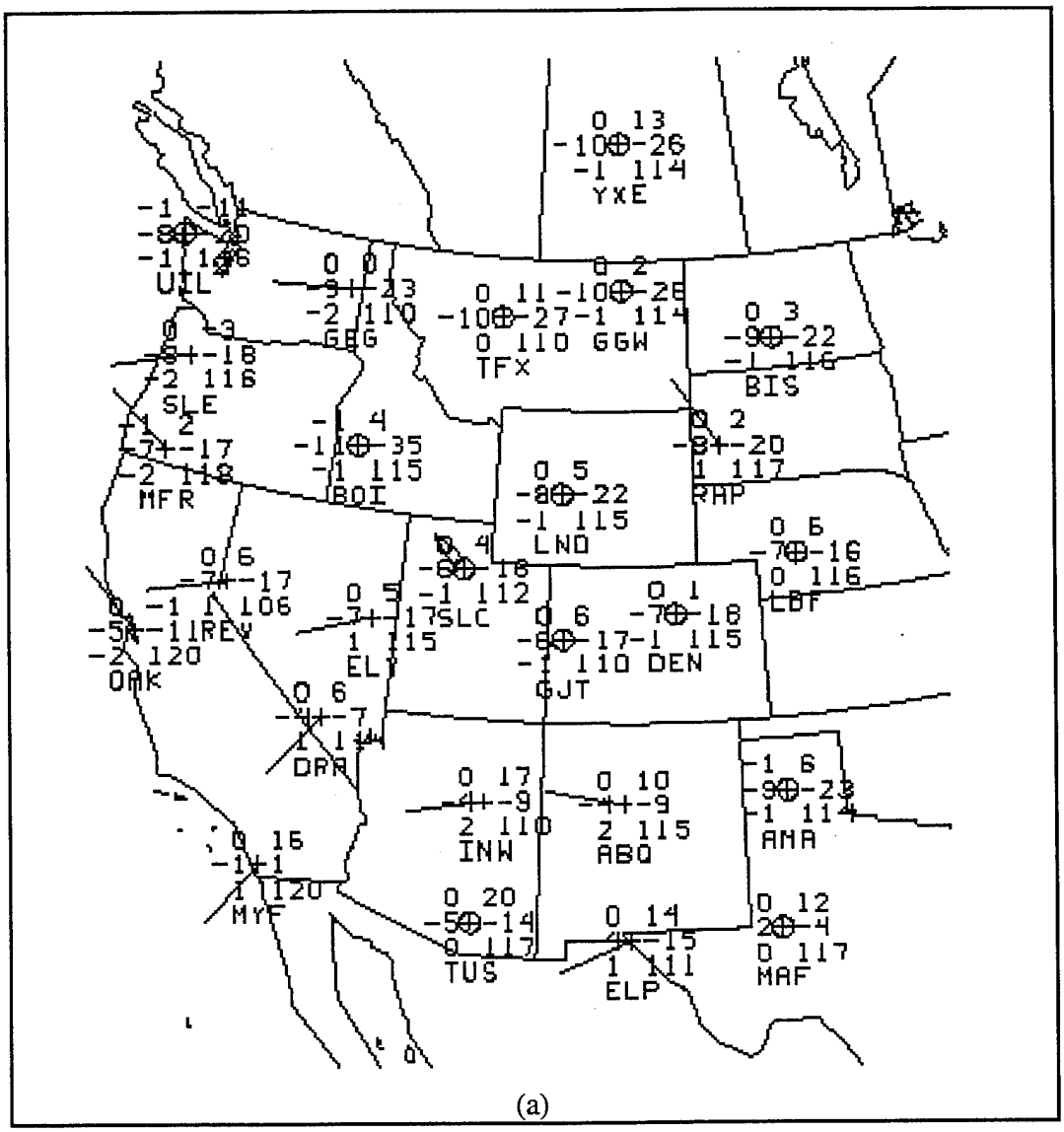

Figure 5.3. Average error of 36-hour MEM forecasts during Winter 1995 for selected variables at: (a) 300 mb; (b) 500 mb; (c) 700 mb; and (d) 850 mb. The errors are computed with respect to rawinsonde observations at the stations identified by the plus sign and three-letter ID numbers. The average errors are plotted for each variable according to the following: temperature (^{o}C, upper left); dew point temperature (^{o}C, middle left); wind speed (m s^{-1}, lower left); geopotential height (m, upper right); relative humidity (%, middle right); number of verified forecasts (lower right); and vector wind (wind barb where a half barb reflects 5 m s^{-1} and a circle around the station indicates a wind speed error less than 2.5 m s^{-1}). Stations whose surface elevations lie above 850 mb verify only geopotential height on the 850 mb surface.

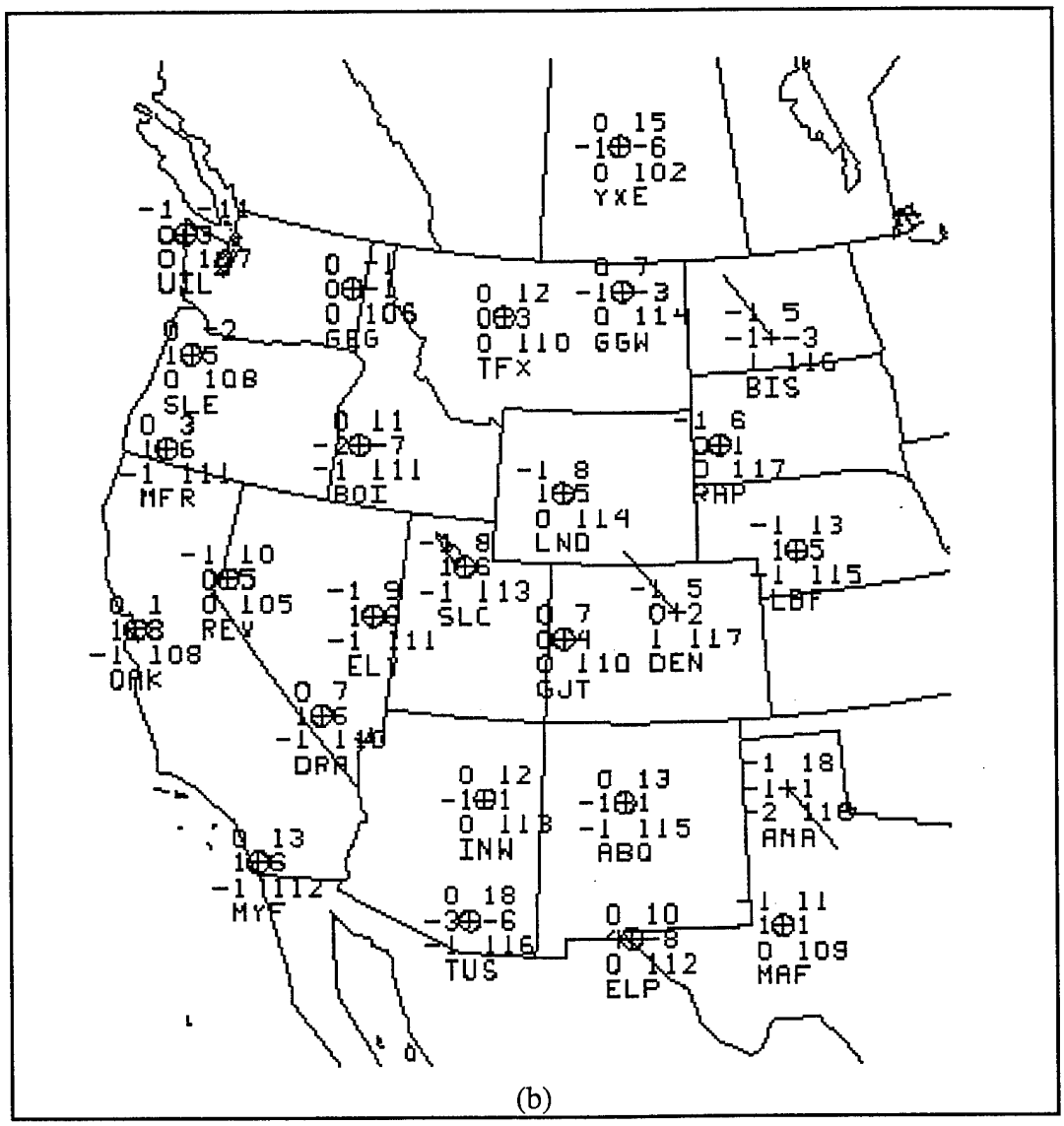

Figure 5.3. (Continued)

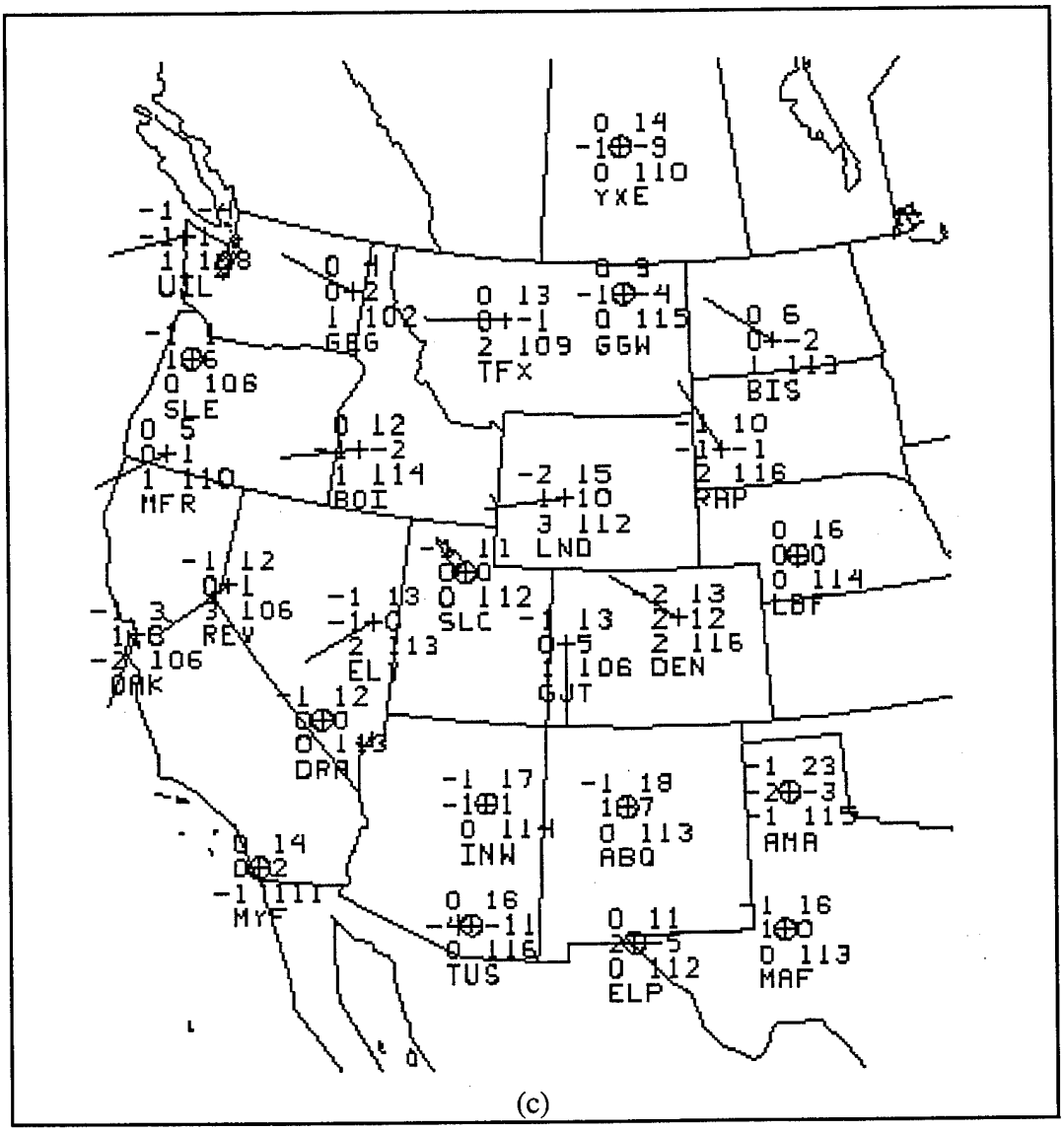

Figure 5.3. (Continued)

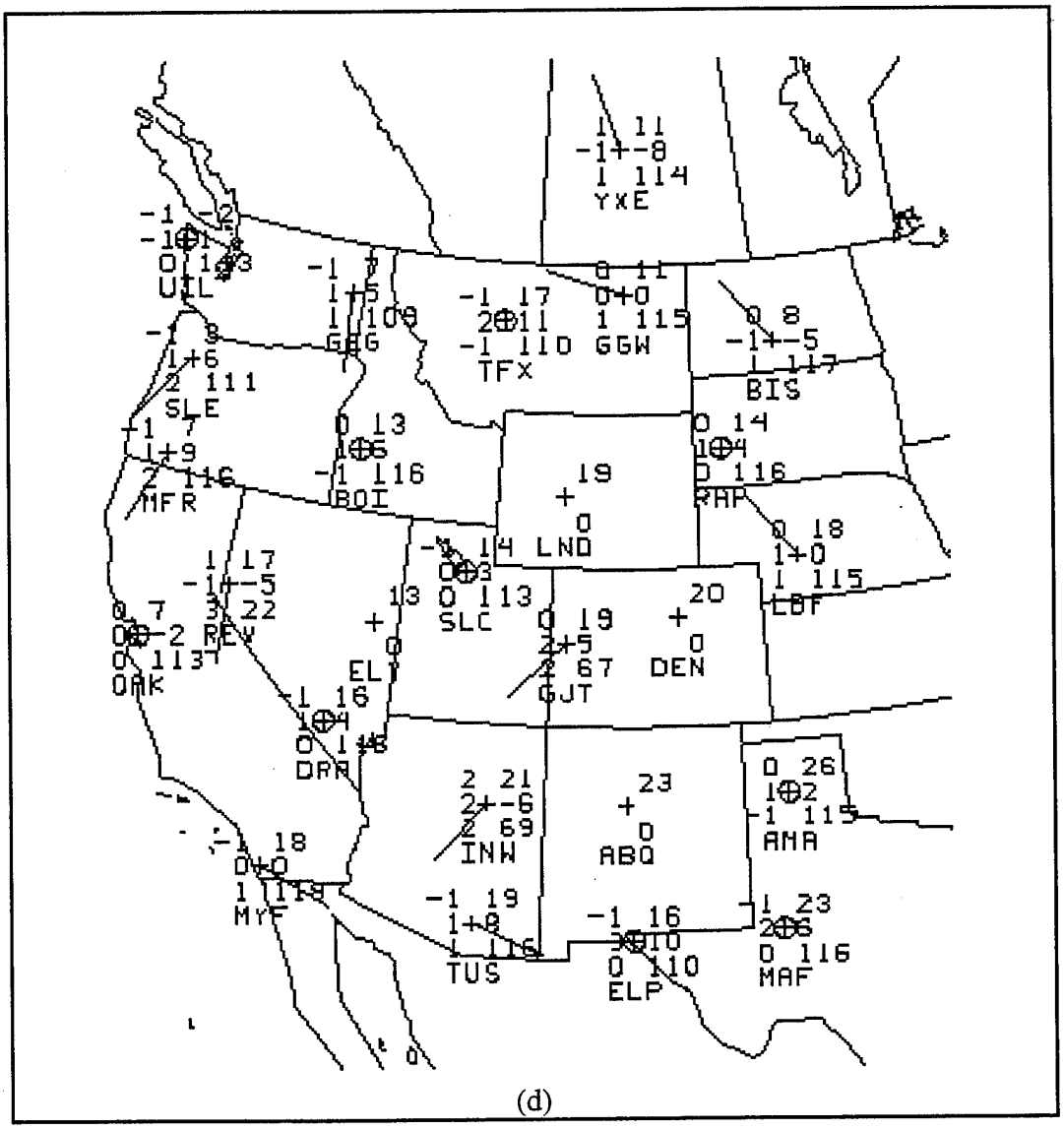

(d)

Figure 5.3. (Continued)

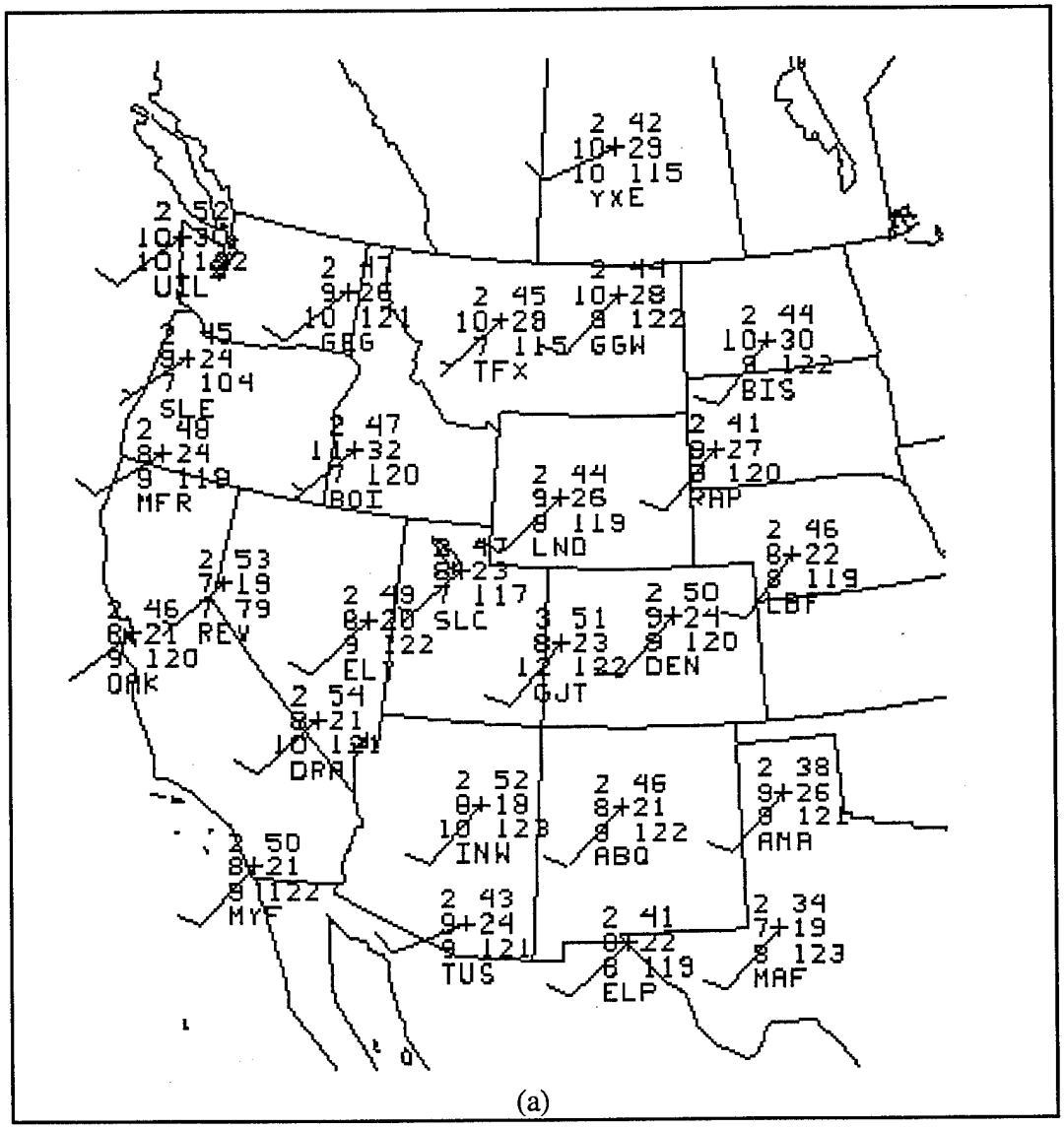

Figure 5.4. RMS error of 36-hour MEM forecasts during Fall 1994 for selected variables at: (a) 300 mb; (b) 500 mb; (c) 700 mb; and (d) 850 mb. The errors are computed with respect to rawinsonde observations at the stations identified by the plus sign and three-letter ID numbers. The average errors are plotted for each variable according to the following: temperature (^{o}C, upper left); dew point temperature (^{o}C, middle left); wind speed (m s^{-1}, lower left); geopotential height (m, upper right); relative humidity (%, middle right); number of verified forecasts (lower right); and vector wind (wind barb where a half barb reflects 5 m s^{-1} and a circle around the station indicates a wind speed error less than 2.5 m s^{-1}). Stations whose surface elevations lie above 850 mb verify only geopotential height on the 850 mb surface.

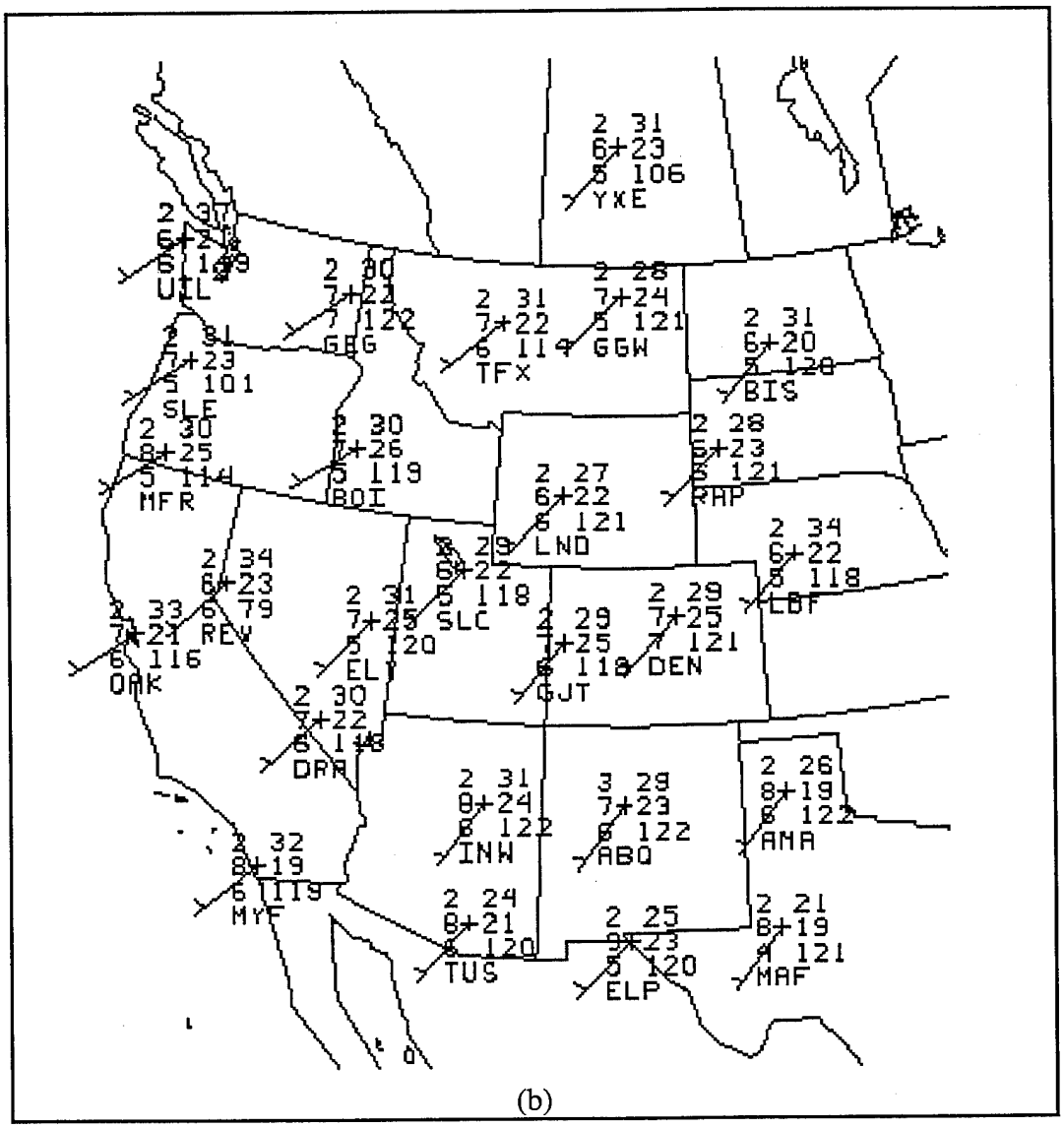

(b)

Figure 5.4. (Continued)

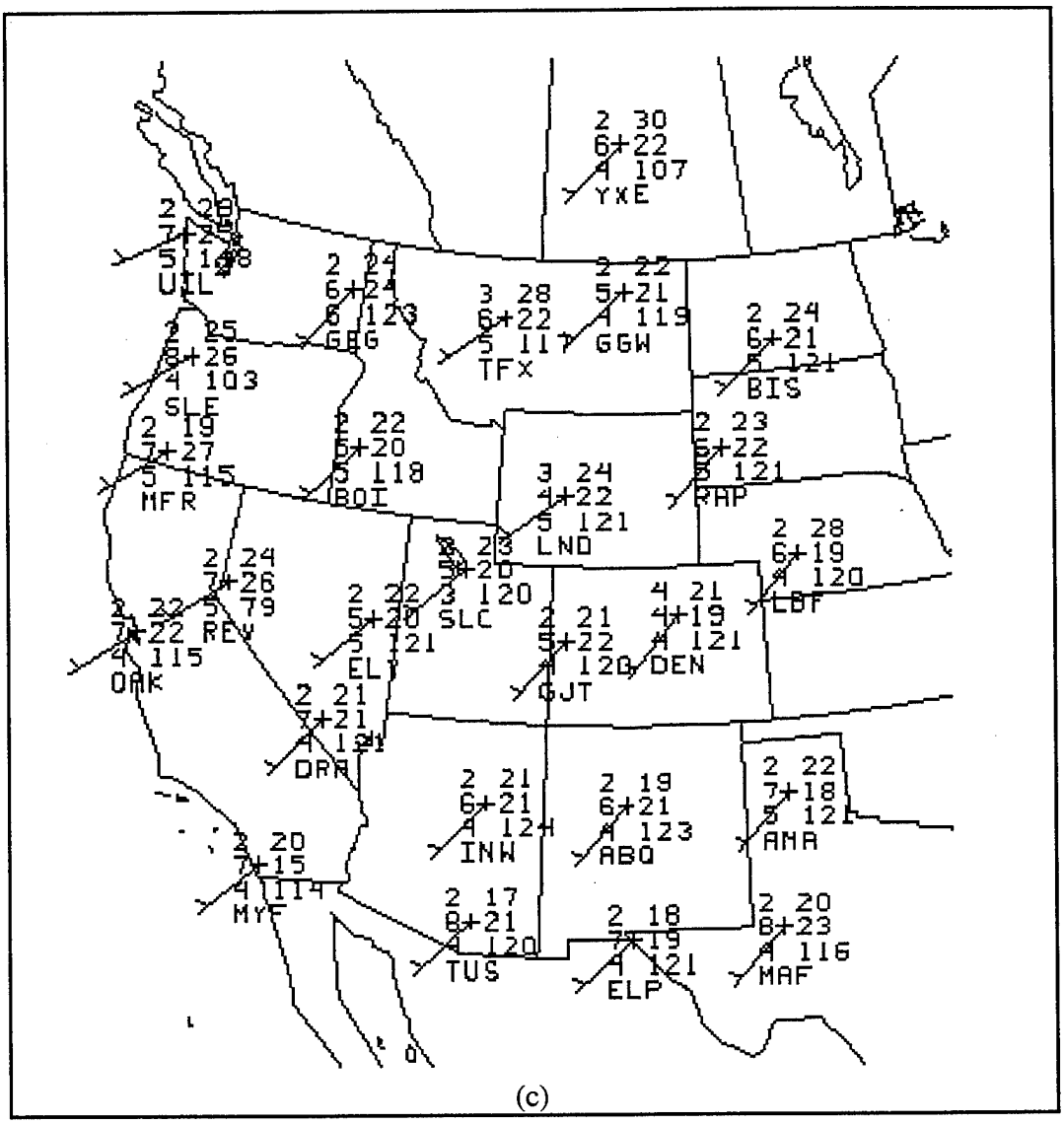

Figure 5.4. (Continued)

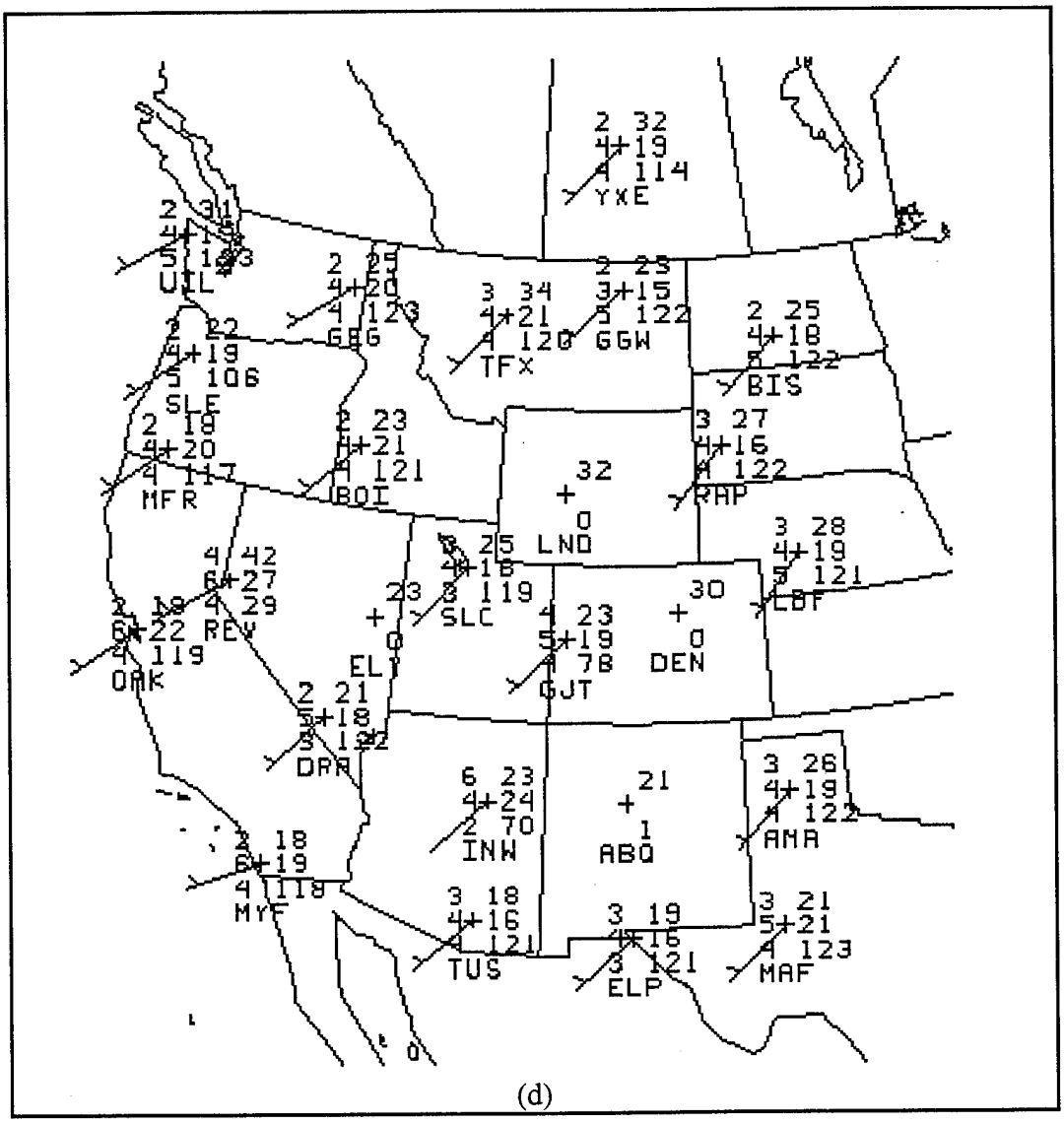

(d)

Figure 5.4. (Continued)

Large RMS errors in moisture are also evident at 700 mb (Figure 5.4c) and 850 mb (Figure 5.4d). With a few exceptions, the magnitude of the RMS error in temperature, dew point temperature, relative humidity, and vector wind tend to be independent of vertical level below 300 mb.

The RMS errors for the 36-hour MEM forecasts during Winter 1995 are shown in Figure 5.5. The 300 mb level errors are similar to the Fall 1994 errors (geopotential height errors on the order of 45-50 m, vector wind errors on the order of 10 m s^{-1}, temperature errors on the order of 2°C, and large dew point temperature and relative humidity errors) indicating that the errors are, for this evaluation period at least, independent of forecast season. As in the 300 mb level case, the 500 mb RMS error magnitudes (Figure 5.5b) are virtually identical to their Fall counterparts and on the same order of magnitude as those at 700 mb (Figure 5.5c) and 850 mb (Figure 5.5d), indicating that the magnitude of the RMS error in temperature, dew point temperature, relative humidity, and vector wind tend to be independent of vertical level below 300 mb.

Further Examination of Vertical Structure

The growth of average error as a function of forecast duration for the Fall 1994 and Winter 1995 seasons is summarized in Figures 5.6 and 5.7, respectively. Figure 5.6 shows the vertical structure of the average error at Salt Lake City for the Fall 1994 season at the analysis (Figure 5.6a), 12-hour forecast (Figure 5.6b), 24-hour forecast (Figure 5.6c), and 36-hour forecast (Figure 5.6d) times. At the analysis time (Figure 5.6a), very small biases are exhibited by the three variables with the exception of dew point temperature above 350 mb where the poor observations of moisture are evident. As the forecast duration increases, the cold bias in the lower troposphere becomes evident, a positive (negative) dew point temperature bias develops below (above) 700 mb, and a small positive height bias develops at nearly all levels.

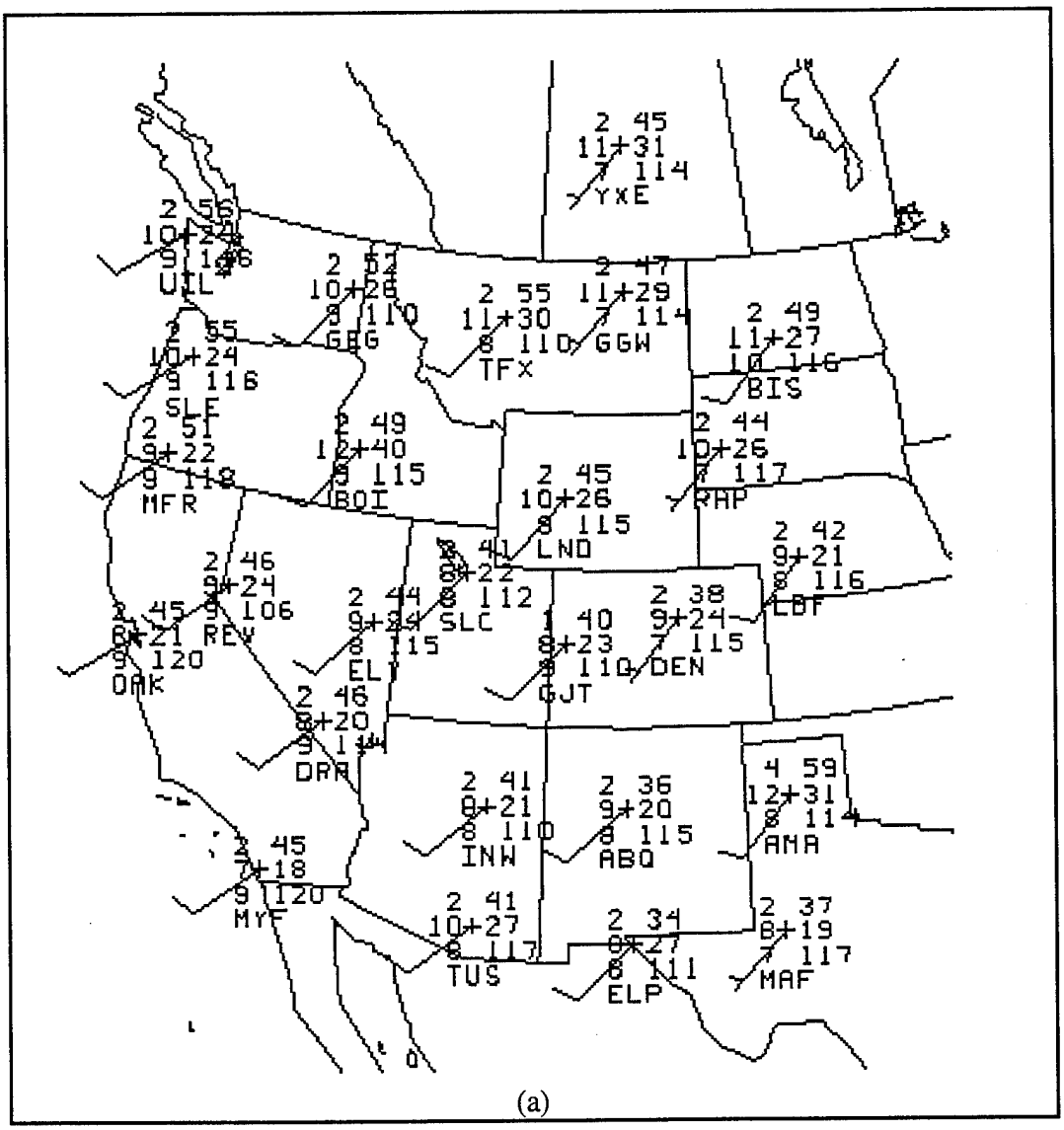

Figure 5.5. RMS error of 36-hour MEM forecasts during Winter 1995 for selected variables at: (a) 300 mb; (b) 500 mb; (c) 700 mb; and (d) 850 mb. The errors are computed with respect to rawinsonde observations at the stations identified by the plus sign and three-letter ID numbers. The average errors are plotted for each variable according to the following: temperature (^{o}C, upper left); dew point temperature (^{o}C, middle left); wind speed (m s^{-1}, lower left); geopotential height (m, upper right); relative humidity (%, middle right); number of verified forecasts (lower right); and vector wind (wind barb where a half barb reflects 5 m s^{-1} and a circle around the station indicates a wind speed error less than 2.5 m s^{-1}). Stations whose surface elevations lie above 850 mb verify only geopotential height on the 850 mb surface.

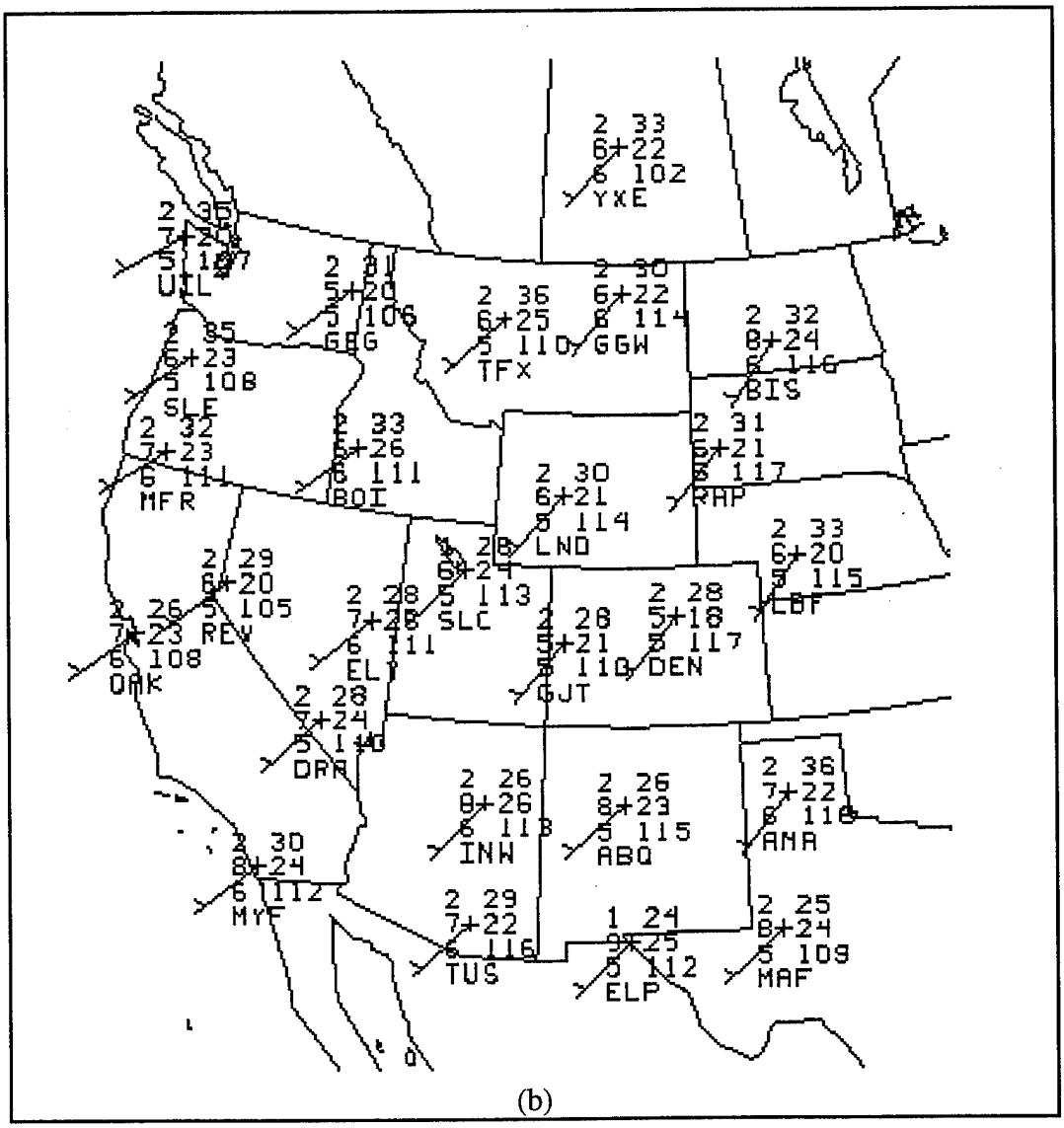

Figure 5.5. (Continued)

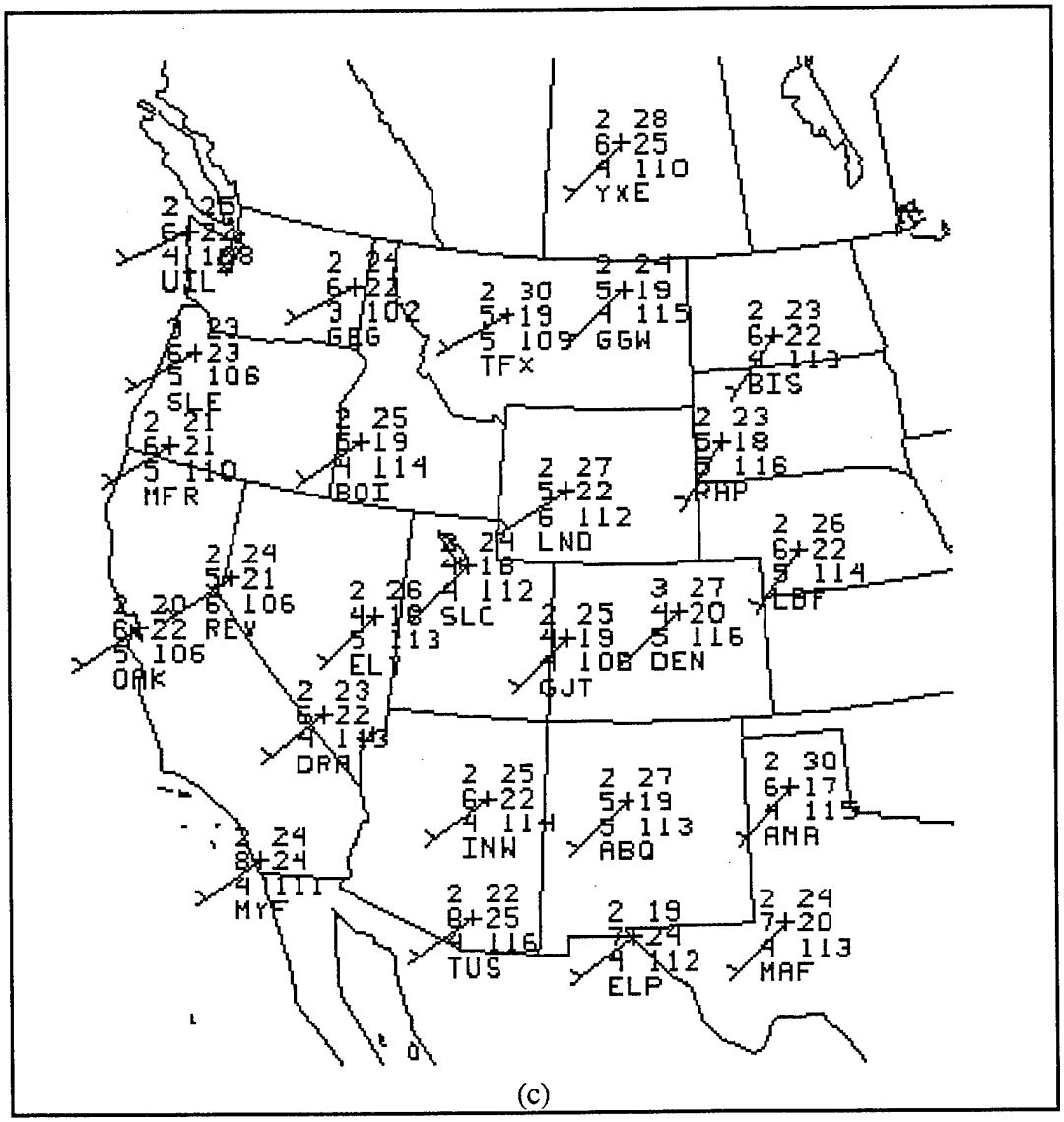

(c)

Figure 5.5. (Continued)

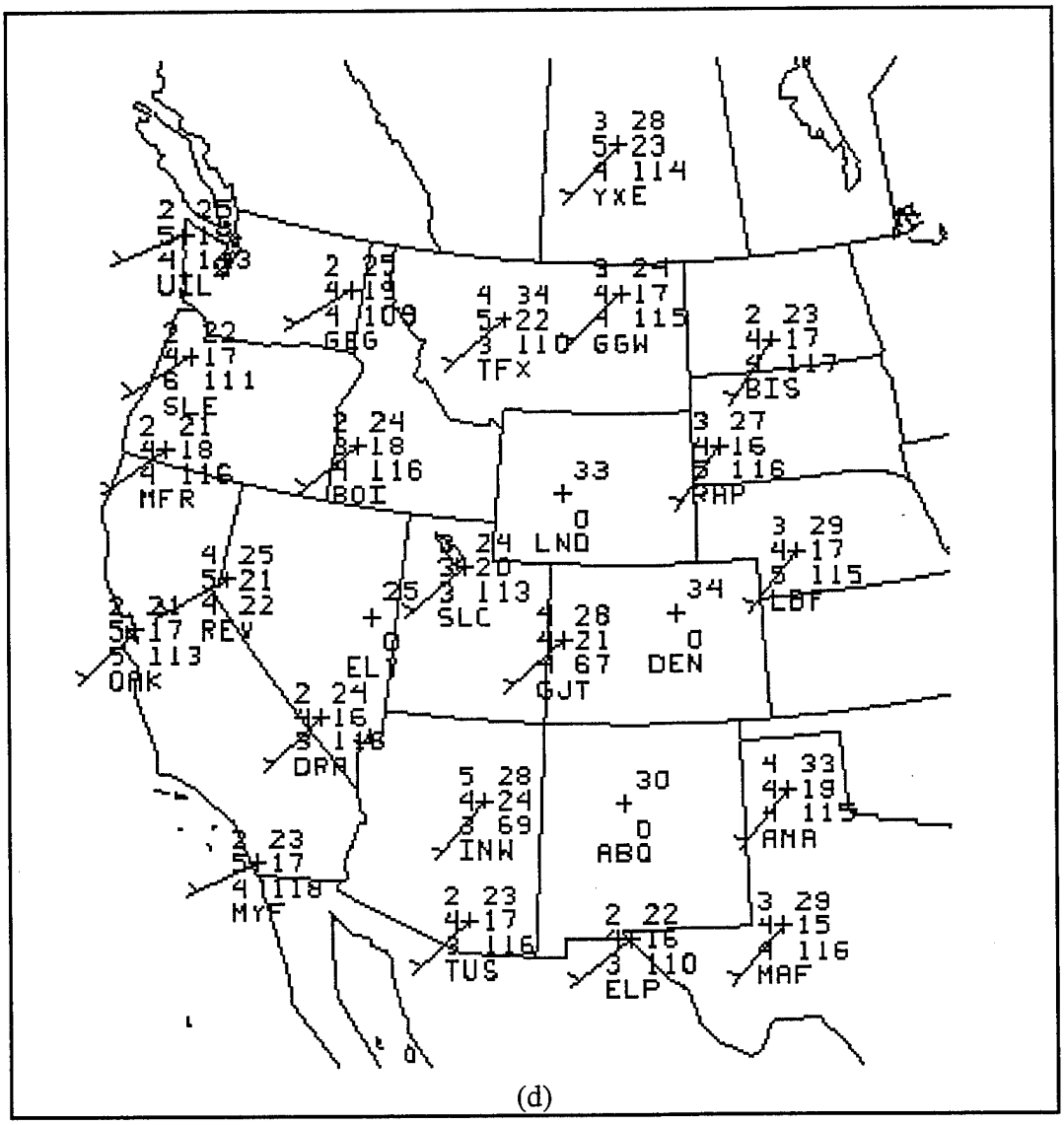

Figure 5.5. (Continued)

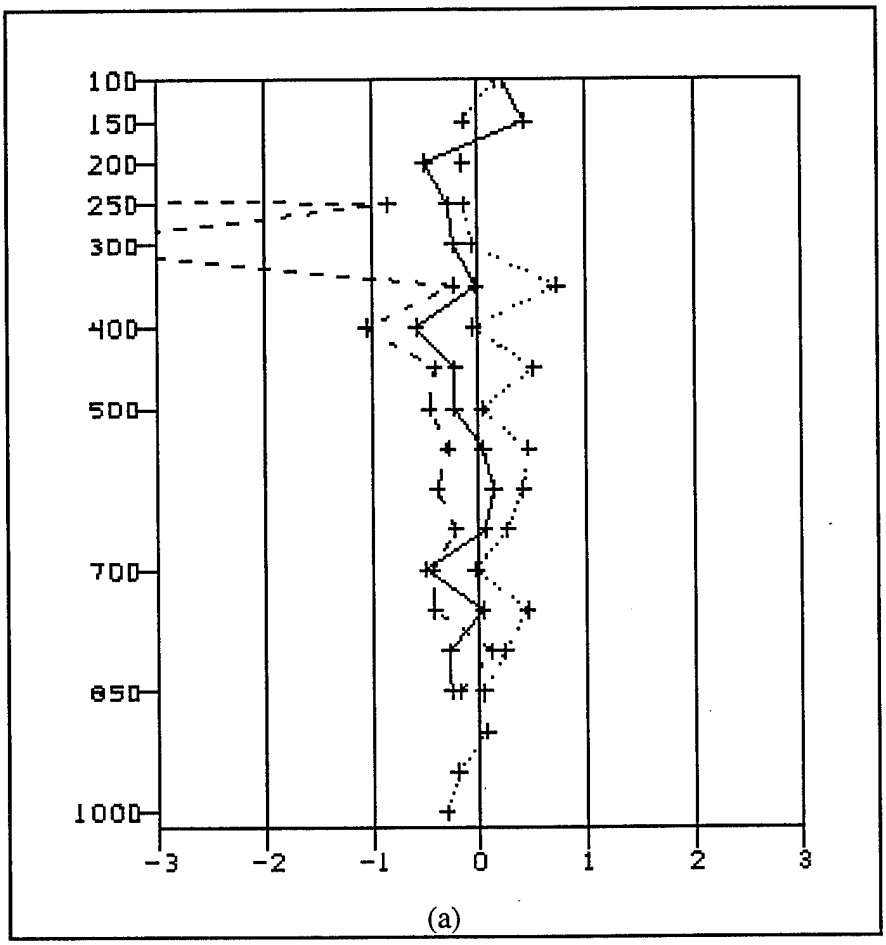

Figure 5.6. Fall seasonal average error of the MEM with respect to the rawinsonde observations at Salt Lake City, Utah as a function of height: (a) the analysis, (b) the 12-hour forecast, (c) the 24-hour forecast, and (d) the 36-hour forecast. The solid line denotes the temperature error in °C, the dashed line shows the dew point error in °C and the dotted line shows the height error in dm.

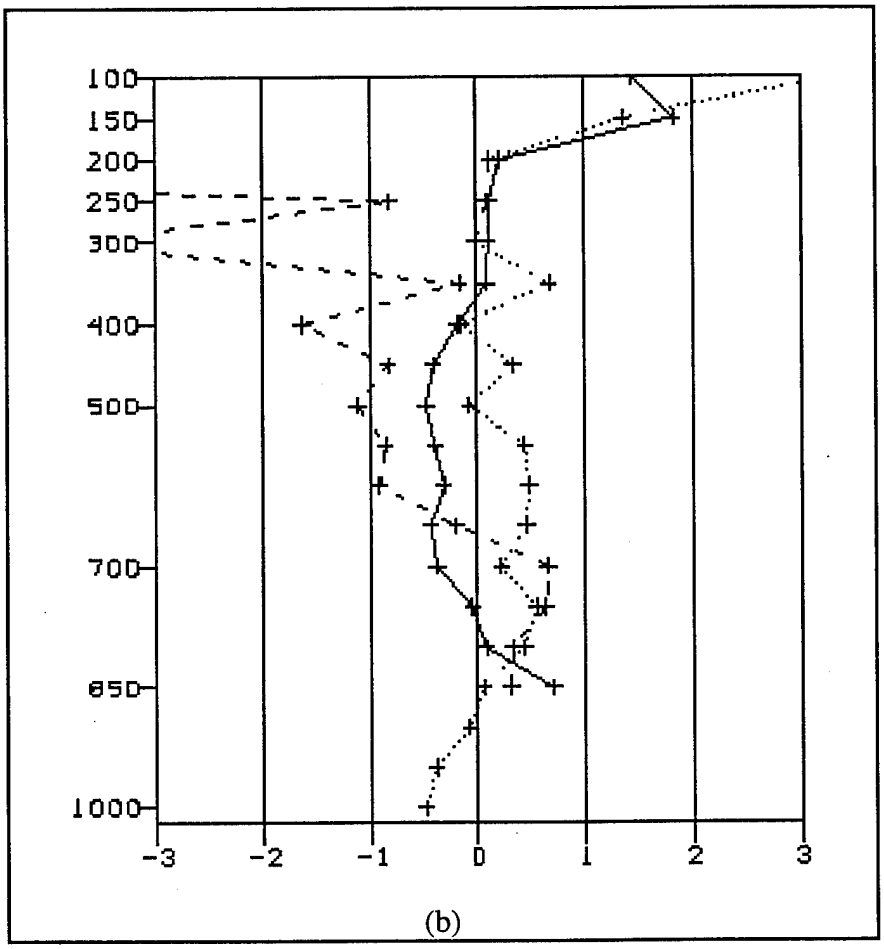

Figure 5.6. (Continued)

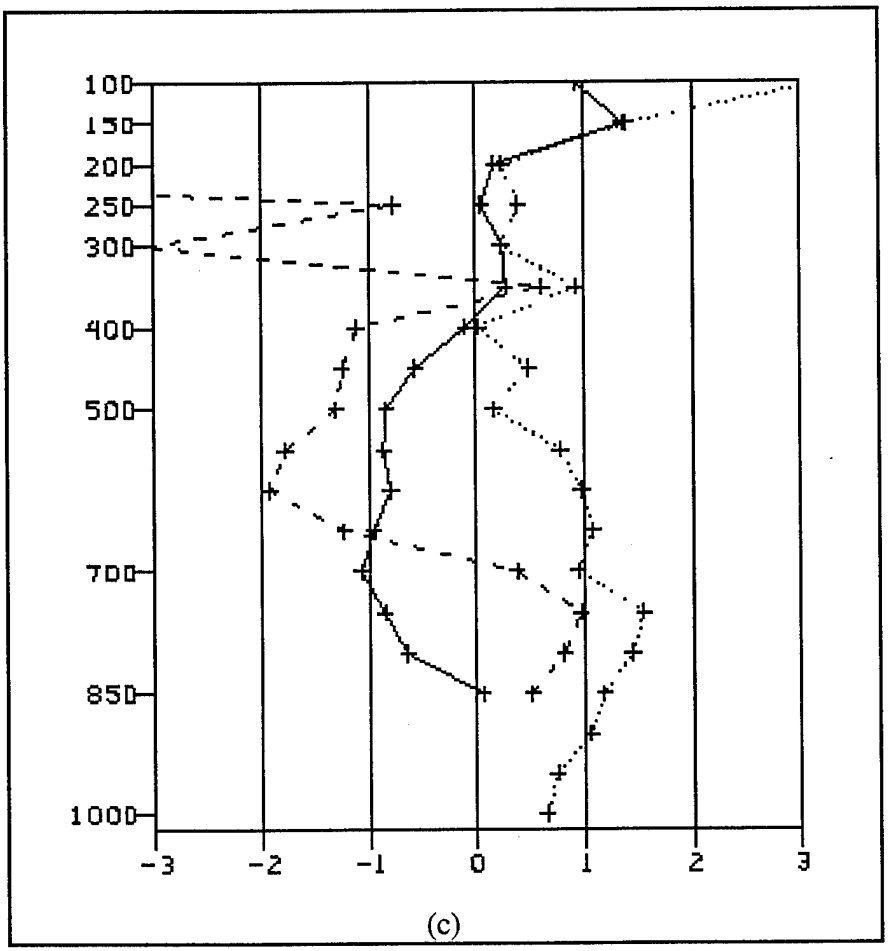

Figure 5.6. (Continued)

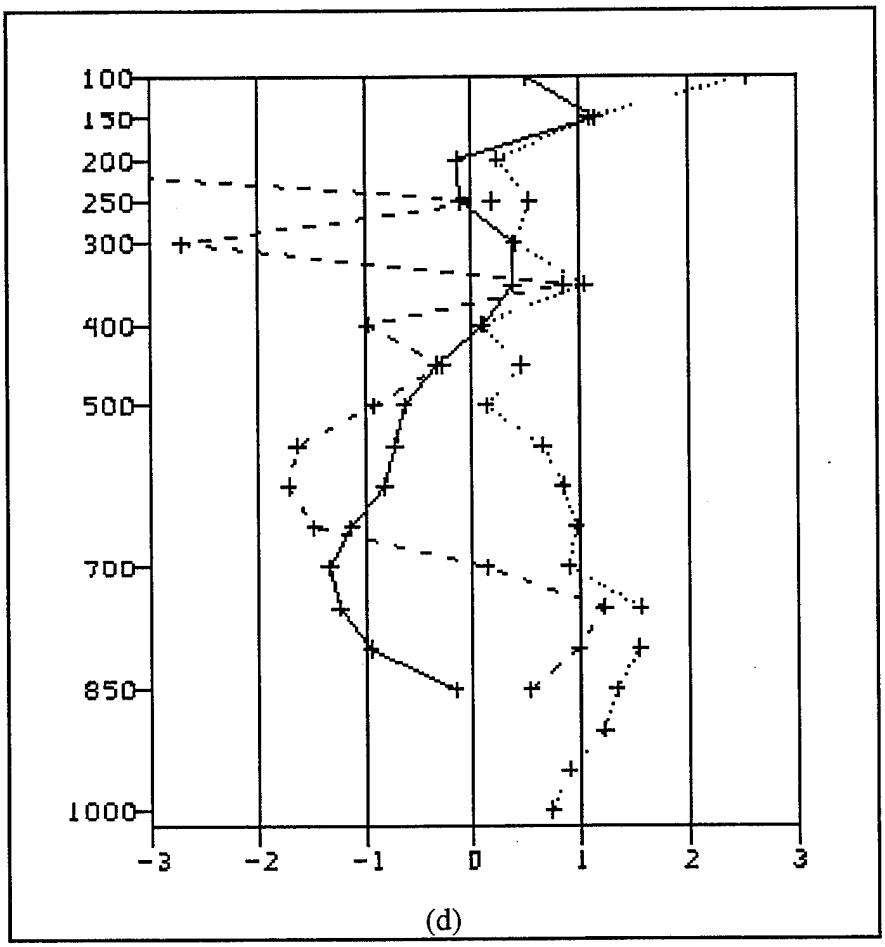

Figure 5.6. (Continued)

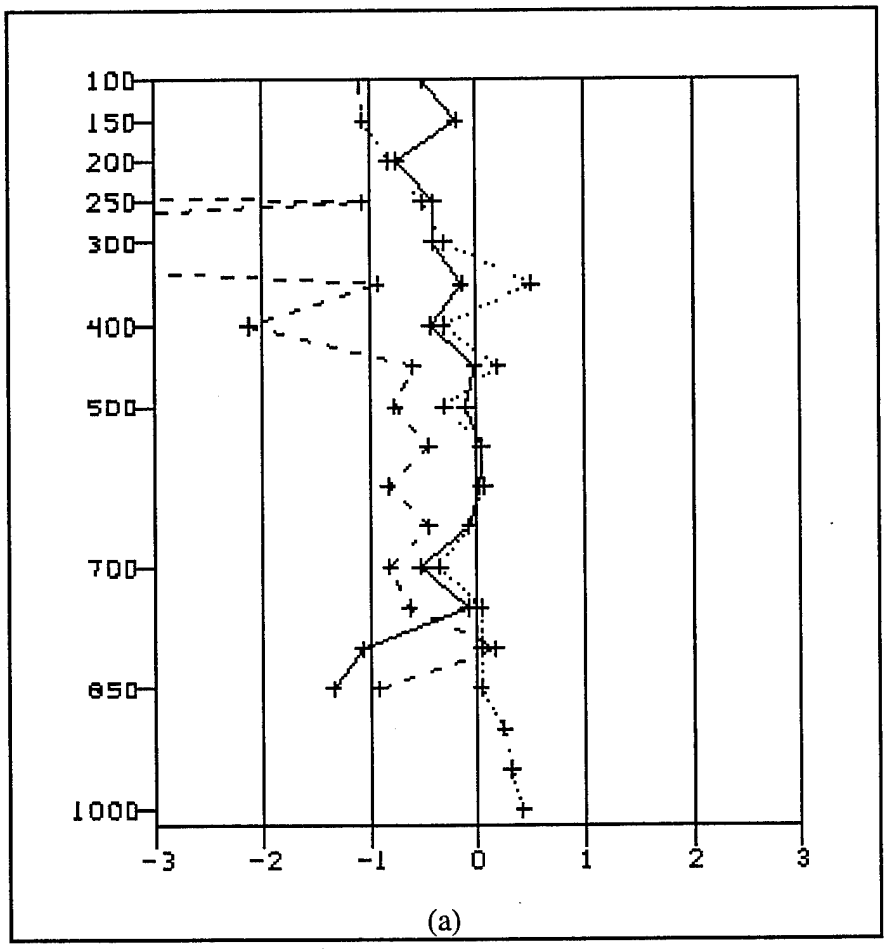

Figure 5.7. Winter seasonal average error of the MEM analyses with respect to the rawinsonde observations at Salt Lake City, Utah for (a) the analysis, (b) the 12-hour forecast, (c) the 24-hour forecast, and (d) the 36-hour forecast. The solid line shows the temperature error in °C, the dashed line shows the dew point error in °C and the dotted line shows the height error in dm.

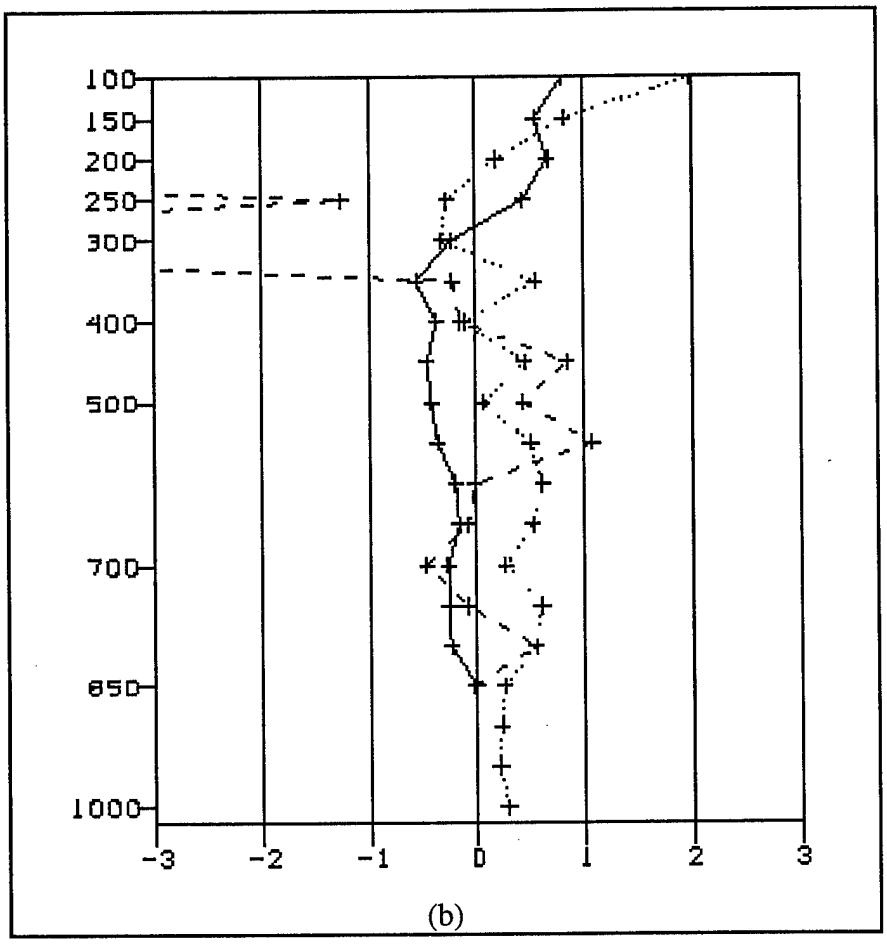

Figure 5.7. (Continued)

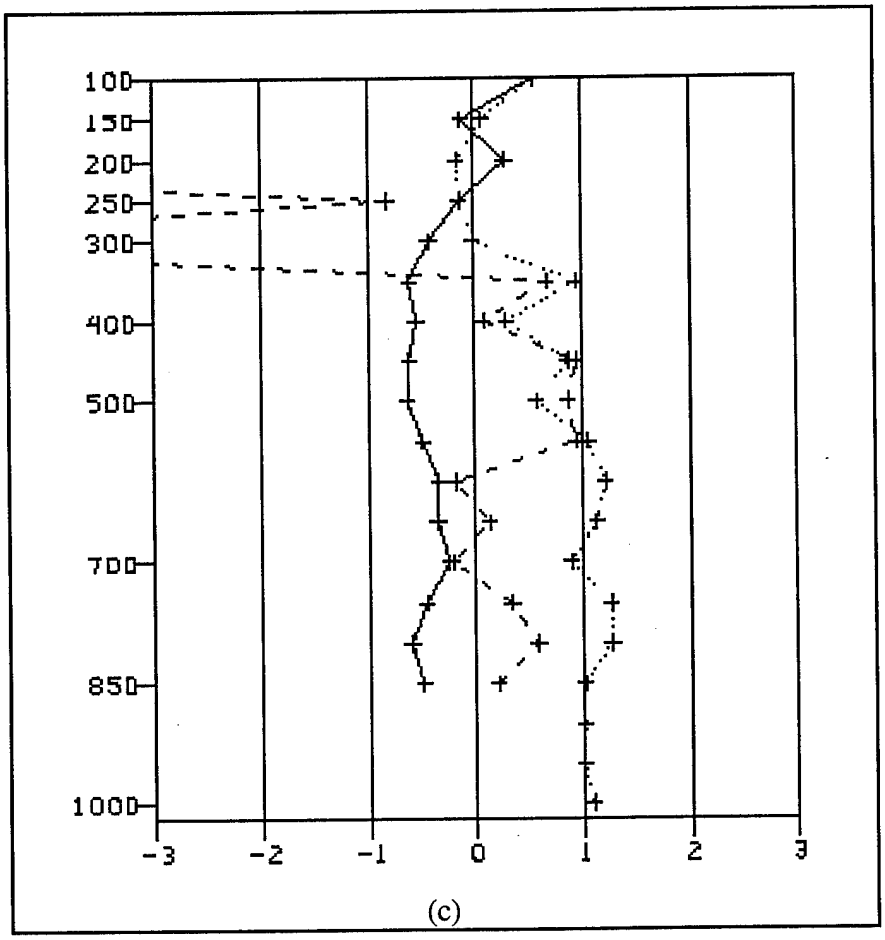

Figure 5.7. (Continued)

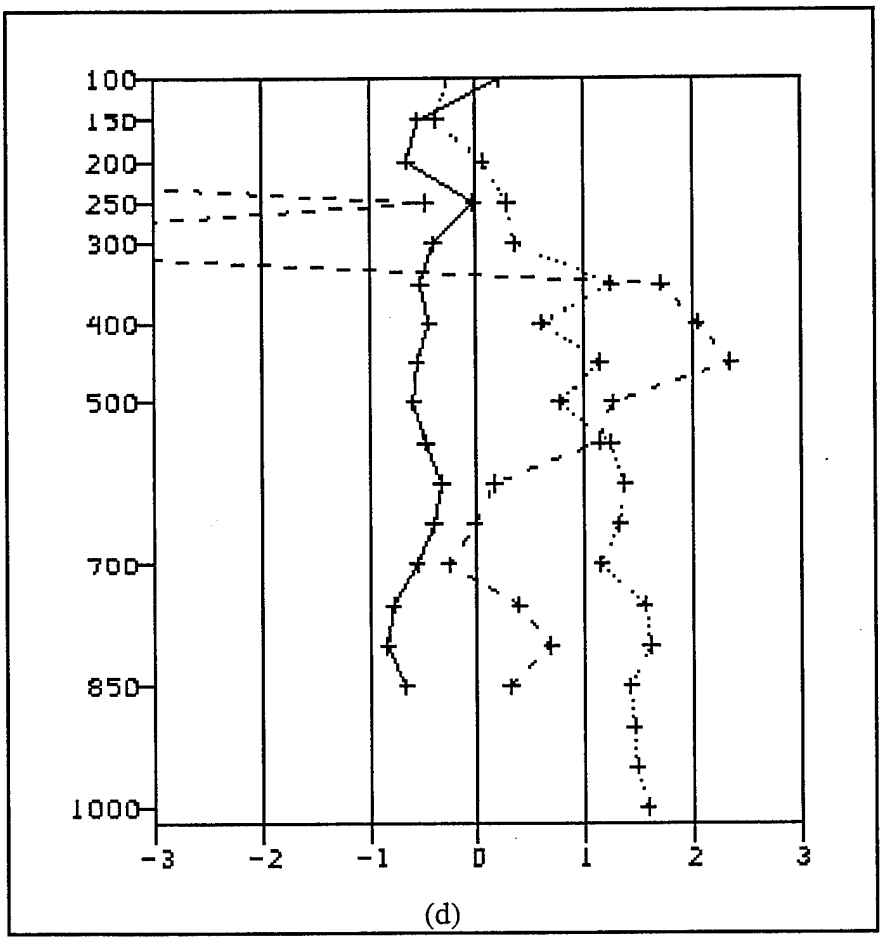

Figure 5.7. (Continued)

Similar evolution of the average errors as a function of forecast duration and vertical level develop at most other stations this can be viewed on-line by accessing URL: **http://www.met.utah.edu/html/meso/meso_seasonal_bias_profile.html**. As a general rule, the lowest verification level above ground level should be treated with caution over elevated terrain where the horizontal interpolation to the sounding location may introduce errors.

The vertical structure of the average error at Salt Lake City for the Winter 1995 season is shown in Figure 5.7. There are some differences between the Fall 1994 and the Winter 1995 seasonal averages that might have been missed if the vertical structure had not been examined. At the analysis time (Figure 5.7a), small dry biases (about -1°C) are present above 800 mb, extending up to 450 mb. By the 12-hour forecast (Figure 5.7b), 24-hour forecast (Figure 5.7c), and 36-hour forecast (Figure 5.7d) this dry bias reverses and intensifies, and by the 36 hour forecast point, the vertical temperature bias is almost the reverse of the Fall seasonal bias (Figure 5.6d) with a +2.2°C moist bias at 450 mb.

Additionally, where the Fall 1994 36-hour seasonal profile displayed a pronounced cold bias between 850 mb and 700 mb, the corresponding Winter 1995 profile shows an almost constant -0.5°C to -1.0°C cold bias with a slight bulge at about 800 mb. As in the Fall 1994 case, the evolution of the average errors as a function of forecast duration and vertical level develop at most other stations also.

The growth of the RMS error as a function of forecast duration for the Fall 1994 season is shown in Figure 5.8. It would be redundant to present the Winter 1995 seasonal statistics as they are similar to the Fall 1994 values. These can be viewed via URL: **http://www.met.utah.edu/html/meso/meso_seasonal_rms_profile.html**. At the analysis time (Figure 5.8a) temperature RMS error remains at about 1°C throughout all the vertical levels. This error grows through the forecast period to a magnitude of about 2°C for most levels at the 36-hour point (Figure 5.8d) with the slightly higher value of 2.5°C below 700 mb.

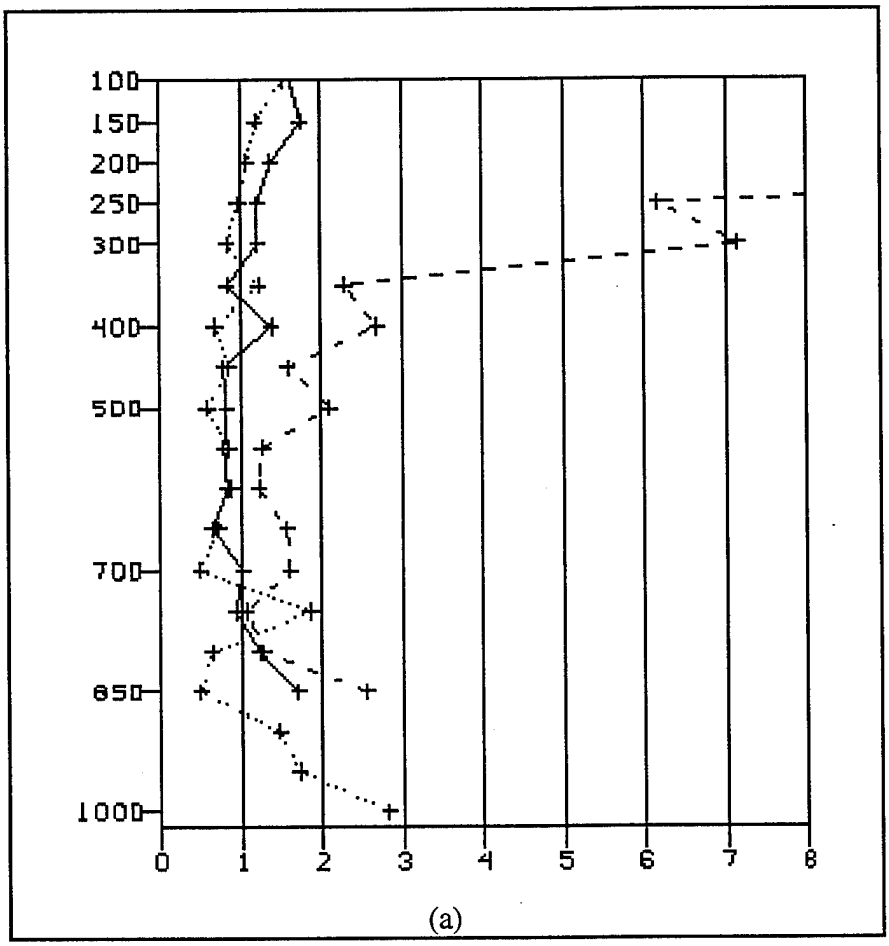

Figure 5.8. Fall RMS error of the MEM analyses with respect to the rawinsonde observations at Salt Lake City, Utah for: (a) the analysis, (b) the 12-hour forecast, (c) the 24-hour forecast, and (d) the 36-hour forecast. The solid line shows the temperature error in °C, the dashed line shows the dew point error in °C and the dotted line shows the height error in dm.

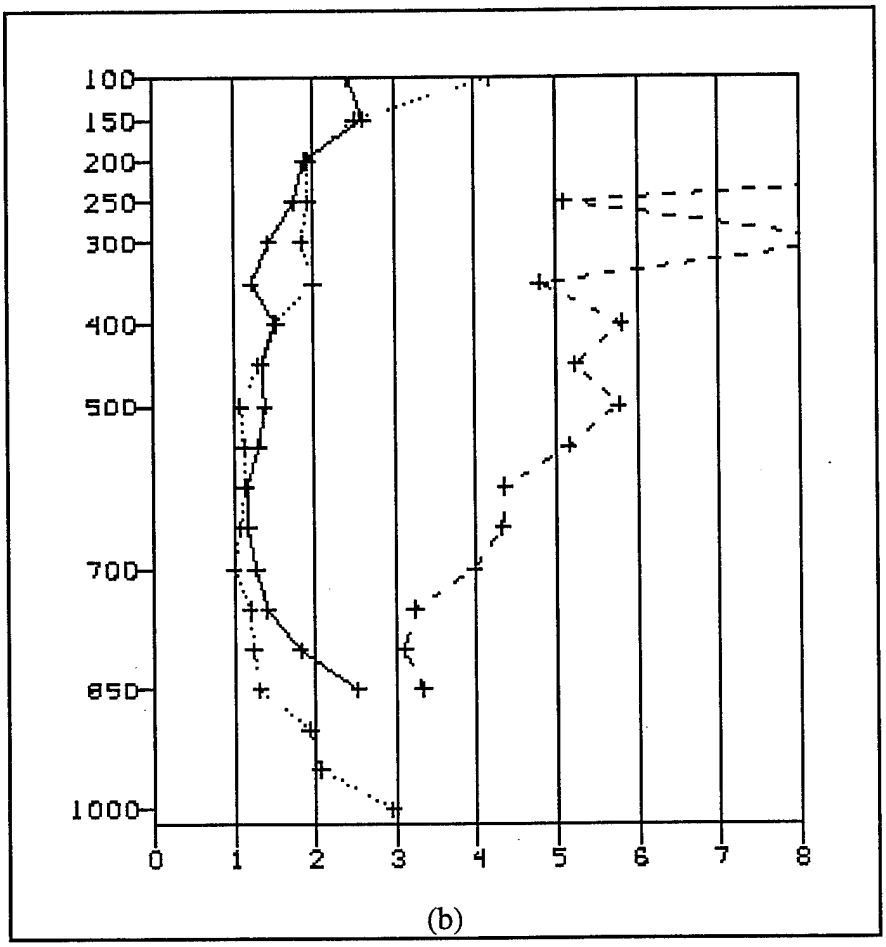

Figure 5.8. (Continued)

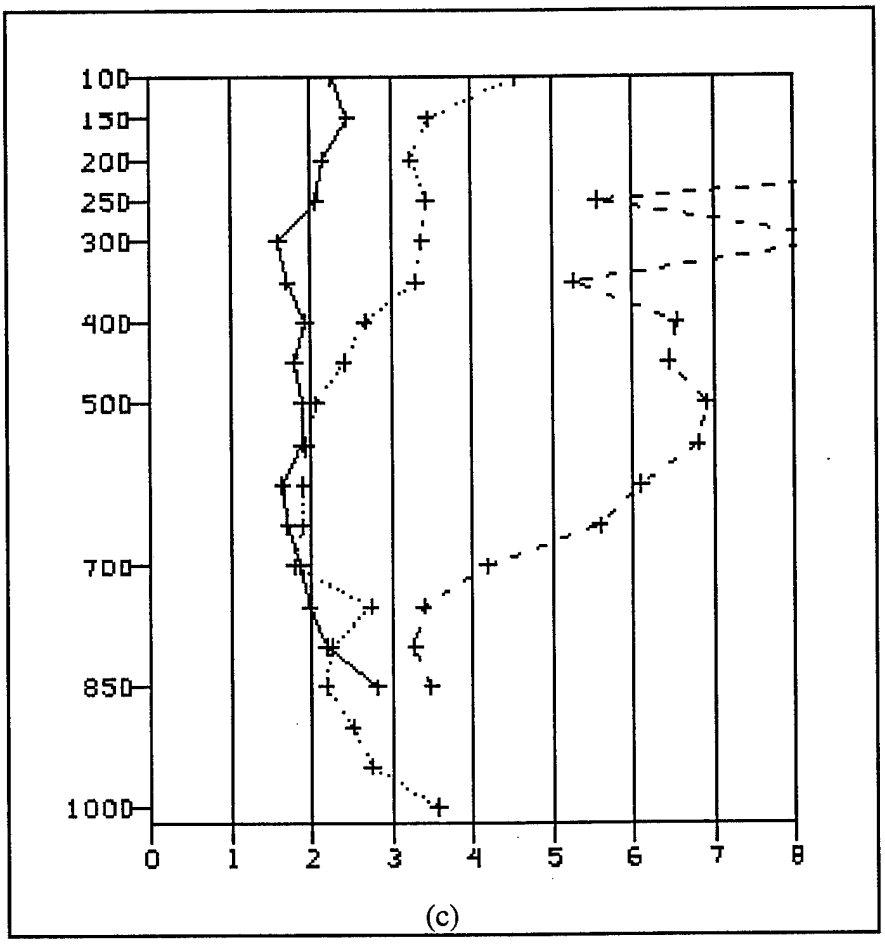

Figure 5.8. (Continued)

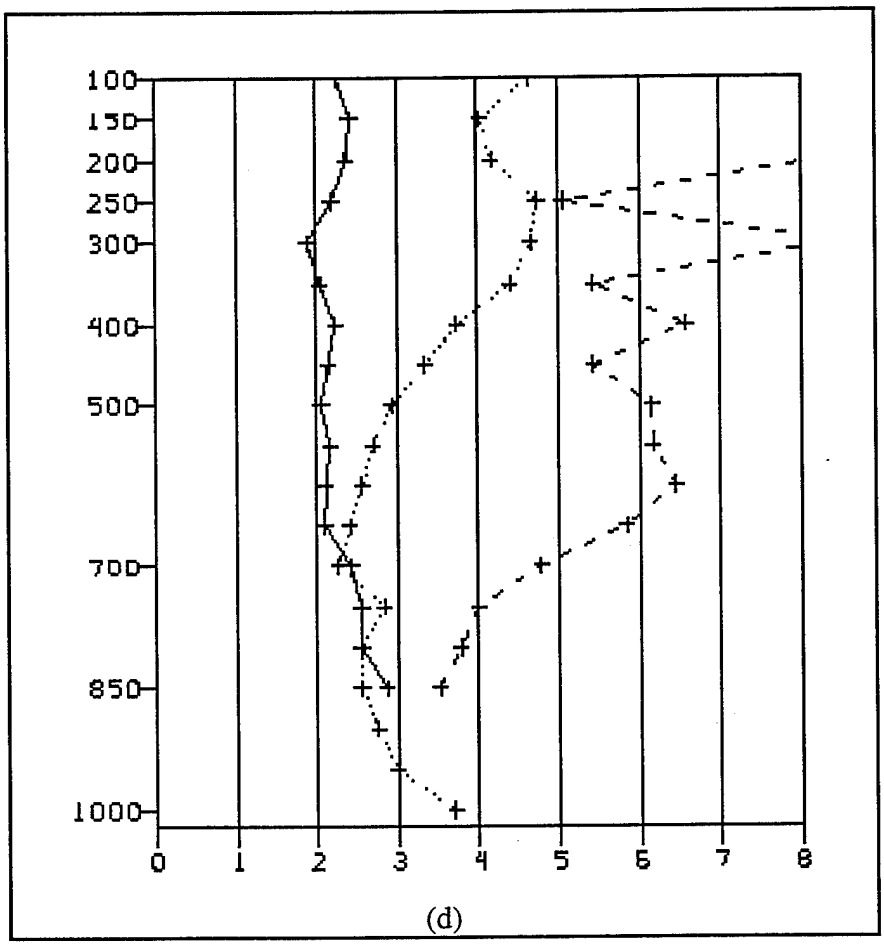

Figure 5.8. (Continued)

The dew point temperature errors start at about 1°C in the analysis (Figure 5.8a) but grow rapidly through the forecast period with a pronounced maximum in the 24-hour forecast (Figure 5.8c) at around 550 mb. The geopotential height RMS error profile develops a 20 m error by the 12-hour forecast (Figure 5.8b) which grows to over 45 m at 36 hours at the 300 mb level. As mentioned earlier, the Winter 1995 profiles show similar RMS error magnitudes. The 700 mb to 400 mb dew point temperature RMS errors are virtually identical in the Fall 1994 and Winter 1995 season even though the average errors are 180° out of phase.

Finally, as a further example of the vertical structure of the errors field, the Fall 1994 average and RMS errors at Oakland (OAK), CA are presented in Figure 5.9 for the 36-hour forecast period only. Notice that the cold bias maximizes in the vertical around 800 mb rather than at 700 mb as at Salt Lake City. Investigation of the cold bias at all stations in the west suggests that lower elevation stations tend to have lower maxima while higher elevation stations exhibit higher maxima. Thus, the cause of this bias may be related to processes in the upper part of the boundary layer. Large RMS errors are evident at Oakland as well (Figure 5.9b). The RMS error exceeds 6°C above 850 mb.

Temporal Evolution of Model Error

The cumulative statistics presented so far in this chapter provide an indication of the errors likely to be found at locations around the west. However, there is considerable day-to-day variation in the model's skill. In order to examine these day-to-day variations, each model's forecast cycle is verified and presented as part of time series for that month as a function of variable, station, and forecast duration. These time series are available on-line using the URL: **http://www.met.utah.edu/html/meso/meso_time_series.html**.

As an example of the fluctuations in model skill, Figure 5.10 presents the time series of 700 mb temperature error at Salt Lake City, Utah over the 6-month period from October 1994 through March 1995. The cold bias in the lower troposphere is clearly evident in the time series, since there are many more negative errors than positive errors,

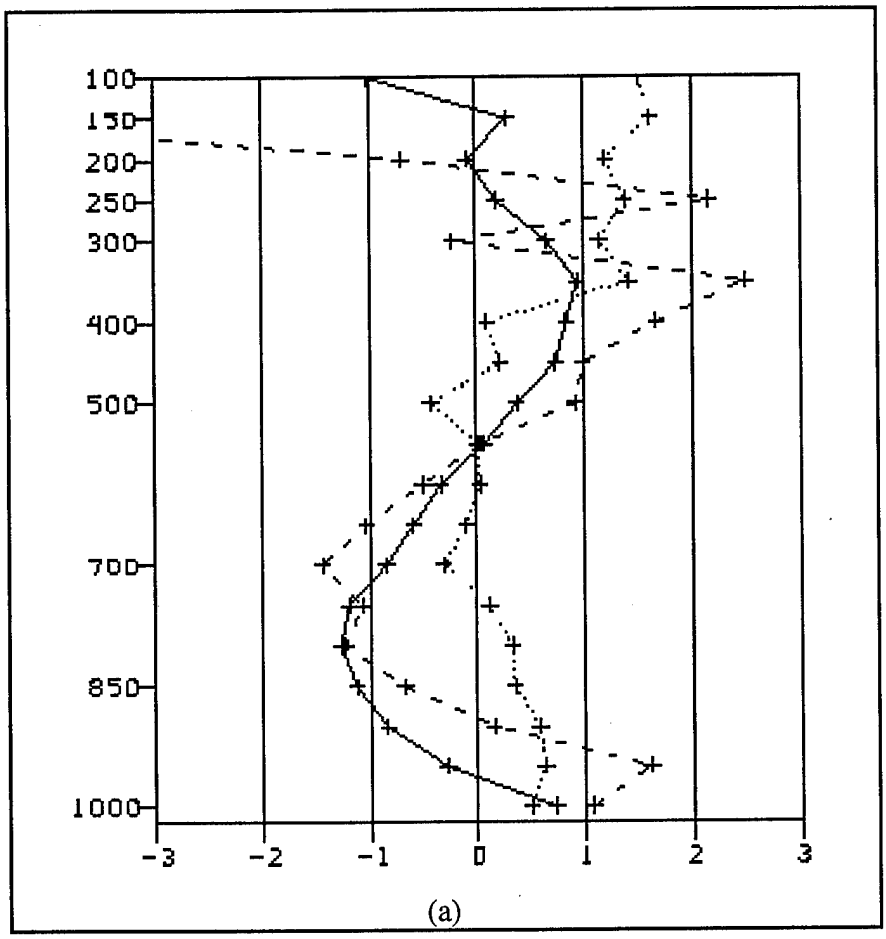

Figure 5.9. Oakland, CA 36-hour forecast Fall seasonal (a) average error (b) RMS error plotted as a function of height. The solid line shows the temperature error in °C, the dashed line shows the dew point error in °C and the dotted line shows the height error in dm.

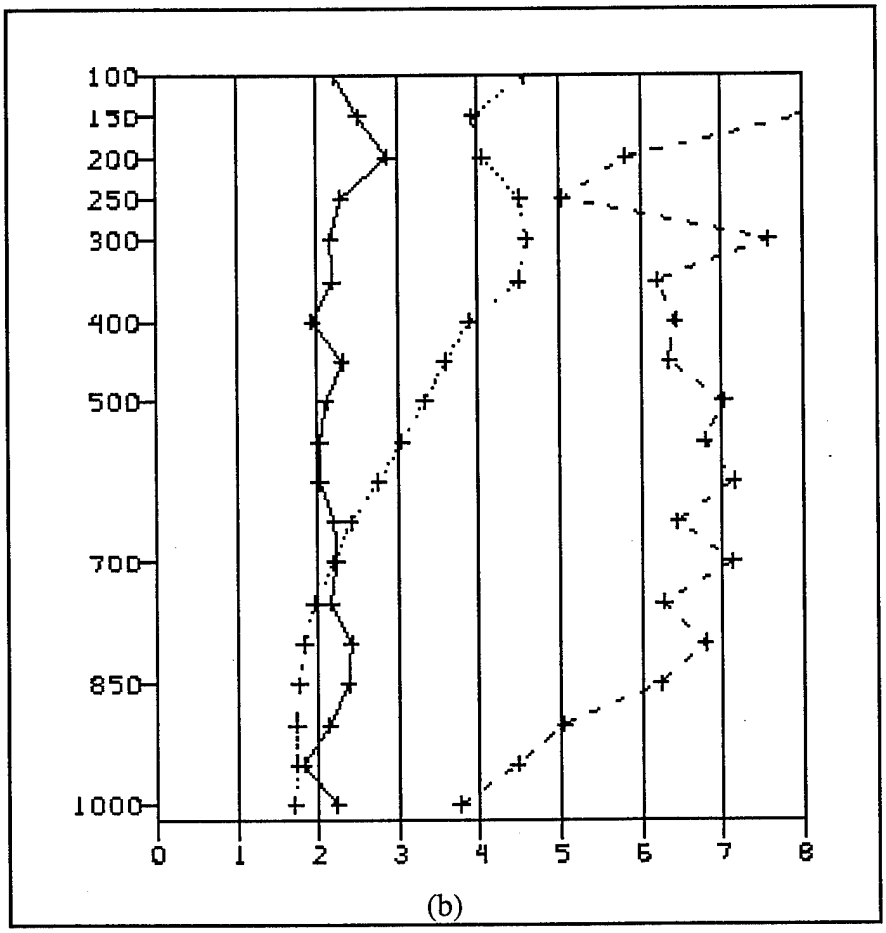

Figure 5.9. (Continued)

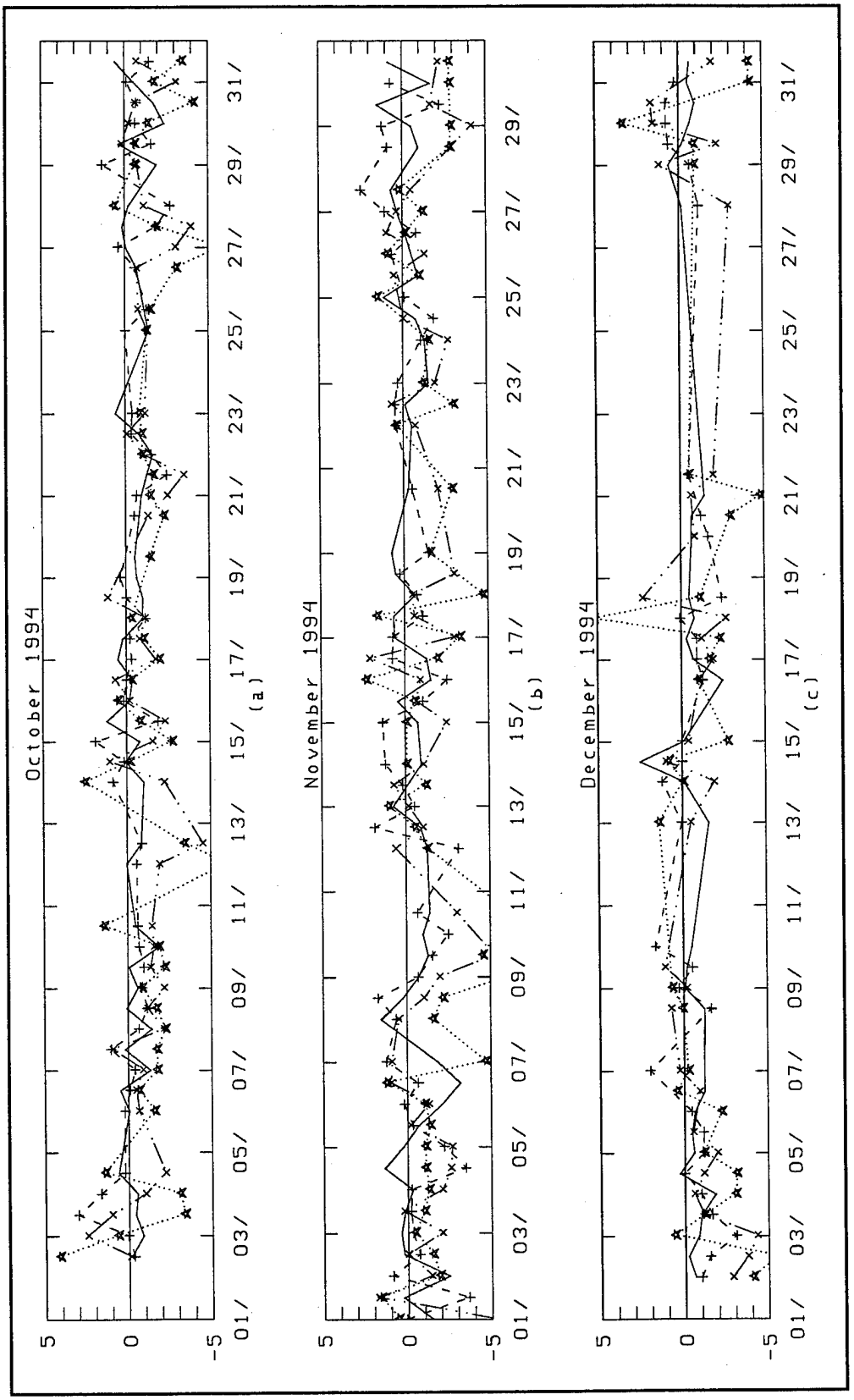

Figure 5.10. Time series of 700 mb temperature error (°C) at Salt Lake City, Utah for (a) October 1994; (b) November 1994; (c) December 1994; (d) January 1995; (e) February 1995; and (f) March 1995. Solid, dashed, dash-dot and dotted lines represent 0, 12, 24, and 36 hour forecasts respectively. The values are plotted at the forecast's initial time.

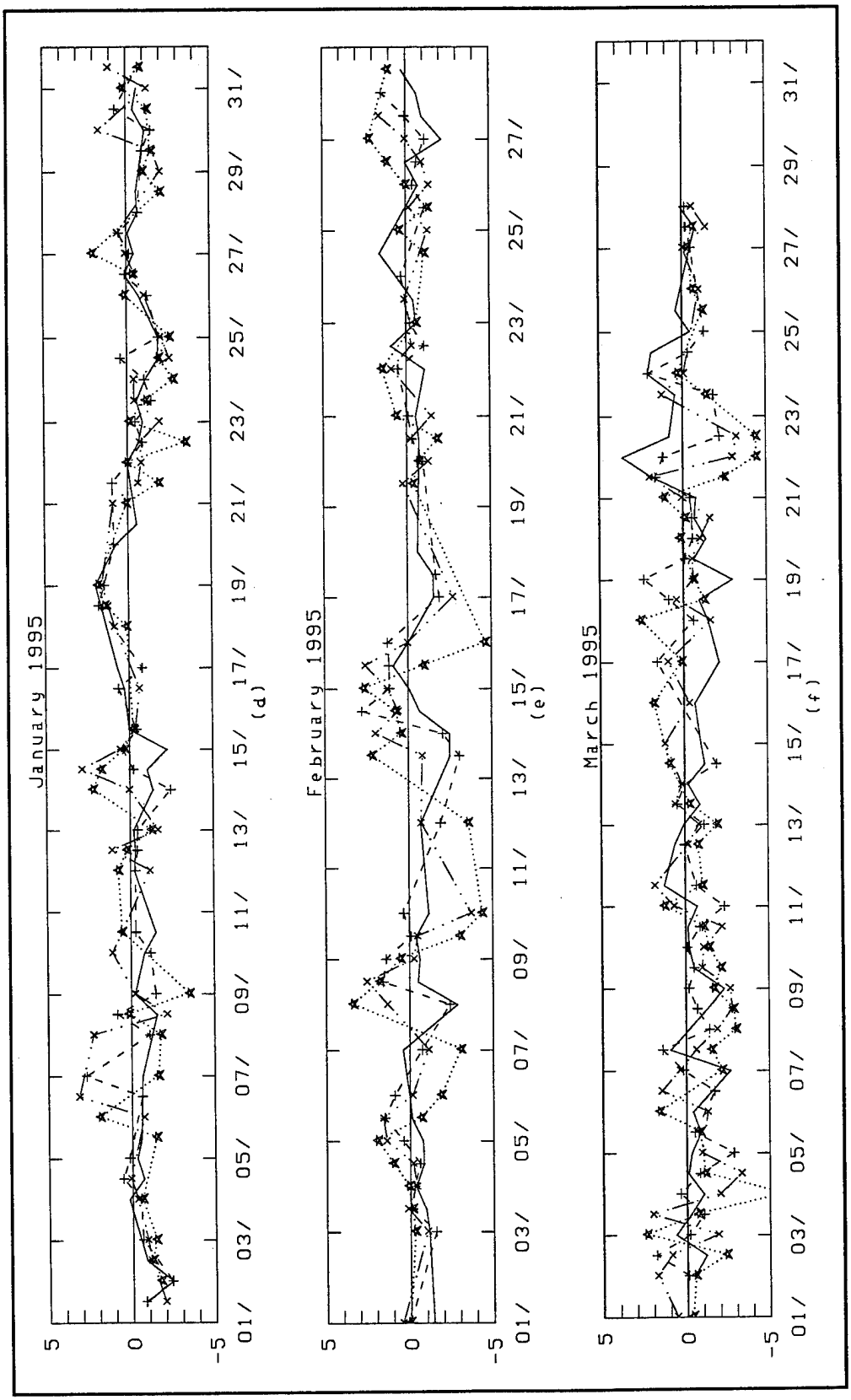

Figure 5.10. (Continued)

especially during the fall months. Infrequently, much larger errors are evident. The following forecasts exhibited 700 mb temperature errors in excess of -5°C:

- 0000 UTC, 12 October, 1994
- 0000 UTC, 27 October 1994
- 0000 UTC, 9 November, 1994
- 0000 UTC, 10 November, 1994
- 1200 UTC, 10 November, 1994
- 1200 UTC, 2 December, 1994
- 0000 UTC, 4 March, 1995.

Only one forecast had a +5°C or greater error: 0000 UTC, December 18 1994. The period studied in Chapter 4 had 3 of the 8 largest model errors in 700 mb temperature at Salt Lake City during this 6-month period. (The forecast initialized on 1200 UTC, 9 November 1994 that was examined in detail in Chapter 4 had an error slightly less than 5°C.)

The synoptic situation associated with each of the large model errors can be examined by accessing the on-line MPEG files available for each month of the upper tropospheric potential vorticity and the 500 mb geopotential height field analyses via URL: **http://www.met.utah.edu/html/meso/meso_mpg.html**. Many of the model forecasts with larger than normal negative errors are associated with developing or approaching troughs over the western United States. The forecasts associated with the largest errors listed above can be characterized as attempts by the model to move the synoptic-scale trough too fast to the east and thereby leading to faster cooling in the lower troposphere than was observed at Salt Lake City. The one case where the model was erroneously warm by more than 5°C is associated with too rapid development of ridging over the intermountain region.

Cumulative Precipitation Statistics

The precipitation amount and distribution forecast by the MEM is of great interest to operational forecasters and model developers. Precipitation represents the integrated

effect of numerous processes in the model. However, verifying precipitation forecasts over the western United States is a difficult task as a result of the relatively sparse data networks in many regions of the west, the many different archival sources for the verification data, and the complex terrain that leads to wide variations in precipitation over short distances.

Precipitation forecasts from the MEM have been contrasted to that forecast by other operational and research models on-line and the observed precipitation field for the California flood periods during January and March 1995. (See the URL: **http://www.met.utah.edu/html/case/case_master.html**). This work will be reported more fully elsewhere.

Here, the cumulative precipitation forecast by the model over the Fall 1994 and Winter 1995 seasons is simply presented without detailed comparison to observed accumulated precipitation. Instead, the focus is on the model's spinup of precipitation and the relative contribution of convective and resolvable-scale precipitation. These figures are available via URL: **http://www.met.utah.edu/html/meso/meso_rain.html**. Figure 5.11a shows the total precipitation forecast by the MEM during the first 12 hours of the model's forecast based on all available model forecasts during Fall 1994. The total precipitation forecast by the model during the next 12 hours (12- to 24-hour forecast period) is shown in Figure 5.11b and the precipitation forecast in the last 12 hours of each model forecast is presented in Figure 5.11c. The spatial distribution of precipitation has many plausible features with large amounts over the coastal areas of Oregon and Washington and secondary maxima over the Cascade Mountains of those states. Large precipitation totals are also forecast over the Sierra Mountains.

If all forecasts were available during the season, then the totals shown in the three panels of Figure 5.11 would be identical. Given that many forecasts are missing, then it might be expected that some differences might crop up. However, there is a clear spinup of precipitation evident with increasing forecast time. For example, over the Wasatch Mountains of Utah, the model forecasts an increasing maximum amount of precipitation

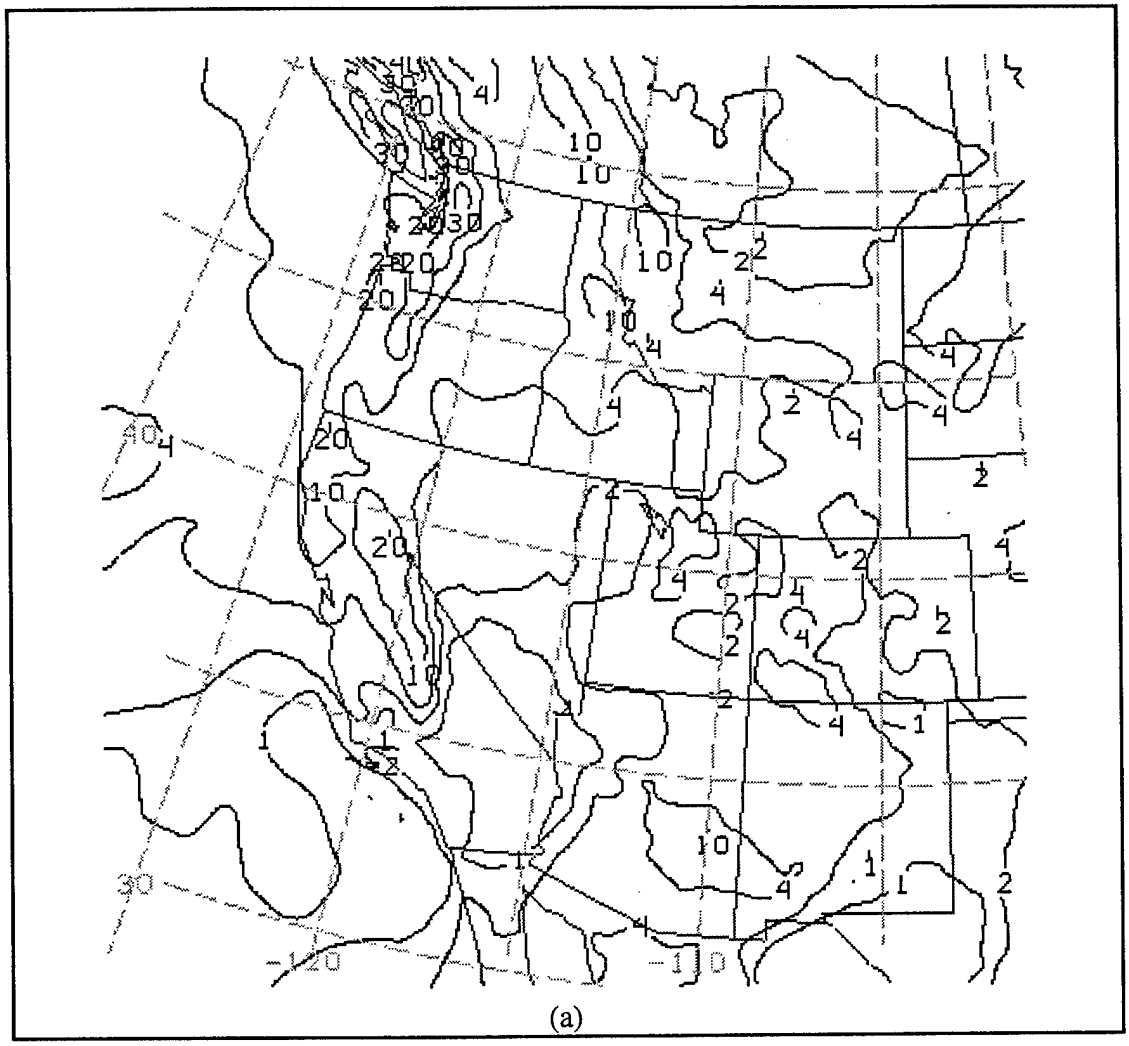

Figure 5.11. Total accumulated precipitation (in inches) forecast by the MEM during Fall 1994 for the periods: (a) 0- to 12-hour forecasts; (b) 12- to 24-hour forecasts; and (c) 24- to 36-hour forecasts. The contours are plotted at intervals of 1, 2, 4, 10, 20, 30, 40 , and 50 inches.

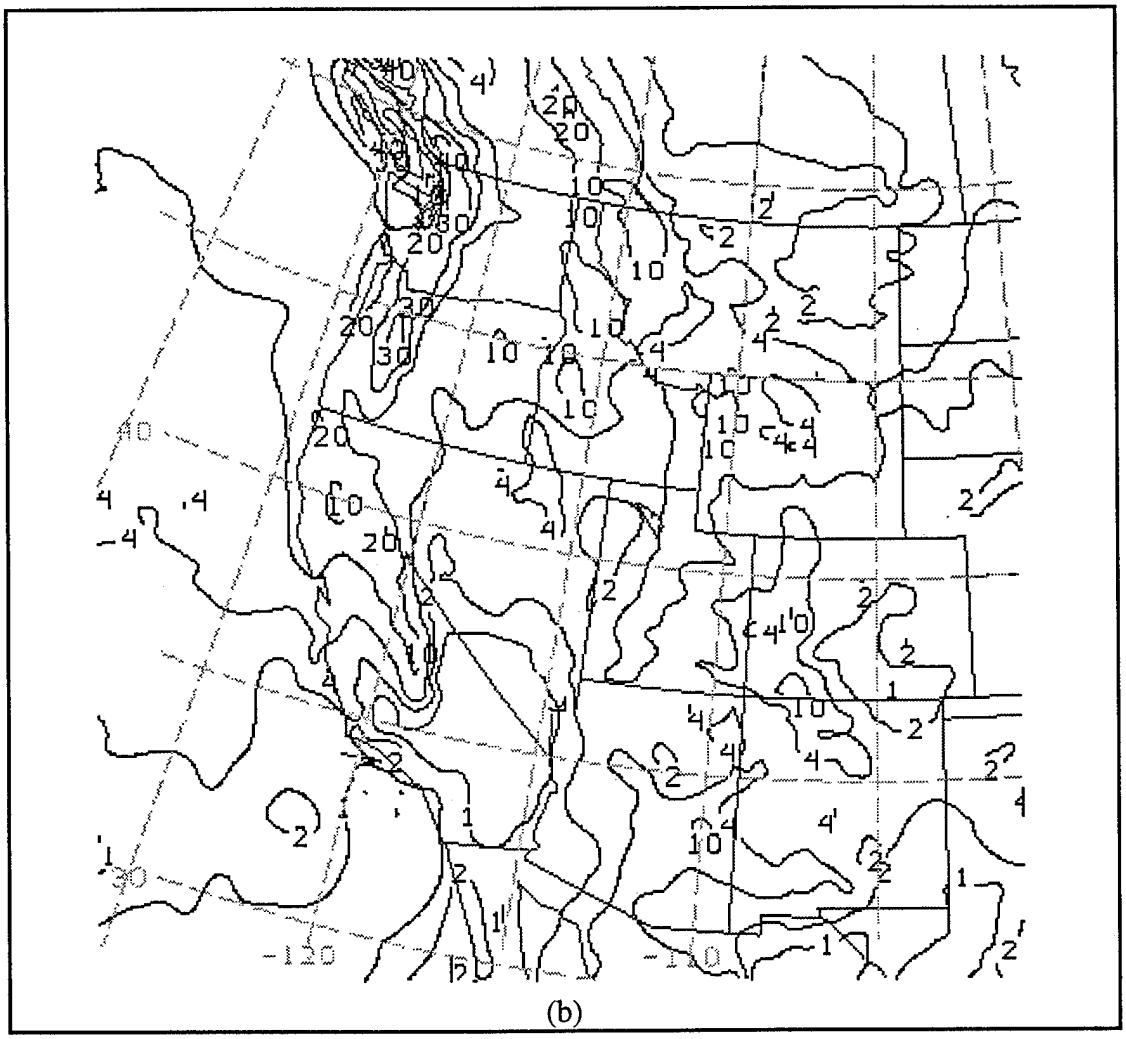

(b)

Figure 5.11. (Continued)

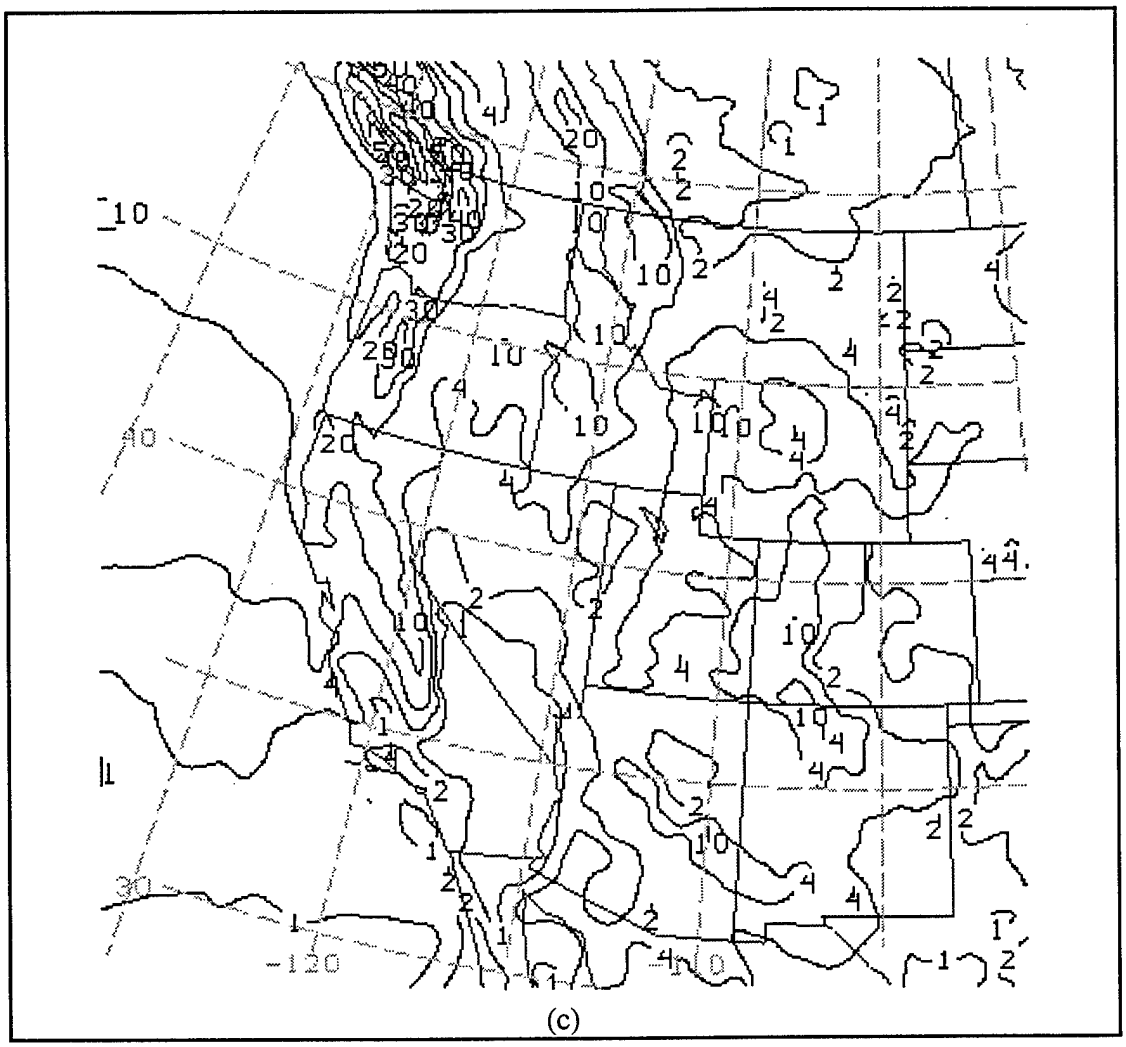

(c)

Figure 5.11. (Continued)

between the first two 12-hour periods. Large increases in precipitation with increasing forecast time are evident in other regions as well, e.g., along the west coast of Vancouver Island. As a general rule, the totals for the 12- to 24-hour and 24- to 36-hour forecast periods appear more consistent, which suggests that the model's spinup of precipitation is, for the most part, complete after 12 hours.

Forecast total precipitation during the Winter 1995 season is presented in Figure 5.12. The largest amounts are forecast along the west slopes of the Sierra Mountains of northern and central California. Local, large maxima are also evident over northwestern California extending southward along the coastal range, and near Santa Barbara, California. These areas were hit hard by the flooding during January and March 1995. The increase in precipitation from the 0- to 12-hour to 12- to 24-hour forecast period remains evident during winter by comparing the magnitudes of total precipitation in the three panels of Figure 5.12.

To provide a simple comparison of the precipitation amounts forecast by the MEM to those observed, Table 5.3 lists the total precipitation observed at Salt Lake City and Alta during the two seasons. Alta lies at an elevation of roughly 8000 feet in the Wasatch Mountains about 40 km from the Salt Lake City airport. The airport site tends to be one of the driest locations along the west slope of the Wasatch Mountains whereas Alta is normally one of the wettest. These two stations then tend to bracket the observed precipitation in this region of northern Utah. The precipitation amounts forecast at Salt Lake City are comparable to those observed; however, given that only roughly 2/3 of all of the model forecasts are available for this comparison, the model has overforecast the total precipitation at the airport. On the other hand, the model underestimates the precipitation totals observed in the Wasatch Mountains to a degree that could not be compensated for by the missing model forecasts. As a general rule, the model underestimates the precipitation over other mountainous regions of the west as well.

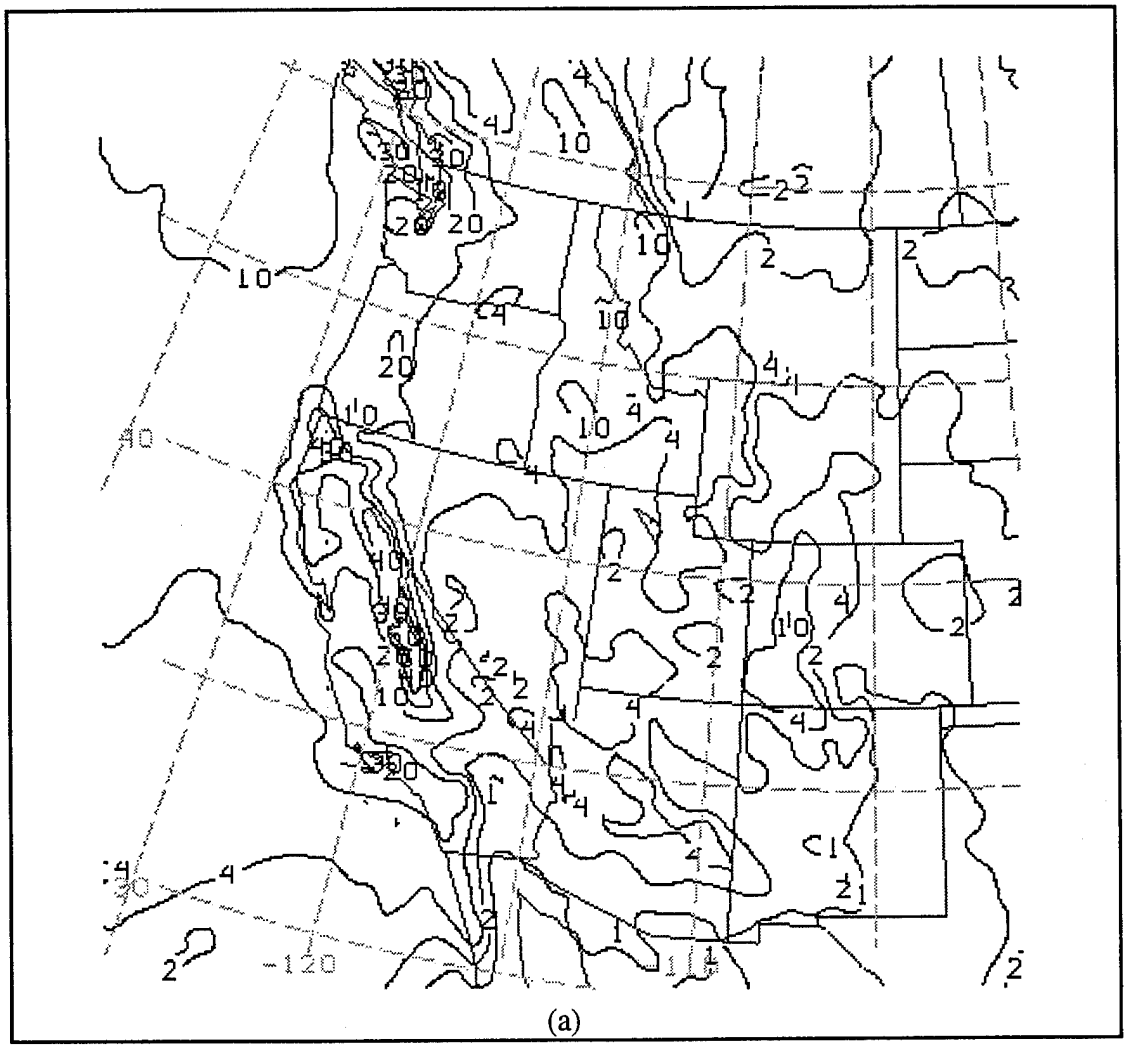

Figure 5.12. Total accumulated precipitation (in inches) forecast by the MEM during Winter 1995 for the periods: (a) 0- to 12-hour forecasts; (b) 12- to 24-hour forecasts; and (c) 24- to 36-hour forecasts. The contours are plotted at intervals of 1, 2, 4, 10, 20, 30, 40 , and 50 inches.

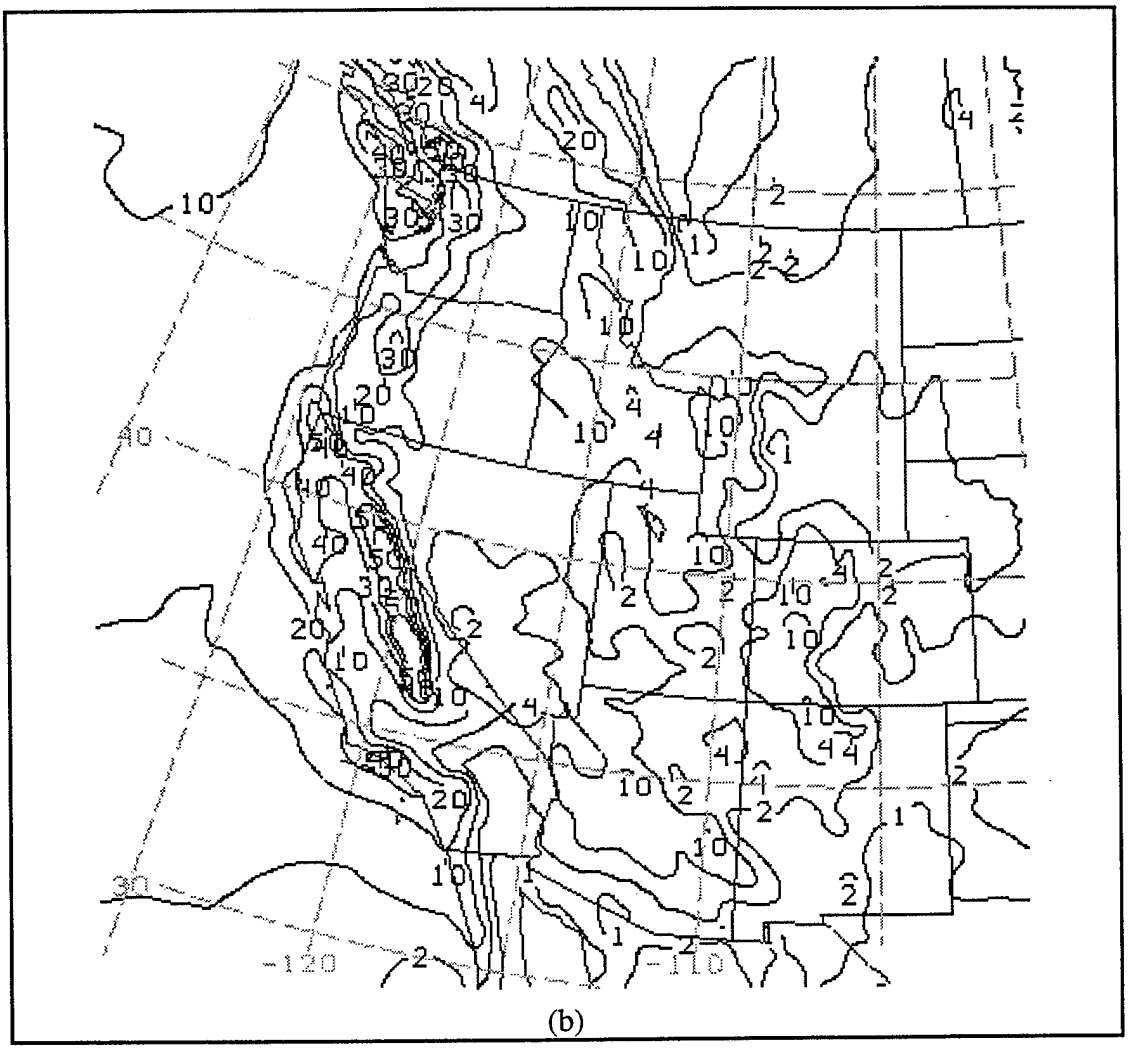

Figure 5.12. (Continued)

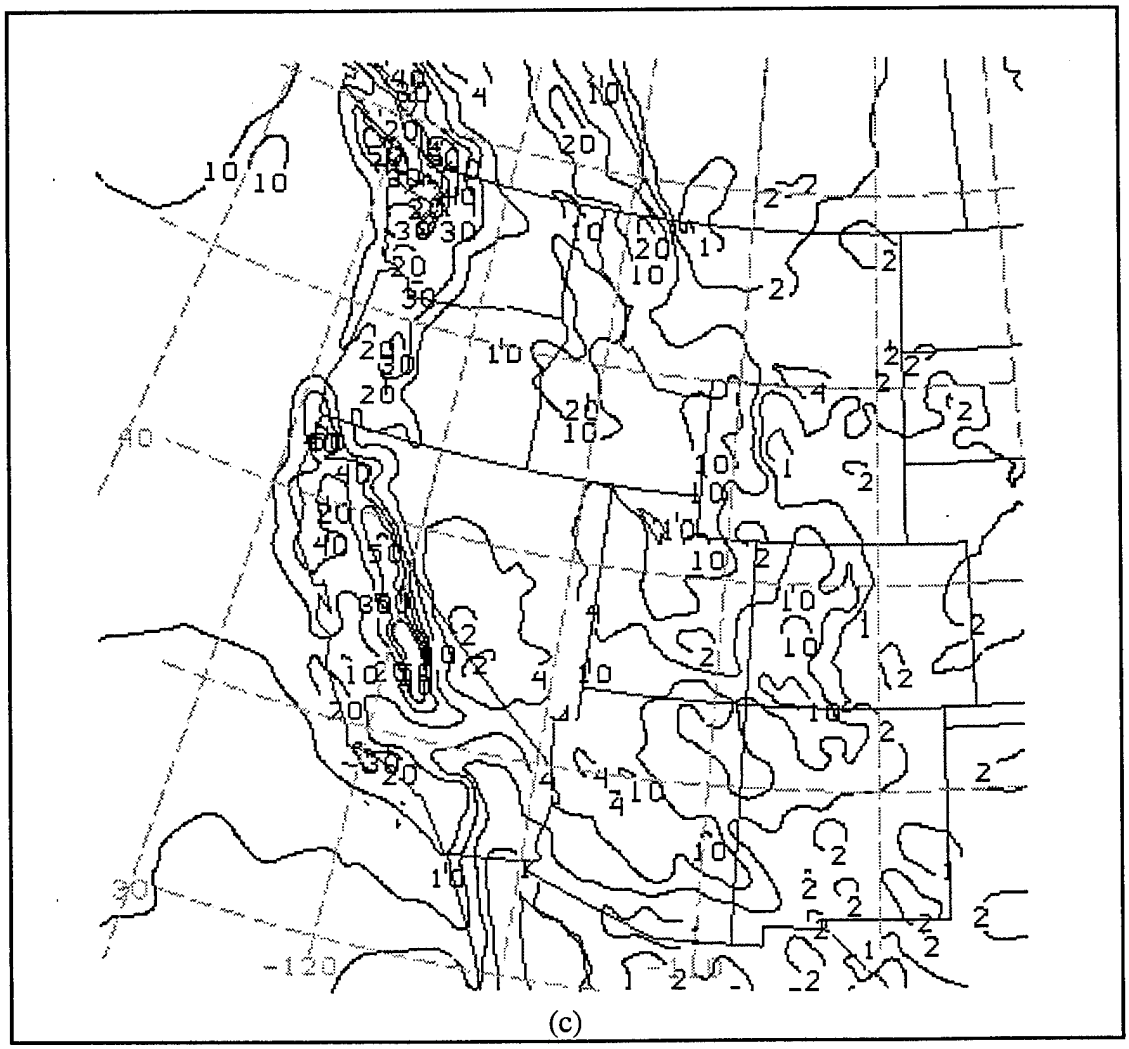

Figure 5.12. (Continued)

Table 5.3. Precipitation (in inches) observed at Salt Lake City and Alta during the Fall 1994 and Winter 1995 seasons contrasted to the total and convective precipitation forecast by the MEM as a function of forecast duration. The precipitation at the model grid point closest to Salt Lake City (Alta) is to the left (enclosed in parentheses).

	Fall 1994	**Winter 1995**
Salt Lake City, Utah	5.24	6.63
Alta, Utah	22.99	35.60
0-12 hour Total	3.59 (4.22)	4.02 (5.25)
12-24 hour Total	4.18 (5.36)	5.78 (7.63)
24-36 hour Total	5.37 (5.69)	6.46 (8.23)
0-12 hour Convective	.01 (.00)	.08 (.19)
12-24 hour Convective	.02 (.03)	.62 (.57)
24-36 hour Convective	.26 (.08)	.85 (.88)

The total precipitation combines the resolvable-scale precipitation arising from excess moisture from the surface to some level in the vertical and the parameterized convective precipitation. As mentioned in Chapter 2, the MEM uses a modified Betts-Miller scheme to parameterize convection (Black 1994). When the Betts-Miller scheme is triggered in the model, the vertical profiles of moisture and temperature are adjusted to a reference profile and excess moisture is counted as precipitation.

As shown in Table 5.3, the amount of convective precipitation observed at the grid points near Salt Lake City and Alta is very small during the Fall 1994 season and represents 10-15% of the total precipitation during Winter 1995. This relatively small contribution of convective precipitation to the total precipitation is found throughout the intermountain west as shown in Figure 5.13. Only the accumulated convective precipitation for the 24- to 36-hour period is presented here. The other panels are available on-line. Very little convective

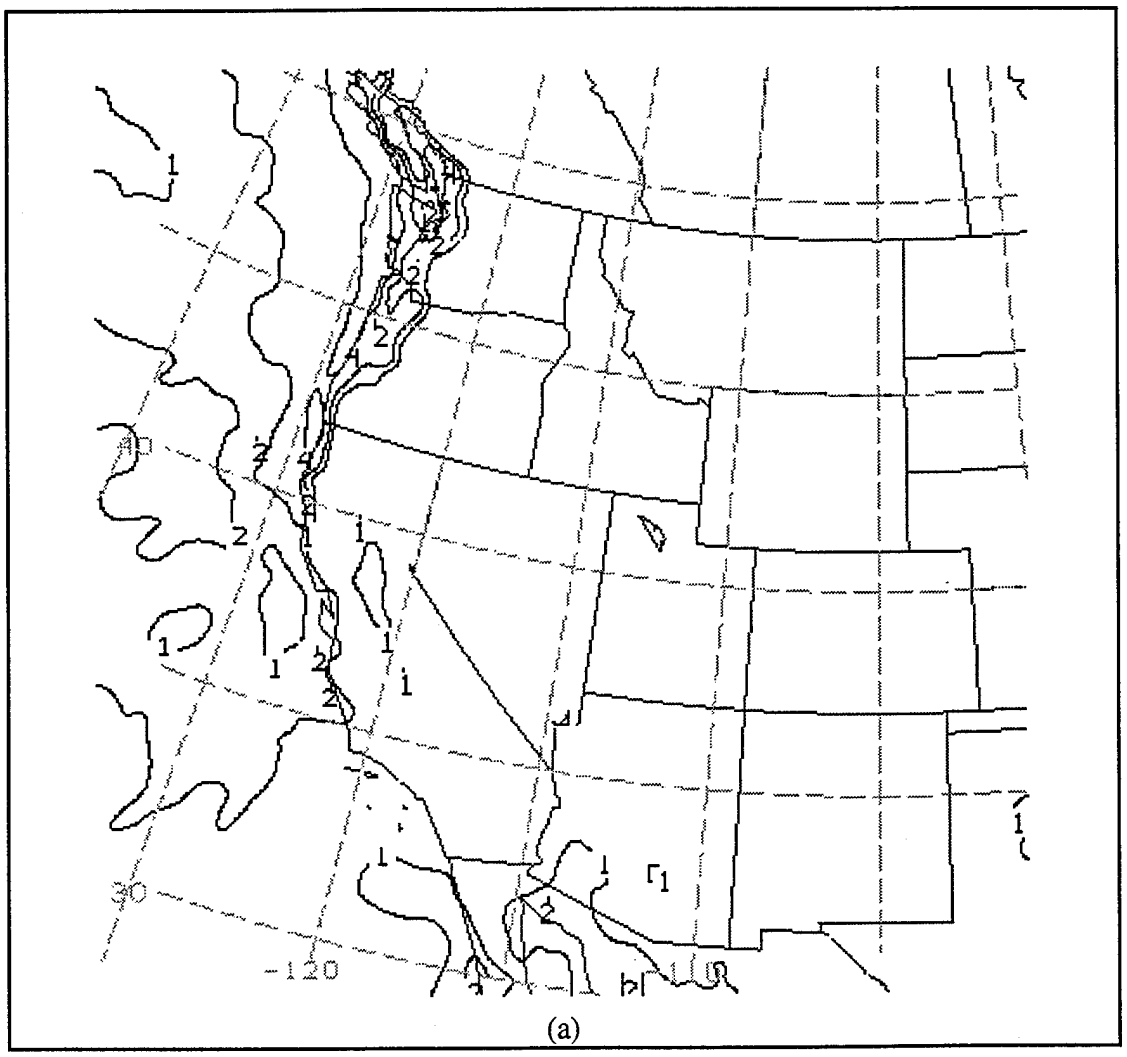

Figure 5.13. Accumulated convective precipitation (in inches) forecast by the MEM between 24 and 36 hours of each forecast during (a) Fall 1994 and (b) Winter 1995. The contours are plotted at intervals of 1, 2, 4, 10, 20, 30, 40, and 50 inches.

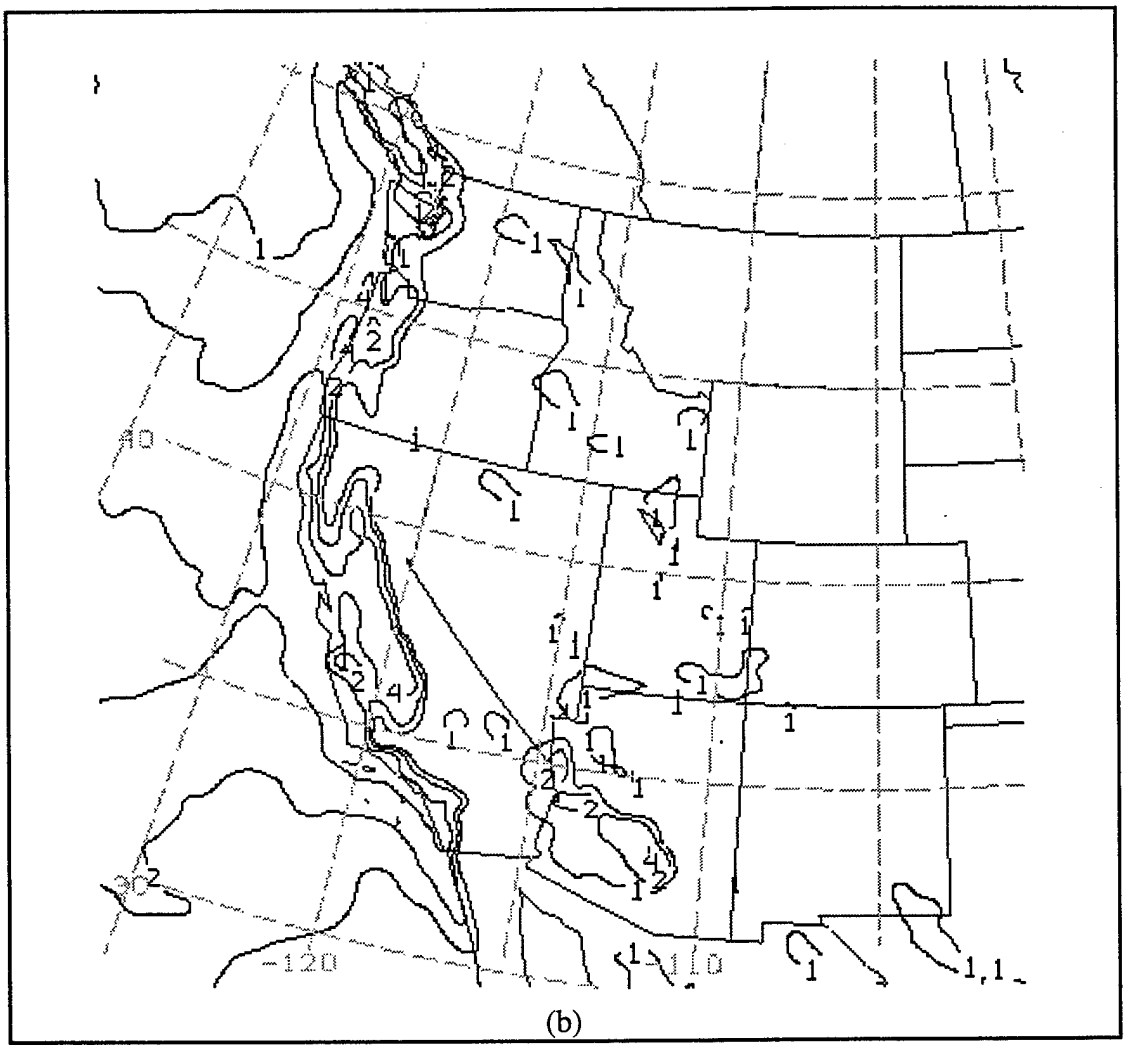

Figure 5.13. (Continued)

precipitation is forecast by the model, with the exception of the coastal zones, where the convective precipitation represents up to 25% of the total precipitation. During Winter 1995 (Figure 5.13b), large amounts of convective precipitation are found also in the Central Valley of California and in the low lying areas of Arizona. The common characteristic of the regions of significant convective precipitation appears to be the underlying low elevation of the grid point. The reasons for the 'offshore' maxima in convective precipitation (Figure 5.13) are not clear.

CHAPTER 6

SUMMARY AND CONCLUSIONS

The MEM forecasts have been archived and processed for over a 6-month period and automated procedures are in place to continue this effort. The 6-month period provides a large enough sample of model forecasts to evaluate the performance of the model over a wide variety of synoptic regimes with respect to its own analyses, those of the RUC, and rawinsonde observations. A novel aspect of this study is that the research results have been made available on-line over the Internet. This activity will continue over the next year.

This analysis provides a baseline of the model's performance in its preoperational state. The general conclusion drawn from this study is that the MEM is performing well over the western United States for dynamical and thermodynamical variables in the free atmosphere. The greatest deficiency is one common to all operational models, i.e., the specification of moisture in the lower and middle troposphere is frequently in error.

Later studies will be able to evaluate improvements to the model planned for May 1995 that will affect the model's treatment of processes in the boundary layer that are very important in the western United States. For example, preliminary analyses of low-level winds forecast by the MEM that have not been presented here suggest that they are too smooth spatially and do not 'feel' the underlying terrain found in the West.

The MEM forecast initialized at 1200 UTC, 9 November 1994 was used as a case study to introduce some of the diagnostic fields available to analyze the MEM. This forecast was chosen because it lies within a period in which the model's forecasts were less skillful than usual. Nonetheless, for many fields, the model's forecasts during this period were

good, including its handling of upper tropospheric potential vorticity anomalies. The largest errors are evident in the lower tropospheric temperature and moisture fields.

The average errors of the model's forecasts for selected variables were examined over the Fall 1994 and Winter 1995 seasons. These errors are presented on-line for each month and season. The average error provides an indication of systematic errors, or biases, that the model may have. For forecast durations of 36 hours or less, the model exhibits little significant bias in the 300 mb wind or 500 mb geopotential height fields. This is encouraging and indicates that operational forecasters need not be overly concerned with systematic tendencies in the model's forecasts in the upper troposphere.

As with many operational models, the MEM exhibits a cold bias in the lower troposphere on the order of 1-2^{o}C. This bias reaches a maximum within 200 mb of the model's surface. The causes for this bias are not clear, but are perhaps tied to the model's treatment of the vertical fluxes of heat and moisture in the boundary layer. The temporal trend of this bias has it largest in the summer and weakest in the winter. This trend may result from the seasonal change in the mean state of the atmosphere.

The RMS errors of the model's forecasts indicate that the typical magnitudes of the MEM errors are comparable to those of other operational models for forecast durations of 36 hours. The largest errors are evident, not surprisingly, in the lower and middle tropospheric moisture fields. Without performing a detailed intercomparison of the errors from all of the models at the NMC, it is not possible from the information provided here to conclude that the skill of the MEM is better than other models. However, Black (1994) and several of the studies cited in Chapter 1 have demonstrated that the precipitation skill of the Eta model is better than that of the NGM.

Time series of the model's skill indicate that the model occasionally has poor forecasts with, for example, 700 mb temperature errors larger than 5^{o}C. Errors of this magnitude reflect significant regional departures between what is forecast and what is observed. An impression gained from these low skill forecasts is that they are associated

predominantly with developing troughs in the west in which many eventually develop cut-off lows over the southwestern United States. The largest errors are present when the model moves such troughs too fast to the east and underforecasts the southward component of their motion. Causes for this behavior remain unclear at this time, but may be associated with the model's smooth terrain. Mountain barriers such as the Sierra Mountains lead to significant lee-side cyclogenesis that may not be adequately handled by the model.

Accumulations of model precipitation over months and seasons indicates that the version of the MEM evaluated here spins up model precipitation as the model forecast evolves during the first 12 hours. This is not surprising and represents a problem that is undergoing evaluation in many research and operational models (Donner 1988, Kasahara et al. 1994). Assimilation procedures intended to be implemented in future version of the EDAS in which observed precipitation is incorporated may alleviate this deficiency. In addition, changes in soil moisture to be implemented during May 1995 may also help. The model appears to underforecast precipitation over major mountain barriers in the intermountain west. A more detailed comparison of the observed and forecasted precipitation is underway.

Another aspect of the model's precipitation distribution is that the convective parameterization is infrequently triggered away from the coastline in the west. The distribution of convective precipitation maximizes to the west of the coastline. Convection is inhibited when the model's surface is more than a few hundred meters above sea level. This suggests that the triggers used to specify when the convective scheme is turned on needs to be examined carefully. It could be argued that the convective scheme should not be triggered frequently during winter in the west, but the absence of convective precipitation in many regions is unlikely to be realistic. Further, the Betts-Miller scheme plays a more important role in the model than simply a way to generate precipitation. It acts to inhibit instabilities that develop when the vertical lapse rate approaches or exceeds the saturated adiabatic lapse rate (Zhang et al. 1994). That the convective scheme is infrequently applied

implies that such instabilities have to be removed through the model's treatment of turbulence.

The results presented here represent the first systematic evaluation of the performance of the MEM over the western United States. Other related research is underway now at the University of Utah that includes: (1) a more detailed evaluation of the distribution of precipitation during the flooding episodes in California during January 1995 and March 1995 and (2) evaluation of the model's forecasts of vertical motion and related quasi-geostrophic diagnostic fields. During the period 15 May 1995 until 1 July 1995, researchers at the University of Utah will participate in the nationwide evaluation of the MEM before its operational release later during the summer. These activities will help to provide information on the model's performance to model developers, researchers, and operational forecasters that has not been available in the past for other operational models.

REFERENCES

Betts, A. K., 1986: A new convective adjustment scheme. Part I: Observational and theoretical basis. *Quart. J. Roy. Meteor. Soc.*, **112**, 677-691.

___, and M. J. Miller, 1986: A new convective adjustment scheme. Part II: Single column tests using GATE wave, BOMEX and arctic air-mass data sets. *Quart. J. Roy. Meteor. Soc.*, **112**, 693-709.

Black, T. L., 1994: The new NMC Mesoscale Eta model: Description and forecast examples. *Wea. Forecasting*, **9**, 265-278.

___, and F. Mesinger, 1989: Forecast performance of the NMC's Eta coordinate regional model. Preprints, 12th Conf. on Weather Analysis and Forecasting, Monterey, CA., Amer. Meteor. Soc., 551-555.

___, and F. Mesinger, 1991: Small scale circulations in NMC's 30 km Eta model. Preprints, Ninth Conf. on Numerical Weather Prediction, Denver, CO., Amer. Meteor. Soc., 229-230.

___, D. G. Deaven, and G. J. DiMego, 1993: The step-mountain eta coordinate model: 80 km "Early" version and objective verifications. Technical Procedures Bulletin 412, NOAA/NMS, 31pp.

___, and M. Baldwin, 1995: Winter forecast characteristics of the NMC Mesoscale model. Preprints, 14th Conf. on Weather Analysis and Forecasting, Dallas, TX, Amer. Meteor. Soc., 157-158.

Bleck, R., and S. G. Benjamin, 1993: Regional weather prediction with a model combining terrain-following and isentropic coordinates. Part I: Model description. *Mon. Wea. Rev.*, **121**, 1770-1785.

Cairns, M. M., R. J. Miller, S. C. Albers, D. L. Birkenheuer, B. D. Jamison, C. S. Hartsough, J. L. Mahoney, A. Marroquin, P. T. McCaslin, J. E. Ramer, and J. M. Schmidt, 1993: *A preliminary evaluation of aviation-impact variables derived from numerical models.* NOAA Tech. Memo., ERL FSL-5, 165pp.

des Jardins, M. L., K. F. Brill, and S. S. Schotz, 1991: *GEMPAK5 User's Guide.* NASA Tech. Memo. 4260.

Donner , L. J., 1988: An initialization for cumulus convection in numerical weather prediction models. *Mon. Wea. Rev.*, **116**, 377-385.

Dunn, L. B., 1993: Evaluation of the National Meteorological Center Mesoscale model for prediction of severe convection over central Arizona. Doctoral dissertation, University of Utah, 152pp.

___, and J. Horel, 1994a: Prediction of central Arizona convection. Part I: Evaluation of the NGM and Eta model precipitation forecasts. *Wea. Forecasting.*, **9**, 495-507.

___, and J. Horel, 1994b: Prediction of central Arizona convection. Part II: Further evaluation of the Eta model forecasts. *Wea. Forecasting.*, **9**, 508-521.

Janjic´, Z. I., 1994: The step-mountain eta coordinate model: Further developments of the convection, viscous sublayer, and turbulence closure schemes. *Mon. Wea. Rev.*, **122**, 927-945.

Kasahara, A., A. P. Mizzi, and L. J. Donner, 1994: Diabatic initialization for improvement in the tropical analysis of divergence and moisture using satellite radiometric imagery data. *Tellus*, **46A**, 242-264.

Kuo, Y., L. Cheng, and J. Bao, 1988: Numerical simulation of the 1981 Sichuan flood. Part I: Evolution of a mesoscale vortex. *Mon. Wea. Rev.*, **116**, 2481-2504.

Gerrity, J. P. Jr., T. L. Black, and R. E. Treadon, 1994: The numerical solution of the Mellor-Yamada level 2.5 turbulent kinetic energy equation in the Eta model. *Mon. Wea. Rev.*, **122**, 1640-1646.

Mesinger, F., Z. I. Janjic´, S. Nickovic´, D. Gavrilov, and D. G. Deaven, 1988: The step-mountain coordinate model description and performance for cases of Alpine lee cyclogenesis and for a case of an Appalachian redevelopment. *Mon. Wea. Rev.*, **116**, 1493-1518.

___, T. L. Black, D. W. Plummer, and J. H. Ward, 1990: Eta model precipitation forecasts for a period including tropical storm Allison. *Wea. Forecasting*, **5**, 483-493.

___, T. L. Black, and M. E. Baldwin, 1994: Dependence of the skill of the Eta model precipitation forecasts on the resolution and the choice of the eta vs. the sigma coordinate. Preprints, 10th Conf. on Numerical Weather Prediction, Portland, OR, Amer. Meteor. Soc., 426-427.

___, and R. E. Treadon, 1995: "Horizontal" reduction of pressure to sea level: Comparison against the NMC's Shuell method. *Mon. Wea. Rev.*, **123**, 59-68.

Phillips, N. A., 1957: A coordinate system having some special advantages for numerical forecasting. *J. Meteor.*, **14**, 184-185.

Pielke, R. A., 1984: *Mesoscale Meteorological Modeling*, Academic Press, Inc., San Diego, 455.

Rogers, E., D. G. Deaven, and G. J. DiMego, 1995: Mesoscale data assimilation with the Eta model at the National Meteorological Center. Preprints, 14th Conf. on Weather Analysis and Forecasting, Dallas, TX, Amer. Meteor. Soc., 159-160.

Slingo, J. M., 1987: The development and verification of a cloud prediction scheme for the ECMWF model. *Quart. J. Roy. Meteor. Soc.*, **113**, 899-927.

Treadon, R. E., 1993: The NMC Eta model: A documentation. NMC Office Note 394, NOAA/NWS, 44pp. [Available from the National Meteorological Center, NOAA Science Center, Room 101, 5200 Auth Road, Camp Springs, MD 20746.]

Zhang, D. L., J. S. Kain, J. M. Fritsch, and K. Gao, 1994: Comments on "Parameterization of convective precipitation in mesoscale numerical models: A critical review". *Mon. Wea. Rev.*, **122**, 2222-2231.

Zhao, Q., F. H. Carr, and G. B. Lesins, 1991: Improvement of precipitation forecasts by including cloud water and cloud ice into NMC's Eta model. Preprints, Ninth Conf. on Numerical Weather Prediction, Denver, CO., Amer. Meteor. Soc., 50-53.